International Applied Mechanics, Vol. 49, No. 2, March, 2013

STATIC AND DYNAMIC PROBLEMS FOR ANISOTROPIC INHOMOGENEOUS SHELLS WITH VARIABLE PARAMETERS AND THEIR NUMERICAL SOLUTION (REVIEW)

Ya. M. Grigorenko and A. Ya. Grigorenko

Studies on the static and dynamic deformation of isotropic and anisotropic elastic shell-like bodies of complex shape performed using classical and refined problem statements are reviewed. To solve two-dimensional boundary-value problems and eigenvalue problems, use is made of a nontraditional discrete-continuum approach based on the spline-approximation of the unknown functions of partial differential equations with variable coefficients. This enables reducing the original problem to a system of one-dimensional problems solved with the discrete-orthogonalization method. An analysis is made of numerical results on the distribution of stress and displacement fields and dynamic characteristics depending on the loading and boundary conditions, geometrical and mechanical parameters of elastic bodies. Emphasis is placed on the accuracy of the results

Keywords: shell structures, static and dynamic problems, variable parameters, models, discrete-continuum methods

Introduction. Many members of modern engineering structures have the form of intricately shaped shells fixed in various ways and subjected to various distributed and local loads. Shell elements are widely used to meet the requirements imposed by the severe operating conditions of machines, aircraft, transportation vehicles, industrial and civil facilities. The complication of the configuration of shell elements necessitates developing a theory and methods for solving static and dynamic problems for shells made of anisotropic inhomogeneous materials.

A typical feature in the development of the theory of plates and shells is the relationship between the setting up of a mathematical model describing a given class of problems and the development of a method for solving them. For example, Kirchhoff's theory of thin plates [101] and the Kirchhoff–Love theory of thin shells [97] tend not only to provide a realistic description of the deformation of plates and shells, but also to make such models so simple as to solve a number of problems with available computational capability. An example of such relationship is the Donnell–Mushtari–Vlasov theory of shells [5, 28, 36]. Its basic equations were simplified so as to find solutions to some classes of problems over wide ranges of their characteristics, which is demonstrated by the names given to this theory: technical theory of shells, theory of shallow shells, theory of shells with highly variable stress state [2, 8, 9, 16, 20, 23, 24, 29, 37]. This relationship is even stronger nowadays when computers are widely used to solve problems in the theory of shells and mathematical models for certain classes of shells are set up so as to provide for all aspects and possibilities associated with the solution of problems [63].

The solution of two-dimensional boundary-value problems of the statics and dynamics of plates, shells, and solids described by partial differential equations with variable coefficients involves severe computational difficulties. To solve them, use is sometimes made of approaches based on separation of variables and reduction of the original problem to one dimension. However, this is often hindered by many factors, such as complex shape, equation coefficients, boundary conditions, etc.

Recent trends in computational mathematics, mathematical physics, and mechanics are toward the wide use of spline functions. This is due to the following advantages of spline-approximations: stability of splines against local perturbations, i.e.,

S. P. Timoshenko Institute of Mechanics, National Academy of Sciences of Ukraine, 3 Nesterova St., Kyiv, Ukraine 03057, e-mail: ayagrigorenko@yandex.ru. Translated from Prikladnaya Mekhanika, Vol. 49, No. 2, pp. 3–70, March–April 2013. Original article submitted June 5, 2012.

the local behavior of a spline in the neighborhood of a point does not affect its overall behavior, unlike polynomial approximation (good convergence of spline-interpolation unlike polynomial interpolation); simplicity and convenience of numerical implementation of spline algorithms [1, 2, 5]. Various numerical approaches to solving problems in the theory of plates and shells are addressed in [64, 66, 85, 86, 96, 98, 99].

Here, to solve problems described by partial differential equations, we will follow a nonconventional approach employing spline-approximation to reduce the original problem to a one-dimensional one that can be solved with the stable numerical discrete-orthogonalization method [16–19]. Some other numerical approaches were used in [38, 43, 45, 51–54] to study the static and dynamic behavior of shell structures.

The discrete-orthogonalization method was for the first time proposed in [3, 6]. The monograph [26] states that the discrete-orthogonalization method was for the first time applied to the statics of shells in [18, 19]. Features of using this method in the theory of shells are outlined in [16] where it was also shown that the memory requirements can be substantially reduced by somewhat modifying the algorithm. The efficiency and high accuracy of the method when applied to the theory of shells is noted in [4, 26] and confirmed in [7].

In [10, 17], it was proposed to use spline-approximation to reduce two-dimensional problems of the static and dynamic deformation of plates and shells to systems of ordinary differential equations.

1. Using Spline Functions to Solve Boundary-Value Problems for Partial Differential Equations. Let us consider an approach to solving two-dimensional boundary-value problems for partial differential equations with coefficients variable in two directions describing the static and dynamic behavior of elastic shells with variable parameters. The approach employs spline-approximation to reduce two-dimensional problems to one-dimensional ones that can be solved with the stable numerical discrete-orthogonalization method [10, 17, 72, 73].

Basics of Spline Functions. Expand a partition $\Delta: a = x_0 < x_i < \ldots < x_N = b$ to include auxiliary points $x_{-m} < \ldots < x_{-1} < a,\ b < x_{N+1} < \ldots < x_{N+m}$ and consider a partition

$$\Delta_1: x_{-m} < \ldots < x_{-1} < x_0 < x_1 < \ldots < x_{N-1} < x_N < x_{N+1} < \ldots < x_{N+m}.$$

Consider a function $\varphi_m(x,t) = (-1)^{m+1}(m+1)(x-t)_+^m$ and form a divided difference of order $(m+1)$ using argument values $t = x_i, \ldots, x_{i+m+1}$. Doing so gives functions of x:

$$\widetilde{B}_m^i = \varphi_m[x, x_i, \ldots, x_{i+m+1}], \qquad i = -m, \ldots, N-1. \tag{1.1}$$

These functions are called basis splines or B-splines of degree m and are splines of degree m over the partition Δ_1 such that the difference between its degree and smoothness is equal to one (defect 1).

With the identity $(x-t)_+^m = (x-t)^m + (-1)^{m+1}(t-x)_+^m$, functions (1.1) can be represented as

$$\widetilde{B}_m^i(x) = (m+1)\sum_{p=i}^{i+m+1}\frac{(x_p - x)_+^m}{\omega'_{m+1,i}(x_p)} \quad (i = -m, \ldots, N-1) \quad \left(\omega_{m+1,i}(t) = \prod_{j=i}^{i+m+1}(t - x_j)\right). \tag{1.2}$$

For practical purposes, it is convenient to use normalized B-splines:

$$B_m^i(x) = \frac{x_{i+m+1} - x_i}{m+1}\widetilde{B}_m^i(x). \tag{1.3}$$

The following recurrence formula holds for such splines:

$$B_m^i(x) = \frac{x - x_i}{x_{i+m} - x_i}B_{m-1}^i(x) + \frac{x_{i+m+1} - x}{x_{i+m+1} - x_{i+1}}B_{m-1}^{i+1}(x). \tag{1.4}$$

It may be used as the definition of B-splines;

$$B_0^i(x) = \begin{cases} 1, & x \in [x_i, x_{i+1}), \\ 0, & x \notin [x_i, x_{i+1}). \end{cases}$$

The functions $B_m^i(x)$ are splines of degree m with defect 1 and finite minimal supports. Moreover, the system of functions $B_m^i(x)(i=-m,\dots,N-1)$ is linearly independent and forms a basis in the space of splines $S_m(\Delta)$. This means that each spline $S_m(x)\in S_m(\Delta)$ can be uniquely expressed as

$$S_m(x)=\sum_{i=-m}^{N-1} b_i B_m^i(x), \tag{1.5}$$

where b_i are some constant coefficients.

The splines $B_m^i(x)$ have the following properties:

(a) $B_m^i(x)>0$ for $x\in[x_i,x_{i+1})$, $B_m^i(x)\equiv 0$ for $x\notin[x_i,x_{i+1})$;

(b) $\int_{-\infty}^{\infty} B_m^i(x)dx=\frac{x_{i+m+1}-x_i}{m+1}$.

Consider a uniform expanded partition

$$\Delta': x_{-m}<\dots<x_{-1}<x_0<\dots<x_N<x_{N+1}<\dots<x_{N+m}\quad (x_{k+1}-x_k=h=\text{const})$$

and set up the first three B-splines of odd degree. They are numbered by numbering the middle knots of their supports.

Therefore, B-splines of odd degree are denoted by $B_m^i(x)$ rather than by $B_m^{i-(m+1)/2}(x)$, i.e., the numbering of splines is shifted by $(m+1)/2$ to the right.

Thus, we have

first-order B-splines

$$B_1^i(x)=\begin{cases}0, & -\infty<x<x_{i-1},\\ t, & x_{i-1}\le x\le x_i,\\ 1-t, & x_i\le x<x_{i+1},\\ 0, & x_{i+1}\le x<\infty,\end{cases} \tag{1.6}$$

cubic B-splines

$$B_3^i(x)=\frac{1}{6}\begin{cases}0, & -\infty<x<x_{i-2},\\ t^3, & x_{i-2}\le x<x_{i-1},\\ -3t^3+3t^2+3t+1, & x_{i-1}\le x<x_i,\\ 3t^3-6t^2+4, & x_i\le x<x_{i+1},\\ (1-t)^3, & x_{i+1}\le x<x_{i+2},\\ 0, & x_{i+2}\le x<\infty,\end{cases} \tag{1.7}$$

quintic B-splines

$$B_5^i(x)=\frac{1}{120}\begin{cases}0, & -\infty<x<x_{i-3},\\ 0, & x_{i-3}\le x<x_{i-2},\\ -5t^5+5t^4+10t^3+10t^2+5t+1, & x_{i-2}\le x<x_{i-1},\\ 10t^5-20t^4-20t^3+20t^2+50t+26, & x_i\le x<x_{i+1},\\ -10t^5+30t^4-60t^2+66, & x_i\le x<x_{i+1},\\ 5t^5-20t^4+20t^3+20t^2-50t+26, & x_{i+1}\le x<x_{i+2},\\ (1-t)^5, & x_{i+2}\le x<x_{i+3},\\ 0 & x_{i+3}\le x<\infty,\end{cases} \tag{1.8}$$

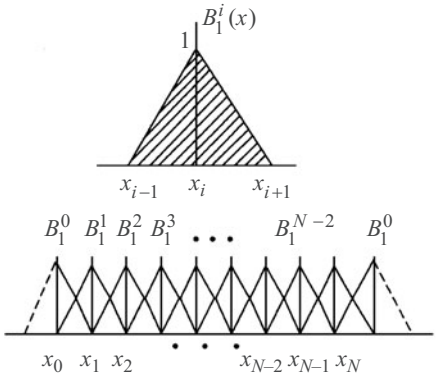

Fig. 1

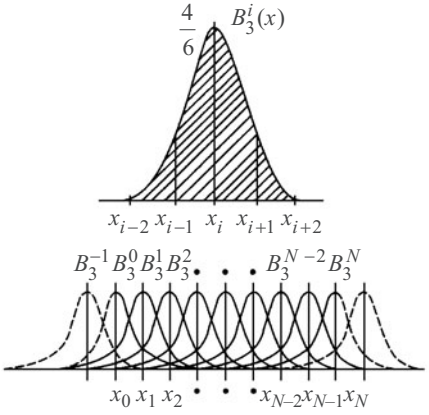

Fig. 2

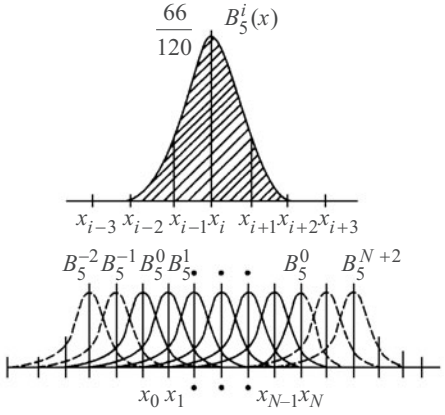

Fig. 3

TABLE 1

x	$B_3^i(x)$	$B_3^{i'}(x)$	$B_3^{i''}(x)$
x_{i-2}	0	0	0
x_{i-1}	$\frac{1}{6}$	$\frac{1}{2h}$	$\frac{1}{2h}$
x_i	$\frac{4}{6}$	0	$-\frac{2}{h^2}$
x_{i+1}	$\frac{1}{6}$	$-\frac{1}{2h}$	$\frac{1}{h^2}$
x_{i+2}	0	0	0

where $t = (x - x_k)/h$ on the interval

$$[x_k, x_{k+1}], \quad k = i = \overline{-\frac{m+1}{2}, i + \frac{m+1}{2} - 1}, \qquad i = \overline{-\frac{m+1}{2} + 1, N + \frac{m+1}{2} - 1}, \qquad m = 1, 3, 5.$$

Figures 1–3 show these B-splines and the associated bases in the spaces $S_m(\Delta)$ $(m = 1, 3, 5)$.

Tables 1 and 2 summarize the values of the splines $B_3^i(x)$ and $B_5^i(x)$ and their derivatives at the knots that belong to their supports.

Using Spline-Approximation to Reduce Two-Dimensional Problems to One-Dimensional. Let us find the solution $\overline{u}(x, y)$ of the following system of linear partial differential equations in the rectangular domain $R\{x_0 \le x \le x_N,\ y_1 \le y \le y_2\}$:

$$\overline{F}\left(x, y, \overline{u}, \frac{\partial \overline{u}}{\partial x}, \frac{\partial \overline{u}}{\partial y}, \frac{\partial^2 \overline{u}}{\partial x^2}, \frac{\partial^2 \overline{u}}{\partial x \partial y}, \frac{\partial^2 \overline{u}}{\partial y^2}, \ldots\right) = 0 \tag{1.9}$$

that satisfies the boundary conditions

$$\overline{G}\left(x, y, \overline{u}, \frac{\partial \overline{u}}{\partial x}, \frac{\partial \overline{u}}{\partial y}\right)\Bigg|_{\Gamma} = 0, \tag{1.10}$$

TABLE 2

x	$B_5^i(x)$	$B_5^{i'}(x)$	$B_5^{i''}(x)$	$B_5^{i^{\mathrm{III}}}(x)$	$B_5^{i^{\mathrm{IV}}}(x)$
x_{i-3}	0	0	0	0	0
x_{i-2}	$\frac{1}{120}$	$\frac{1}{24h}$	$\frac{1}{6h^2}$	$\frac{1}{2h^3}$	$\frac{1}{h^4}$
x_{i-1}	$\frac{26}{120}$	$\frac{10}{24h}$	$\frac{2}{6h^2}$	$-\frac{1}{h^3}$	$-\frac{4}{h^4}$
x_i	$\frac{66}{120}$	0	$-\frac{1}{h^2}$	0	$\frac{6}{h^4}$
x_{i+1}	$\frac{26}{120}$	$-\frac{10}{24h}$	$\frac{2}{6h^2}$	$\frac{1}{h^3}$	$-\frac{4}{h^4}$
x_{i+2}	$\frac{1}{120}$	$-\frac{1}{24h}$	$\frac{1}{6h^2}$	$-\frac{1}{2h^3}$	$\frac{1}{h^4}$
x_{i+3}	0	0	0	0	0

where $\overline{F}$ and $\overline{G}$ are linear vector functions; Γ is the boundary of the domain R. We will approximate the solution of the boundary-value problem (1.9), (1.10) along the Ox-axis. Let us introduce a partition $\Delta: x_0 < x_1 < \ldots < x_N$ on the interval $[x_0, x_N]$. Let the solution of the boundary-value problem have the form

$$\overline{u}(x, y) = \sum_{i=0}^{N} \overline{u}_i(y) * \overline{\psi}_i(x), \tag{1.11}$$

where $\overline{u}_i(y)$ are unknown vector functions; the components of the vector functions $\psi_i(x)$ are linear combinations of B-splines satisfying the boundary conditions (1.10) on the sides $x = x_0$ and $x = x_N$ of the rectangle R.

The symbol $\overline{a} * \overline{b}$ denotes a vector whose elements are products of the respective elements of the vectors $\overline{a}$ and $\overline{b}$. B-splines should be selected so that their degree is greater than the order of the highest derivative of the component of the solution $\overline{u}$ in the equations of system (1.9).

Substituting solution (1.11) into the system of equations (1.9) and requiring that its residual be equal to zero on the straight lines $x = \xi_k$ $(k = 0, 1, 2, \ldots, N)$ in the rectangle R that emerge from the collocation points (ξ_k, y_1) on the side $y = y_1$, we obtain a system of ordinary differential equations of high order:

$$\overline{F}\left(\xi_k,\ y,\ \sum_i \overline{u}_i(y) * \overline{\psi}(\xi_k),\quad \sum_i \overline{u}_i(y) * \frac{d\overline{\psi}_i(\xi)}{dx},\right.$$

$$\sum_i \frac{d\overline{u}_i(y)}{dy} * \overline{\psi}_i(\xi_k),\quad \sum_i \overline{u}_i(y) * \frac{d^2\overline{\psi}_i(\xi_k)}{dx^2},$$

$$\left. \sum_i \frac{d\overline{u}_i(y)}{dy} * \frac{d\overline{\psi}_i(\xi_k)}{dx},\quad \sum_i \frac{d^2\overline{u}_i(y)}{dy^2} * \overline{\psi}_i(\xi_k), \ldots \right) = 0. \tag{1.12}$$

With (1.11), the boundary conditions (1.10) at the points $(\xi_k, y_1), (\xi_k, y_2)\ (k = 0, 1, \ldots, N)$ on the sides $y = y_1$ and $y = y_2$ of the rectangle R become

$$\overline{G}\left(\xi_k, y_j, \sum_i \overline{u}_i(y_j) * \overline{\psi}_i(\xi_k), \sum_i \overline{u}_i(y_j) * \frac{d\overline{\psi}_i(\xi_k)}{dx}; \right.$$

$$\left. \sum_i \frac{d\overline{u}_i(y_j)}{dy} * \overline{\psi}_i(\xi_k), \ldots \right) = 0 \quad (j = 1, 2, k = 0, 1, \ldots, N). \tag{1.13}$$

The one-dimensional boundary-value problem (1.12), (1.13) can be solved, for example, with the discrete-orthogonalization method. To this end, we represent the problem in Cauchy's normal form. One of the important stages of approximation is to set up a combination of vector functions $\overline{\psi}_i(x)$ satisfying given boundary conditions.

Some boundary conditions and associated linear combinations of cubic *B*-splines have been given above. In what follows, we will also use quintic *B*-splines. For simplicity, we assume that the solution of the boundary-value problem is a scalar function $u(x, y)$.

Let us set up linear combinations of quintic *B*-splines for some boundary conditions on the sides $x = \text{const}$ of the rectangle *R*. To this end, we will use the values of $B_5^i(x)$ at the knots of the partition Δ from Table 2 and the properties of *B*-splines. Consider the following boundary conditions:

$$u(x_0, y_j) = \frac{\partial u(x_0, y_j)}{\partial x} = u(x_N, y_j) = \frac{\partial u(x_N, y_j)}{\partial x} = 0,$$

$$\psi_0(x) = \frac{165}{4} B_5^{-2}(x) - \frac{33}{8} B_5^{-1}(x) + B_5^0(x), \qquad \psi_1(x) = B_5^{-1}(x) - \frac{26}{33} B_5^0(x) + B_5^1(x),$$

$$\psi_2(x) = B_5^{-2}(x) - \frac{1}{33} B_5^0(x) + B_5^2(x), \qquad \psi_i(x) = B_5^i(x) \quad (i = 3, 4, \ldots, N-3),$$

$$\psi_{N-2}(x) = B_5^{N-2}(x) - \frac{1}{33} B_5^N(x) + B_5^{N+2}(x), \qquad \psi_{N-1}(x) = B_5^{N-1}(x) - \frac{26}{33} B_5^N(x) + B_5^{N+1}(x),$$

$$\psi_N(x) = B_5^N(x) - \frac{33}{8} B_5^{N+1}(x) + \frac{164}{4} B_5^{N+2}(x), \tag{1.14}$$

$$u_0(x_0, y_j) = \frac{\partial^2 u(x_0, y_j)}{\partial x^2} = u(x_N, y_j) = \frac{\partial^2 u(x_N, y_j)}{\partial x^2} = 0,$$

$$\psi_0(x) = 12 B_5^{-2}(x) - 3 B_5^{-1}(x) + B_5^0(x), \qquad \psi_1(x) = -B_5^{-1}(x) + B_5^1(x),$$

$$\psi_2(x) = -B_5^{-2}(x) + B_5^2(x), \qquad \psi_i(x) = B_5^i(x) (i = 3, 4, \ldots, N-3),$$

$$\psi_{N-2}(x) = B_5^{N-2}(x) - B_5^{N+2}(x), \qquad \psi_{N-1}(x) = B_5^{N-1}(x) - B_5^{N+1}(x),$$

$$\psi_N(x) = B_5^N(x) - 3 B_5^{N+1}(x) + 12 B_5^{N+2}(x), \tag{1.15}$$

$$\frac{\partial u(x_0, y_j)}{\partial x} = \frac{\partial^3 u(x_0, y_j)}{\partial x^3} = \frac{\partial u(x_N, y_j)}{\partial x} = \frac{\partial^3 u(x_N, y_j)}{\partial x^3} = 0,$$

$$\psi_0(x) = B_5^0(x), \qquad \psi_1(x) = B_5^{-1}(x) + B_5^1(x), \qquad \psi_2(x) = B_5^{-2}(x) + B_5^2(x),$$

$$\psi_i(x) = B_5^i(x) (i = 3, 4, \ldots, N-3), \qquad \psi_{N-2}(x) = B_5^{N-2}(x) + B_5^{N+2}(x),$$

$$\psi_{N-1}(x) = B_5^{N-1}(x) + B_5^{N+1}(x), \qquad \psi_N(x) = B_5^N(x). \tag{1.16}$$

Combining these conditions on the sides $x = \text{const}$ of the rectangle, we can increase the number of possible boundary conditions.

Discrete-Orthogonalization Method. Consider the linear boundary-value problem

$$\frac{d\bar{g}}{dt} = A(t)\bar{g}(t) + \bar{f}(t) (a \le t \le b) \tag{1.17}$$

with the boundary conditions

$$B_1\bar{g}(a) = \bar{b}_1, \tag{1.18}$$

$$B_2\bar{g}(b) = \bar{b}_2, \tag{1.19}$$

where $\bar{g} = \{g_1, g_2, \ldots, g_n\}^T$ is a column vector; $\bar{f}$ is the column vector of the right-hand side; $A(t)$ is a given square matrix of order n; B_1 and B_2 are given rectangular matrices of orders $k \times n$ and $(n-k) \times n\ (k < n)$, respectively; $\bar{b}_1$ and $\bar{b}_2$ are given vectors.

The solution of the boundary-value problem (1.17)–(1.19) is represented as

$$\bar{g}(t) = \sum_{j=1}^{m} C_j \bar{g}_j(t) + \bar{g}_{m+1}(t), \tag{1.20}$$

where $m = \min\{k, n-k\}$ (let $m = n-k$ for definiteness); $\bar{g}_j$ are the solutions of Cauchy problems for the system of equations (1.17) for $\bar{f} = 0$ with initial conditions satisfying the boundary conditions at the left endpoint of interval (1.18) for $\bar{b}_1 = 0$; $\bar{g}_{m+1}$ is the solution of the Cauchy problem for system (1.17) with initial conditions satisfying the boundary conditions (1.19); m is the number of boundary conditions at the right endpoint of the interval of integration.

The discrete-orthogonalization method makes it possible to run a stable computational process owing to the orthogonalization of vector solutions of the Cauchy problem at a finite number of points of the interval of variation in the argument. Let us partition the interval $[a, b]$ with points of integration $t_s\ (s = 0, 1, \ldots, N)$ so that $t_0 = a$ and $t_N = b$. Among these points we choose points of orthogonalization $T_i\ (i = 0, 1, \ldots, M)$. These points are usually selected so as to ensure the required accuracy of the solution of the problem.

Let the solutions $\bar{u}_r(T_i)\ (r = 1, 2, \ldots, m+1)$ of the Cauchy problems at the point T_i have been found with some numerical method, say, the Runge–Kutta method.

Thus, we have the following vectors at the point T_i before orthogonalization:

$$\bar{u}_1(T_i), \quad \bar{u}_2(T_i), \ldots, \quad \bar{u}_m(T_i), \quad \bar{u}_{m+1}(T_i). \tag{1.21}$$

Let us orthonormalize the vectors $\bar{u}_j(T_j)\ (j = 1, 2, \ldots, m)$ at the point T_i and denote them by $\bar{z}_1(T_i), \bar{z}_2(T_i), \ldots, \bar{z}_m(T_i)$. The vectors $\bar{z}_i$ are expressed in terms of the vectors $\bar{u}_i$ as

$$\bar{z}_r = \frac{1}{w_{rr}}\left(\bar{u}_r - \sum_{j=1}^{r-1} w_{rj}\,\bar{z}_j\right) \quad (r = 1, 2, \ldots, m)$$

$$\left(w_{rj} = (\bar{u}_r, \bar{z}_j)\ (j < r), w_{rr} = \sqrt{(\bar{u}_r, \bar{z}_r) - \sum_{j=1}^{r-1} w_{rj}^2}\right). \tag{1.22}$$

The vector $\bar{z}_{m+1}$ is not normalized and is calculated with the formula

$$\bar{z}_{m+1} = \bar{u}_{m+1} - \sum_{j=1}^{m} w_{m+1,j}\,\bar{z}_j. \tag{1.23}$$

Using (4.7) and (4.8) at $t = T_i$, we get

$$w_{11}\bar{z}_1 = \bar{u}_1, \quad w_{22}\bar{z}_2 = \bar{u}_2 - w_{21}\bar{z}_1, \quad w_{33}\bar{z}_3 = \bar{u}_3 - w_{31}\bar{z}_1 - w_{32}\bar{z}_2,$$

.....

$$w_{mm}\bar{z}_m = \bar{u}_m - w_{m1}\bar{z}_1 - w_{m2}\bar{z}_2 - \ldots - w_{m,m-1}\bar{z}_{m-1},$$

$$\bar{z}_{m+1} = \bar{u}_{m+1} - w_{m+1,1}\bar{z}_1 - w_{m+1,2}\bar{z}_2 - \ldots - w_{m+1,m-1}\bar{z}_{m-1} - w_{m+1,m}\bar{z}_m.$$

Performing transformations, we obtain the matrix equality

$$\begin{vmatrix} \bar{u}_1(T_i) \\ \bar{u}_2(T_i) \\ \cdot \\ \cdot \\ \cdot \\ \bar{u}_m(T_i) \\ \bar{u}_{m+1}(T_i) \end{vmatrix} = \Omega_i \begin{vmatrix} \bar{z}_1(T_i) \\ \bar{z}_2(T_i) \\ \cdot \\ \cdot \\ \cdot \\ \bar{z}_m(T_i) \\ \bar{z}_{m+1}(T_i) \end{vmatrix},$$

$$\left(\Omega_i = \Omega(T_i) = \begin{vmatrix} w_{11}(T_i) & 0 & 0 & \ldots & 0 \\ w_{21}(T_i) & w_{22}(T_i) & 0 & \ldots & 0 \\ w_{31}(T_i) & w_{32}(T_i) & w_{33}(T_i) & \ldots & 0 \\ \ldots & \ldots & \ldots & \ldots & \cdot \\ w_{m1}(T_i) & w_{m2}(T_i) & w_{m_3}(T_i) & \ldots & 0 \\ w_{m+1,1}(T_i) & w_{m+1,2}(T_i) & w_{m+1,3}(T_i) & \ldots & 1 \end{vmatrix} \right). \tag{1.24}$$

The vectors $\bar{z}_r(T_i)$ are the initial values of the Cauchy problems for homogeneous $(r = 1, 2, \ldots, m)$ and inhomogeneous $(r = m+1)$ systems of differential equations (1.17) on the interval $T_i \le t \le T_{i+1}$.

At each orthogonalization point T_i, the solution of the system of equations (1.17) satisfying the boundary conditions at the left endpoint of interval (1.18) can be represented by two expressions:

$$\bar{g}(T_i) = \sum_{j=1}^{m} C_j^{(i-1)} \bar{u}_j(T_i) + \bar{u}_{m+1}(T_i) \text{ (before orthogonalization)}$$

and

$$\bar{g}(T_i) = \sum_{j=1}^{m} C_j^{(i)} \bar{z}_j(T_i) + \bar{z}_{m+1}(T_i) \text{ (after orthogonalization).}$$

The solution of the system of equations (1.17) in the interval $T_i \le t \le T_{i+1}$ can be represented as

$$\bar{g}(t) = \sum_{j=1}^{m} C_j^{(i)} \bar{z}_j(t) + \bar{z}_{m+1}(t).$$

After integration on the last interval $T_{M-1} \le t \le T_M$ and orthogonalization at the point T_M, we get

$$\bar{g}(T_M) = \sum_{j=1}^{m} C_j^{(M)} \bar{z}_j(T_M) + \bar{z}_{m+1}(T_M). \tag{1.25}$$

Satisfying the boundary conditions at the right endpoint of the interval of integration, i.e., substituting (1.25) into (1.19), we obtain a system of m linear algebraic equations for the unknowns $C_j^{(M)}$ $(j = 1, 2, \ldots, m)$. After $C_j^{(M)}$ is found, the solution of

the boundary-value problem (1.17)–(1.19) at the point $t = T_M$ is given by (1.25). This completes the forward elimination part of solution.

The back substitution part of solution involves the determination of the constants $C_j^{(i-1)}$ from the constants $C_j^{(i)}$ $(j = 1, 2, \ldots, m)$ beginning with $i = M$.

To this end, we equate

$$\sum_{j=1}^{m} C_j^{(i-1)} \bar{u}_j(T_i) + \bar{u}_{m+1}(T_i) = \sum_{j=1}^{m} C_j^{(i-1)} \bar{z}_j(T_i) + \bar{z}_{m+1}(T_i). \tag{1.26}$$

Replacing $\bar{u}_j$ with (1.24) at $t = T_i$, we get

$$C_1^{(i-1)} w_{11} \bar{z}_1 + C_2^{(i-1)} (w_{21} \bar{z}_1 + w_{22} \bar{z}_2) + C_3^{(i-1)} (w_{31} \bar{z}_1 + w_{32} \bar{z}_2 + w_{33} \bar{z}_3) + \ldots$$

$$\ldots + C_m^{(i-1)} (w_{m1} \bar{z}_1 + w_{m2} \bar{z}_2 + \ldots + w_{mm} \bar{z}_m)$$

$$+ (w_{m+1_{,1}} \bar{z}_1 + w_{m+1,2} \bar{z}_2 + \ldots + w_{m+1,m} \bar{z}_m + \bar{z}_{m+1}) = C_1^{(i)} \bar{z}_1 + C_2^{(i)} \bar{z}_2 + \ldots + C_m^{(i)} \bar{z}_m + \bar{z}_{m+1}.$$

Equating the coefficients of the vectors $\bar{z}_j$ $(j = 1, 2, \ldots, m)$, we find

$$\Omega_i' \bar{C}^{(i-1)} = \bar{C}^{(i)} (i = 1, 2, \ldots, M) \quad \text{or} \quad \bar{C}^{(i-1)} = [\Omega_i']^{-1} \bar{C}^{(i)}, \tag{1.27}$$

where Ω_i' is a transposed matrix; $\bar{C}^{(i)}$ is a column vector with elements $C_1^{(i)}$, $C_2^{(i)}, \ldots, C_m^{(i)}, 1$.

Thus, equalities (1.27) can be used to determined the constants $C_j^{(i)}$ at all points, beginning with $i = M$. Next we can find the solutions $\bar{g}(T_i)$ of the boundary-value problem.

2. Stress–Strain State of Orthotropic Shallow Shells (Classical Formulation). Due to the wide use of composite materials, not only isotropic shallow shells [5] but also orthotropic shells [2] are used as structural members.

In what follows, we will outline an approach to solving two-dimensional problems of the statics of orthotropic shallow shells [27] that employs spline-approximation to reduce them to one-dimensional problems that can be solved numerically with the discrete-orthogonalization method. Such an approach was used in [81–83] to solve problems in the theory of plates and shells.

To describe the deformation of shallow orthotropic shells with rectangular planform, we will use the equations of the Donnell–Mushtari–Vlasov theory of shells:

the kinematic equations

$$\varepsilon_1 = \frac{\partial u}{\partial x} + \frac{w}{R_1}, \quad \varepsilon_2 = \frac{\partial \nu}{\partial y} + \frac{w}{R_2}, \quad \varepsilon_{12} = \frac{\partial u}{\partial y} + \frac{\partial \nu}{\partial x},$$

$$\kappa_1 = -\frac{\partial^2 w}{\partial x^2}, \quad \kappa_2 = \frac{\partial^2 w}{\partial y^2}, \quad \kappa_{12} = -\frac{\partial^2 w}{\partial x \partial y}, \tag{2.1}$$

the equilibrium equations

$$\frac{\partial N_1}{\partial x} + \frac{\partial S}{\partial y} = 0, \quad \frac{\partial N_2}{\partial y} + \frac{\partial S}{\partial x} = 0,$$

$$\frac{\partial M_1}{\partial x} + \frac{\partial H}{\partial y} = Q_1, \quad \frac{\partial M_2}{\partial y} + \frac{\partial H}{\partial x} = Q_2,$$

$$\frac{\partial Q_1}{\partial x}+\frac{\partial Q_2}{\partial y}-\frac{1}{R_1}N_1-\frac{1}{R_2}N_2+q=0, \tag{2.2}$$

the constitutive equations

$$\begin{gathered}
N_1=C_{11}\varepsilon_1+C_{12}\varepsilon_2, \quad N_2=C_{12}\varepsilon_1+C_{22}\varepsilon_2, \quad S=C_{66}\varepsilon_{12}, \\
M_1=D_{11}\kappa_1+D_{12}\kappa_2, \quad M_2=D_{12}\kappa_1+D_{22}\kappa_2, \quad H=2C_{66}\kappa_{12}, \\
C_{11}=\frac{E_1h}{1-\nu_1\nu_2}, \quad C_{12}=\frac{\nu_1E_2h}{1-\nu_1\nu_2}=\frac{\nu_2E_1h}{1-\nu_1\nu_2}, \quad C_{22}=\frac{E_2h}{1-\nu_1\nu_2}, \quad C_{66}=G_{12}h,
\end{gathered} \tag{2.3}$$

$$D_{11}=\frac{E_1h^3}{12(1-\nu_1\nu_2)}, \quad D_{12}=\frac{\nu_1E_2h^3}{12(1-\nu_1\nu_2)}=\frac{\nu_2E_1h^3}{12(1-\nu_1\nu_2)},$$

$$D_{22}=\frac{E_2h^3}{12(1-\nu_1\nu_2)}, \quad D_{66}=G_{12}\frac{h^3}{12}, \tag{2.4}$$

where x and y are coordinates ($0\le x\le a$, $0\le y\le b$); u,ν,w are the displacements along the coordinate axes and along the normal to the coordinate plane; $\varepsilon_1,\varepsilon_2,\varepsilon_{12},\kappa_1,\kappa_2,\kappa_{12}$ are the tangential and flexural strains; $N_1,N_2,S,Q_1,Q_2,M_1,M_2,H$ are forces and moments; $E_1,E_2,G_{12},\nu_1,\nu_2$ are the elastic and shear moduli and Poisson's ratios; R_1 and R_2 are the radii of curvature in two directions; $h=h(x,y)$ is the thickness of the shell.

Eliminating Q_1 and Q_2 from Eqs. (2.2), expressing the forces and moments in Eqs. (2.3) in terms of the displacements using (2.1), and substituting them into Eqs. (2.2), we obtain three governing differential equations for the displacements:

$$\begin{gathered}
C_{11}\frac{\partial^2u}{\partial x^2}+C_{66}\frac{\partial^2u}{\partial y^2}+(C_{12}+C_{66})\frac{\partial^2\nu}{\partial x\partial y}+\frac{\partial C_{11}}{\partial x}\frac{\partial u}{\partial x}+\frac{\partial C_{66}}{\partial y}\frac{\partial u}{\partial y} \\
+\frac{\partial C_{66}}{\partial y}\frac{\partial \nu}{\partial x}+\frac{\partial C_{12}}{\partial x}\frac{\partial \nu}{\partial \nu}+\frac{\partial}{\partial x}\left(\frac{C_{11}}{R_1}+\frac{C_{12}}{R_2}\right)w+\left(\frac{C_{11}}{R_1}+\frac{C_{12}}{R_2}\right)\frac{\partial w}{\partial x}=0, \\
C_{22}=\frac{\partial^2\nu}{\partial y^2}+C_{66}\frac{\partial^2\nu}{\partial x^2}+(C_{12}+C_{66})\frac{\partial^2u}{\partial x\partial y}+\frac{\partial C_{22}}{\partial y}\frac{\partial \nu}{\partial y}+\frac{\partial C_{66}}{\partial x}\frac{\partial \nu}{\partial x} \\
+\frac{\partial C_{66}}{\partial x}\frac{\partial u}{\partial y}+\frac{\partial C_{12}}{\partial y}\frac{\partial u}{\partial x}+\frac{\partial}{\partial y}\left(\frac{C_{12}}{R_1}+\frac{C_{22}}{R_2}\right)w+\left(\frac{C_{12}}{R_1}+\frac{C_{22}}{R_2}\right)\frac{\partial w}{\partial y}=0, \\
D_{11}=2\frac{\partial^4w}{\partial x^4}+D_{22}\frac{\partial^4w}{\partial y^4}+(2D_{12}+4D_{66})\frac{\partial^4w}{\partial x^2\partial y^2}+2\frac{\partial D_{11}\partial^3w}{\partial x\ \partial x^3}+2\frac{\partial D_{22}\partial^3w}{\partial y\ \partial y^3} \\
+\left(2\frac{\partial D_{12}}{\partial y}+4\frac{\partial D_{66}}{\partial y}\right)\frac{\partial^3w}{\partial x^2\partial y}+\left(2\frac{\partial D_{12}}{\partial x}+4\frac{\partial D_{66}}{\partial x}\right)\frac{\partial^3w}{\partial x\partial y^2}+\left(\frac{\partial^2D_{11}}{\partial x^2}+\frac{\partial D_{12}}{\partial y^2}\right)\frac{\partial^2w}{\partial x^2} \\
+\left(\frac{\partial^2D_{12}}{\partial x^2}+4\frac{\partial^2D_{22}}{\partial y^2}\right)\frac{\partial^2w}{\partial y^2}+4\frac{\partial^2D_{66}}{\partial x\partial y}\cdot\frac{\partial^2w}{\partial x\partial y}+\frac{C_{11}}{R_1}\cdot\frac{\partial u}{\partial x}+\frac{C_{12}}{R_1}\cdot\frac{\partial \nu}{\partial y}+\frac{1}{R_1}\left(\frac{C_{11}}{R_1}+\frac{C_{12}}{R_2}\right)w \\
\frac{C_{12}}{R_2}\cdot\frac{\partial u}{\partial x}+\frac{C_{22}}{R_2}\cdot\frac{\partial \nu}{\partial y}+\frac{1}{R_1}\left(\frac{C_{12}}{R_1}+\frac{C_{22}}{R_2}\right)w-q_z=0.
\end{gathered} \tag{2.5}$$

Boundary conditions, which can be expressed in terms of displacements, are set on the boundaries $x = \text{const}$ and $y = \text{const}$ of the shell. Resolve the system of equations (2.5) for the derivatives $\frac{\partial^2 u}{\partial x^2}, \frac{\partial^2 \nu}{\partial x^2}, \frac{\partial^4 \omega}{\partial x^4}$.

The solution of the boundary-value problem for the system of differential equations (2.5) can be represented as

$$u(x, y) = \sum_{i=0}^{N} u_i(x)\varphi_i(y),$$

$$\nu(x, y) = \sum_{i=0}^{N} \nu_i(x)\varphi_i(y),$$

$$w(x, y) = \sum_{i=0}^{N} w_i(x)\psi_i(y), \tag{2.6}$$

where u_i, ν_i, w_i $(i = \overline{0, N})$ are unknown functions of the variable x; φ_i and ψ_i $(\overline{0, N})$, $N \geq 6$, are functions set up using cubic and quintic B-splines, respectively, that allow composing linear combinations so as to satisfy various boundarie conditions on the boundaries $y = 0$ and $y = b$ of the shell.

Composing functions $\varphi_i(y)$ and $\psi_i(y)$ as linear combinations of B-splines that satisfy certain boundary conditions on $y = 0$ and $y = b$, substituting expressions (2.6) into the governing equations (2.5), and requiring them to be satisfied at the collocation points y_k $(k = \overline{0, N})$, we obtain a system of $3(N + 1)$ equations. The boundary conditions on the boundaries $x = 0$ and $x = a$ are dealt with in a similar way. The resulting system of ordinary differential equations and the boundary conditions constitute a two-point boundary-value problem on the interval $0 \leq x \leq a$.

If

$$\overline{Y} = \{\bar{y}_1, \bar{y}_2, \ldots, \bar{y}_8, \}^T = \{\bar{u}, \bar{u}', \bar{\nu}, \bar{\nu}', \bar{w}, \bar{w}', \bar{w}'', \bar{w}'''\}^T, \tag{2.7}$$

where $\bar{y}_m = \{\bar{y}_{m_0}, \bar{y}_{m_1}, \ldots, \bar{y}_{m_N}\}^T$ $(m = \overline{1, 8})$, then the boundary-value problem can be represented in the form

$$\frac{d\overline{Y}}{dx} = A(x)\overline{Y} + \bar{f}(x) \quad (0 \leq x \leq a), \tag{2.8}$$

$$B_1\overline{Y}(0) = \bar{b}_1, \quad B_2\overline{Y}(0) = \bar{b}_2. \tag{2.9}$$

To solve the boundary-value problem for the system of equations (2.8) with the boundary conditions (2.9), we use the stable numerical discrete-orthogonalization method. Substituting the functions $u_i(x)$, $\nu_i(x)$, $w_i(x)$ $(i = \overline{0, N})$ into (2.6), we find the solution of the original problem for displacements and then use them to determine the stress–strain state of the shell.

Let us discuss solutions to some problems obtained with this approach. Consider orthotropic shallow shells made of materials with five different sets of elastic constants. Assume that the elastic modulus E_x is constant ($E_x = E = \text{const}$), while the elastic modulus $E_y = \mu E$, the shear modulus $G_{xy} = \lambda E$, and Poisson's ratio ν_x are variable. The sets of elastic constants of the shell material are as follows [2]:

(i) $\mu = 2, \quad \lambda = 0.3, \quad \nu_x = 0.075,$

(ii) $\mu = 1.35, \quad \lambda = 0.215, \quad \nu_x = 0.122,$

(iii) $\mu = 1, \quad \lambda = 0.385, \quad \nu_x = 0.3,$

(iv) $\mu = 0.741, \quad \lambda = 0.159, \quad \nu_x = 0.165,$

(v) $\mu = 0.5, \quad \lambda = 0.125, \quad \nu_x = 0.15.$ (2.10)

Set (iii) represents the isotropic case. The input data are: $a = 12$, $b = 10$, $h = 0.4$, $R_1 = 22.9$, $R_2 = 13$.

TABLE 3

y	$\omega / \frac{E}{q_0}$				
	1	2	3	4	5
	$x = 6$				
0	0	0	0	0	0
1	40.0	56.7	65.3	98.2	141.7
2	120.9	169.0	188.0	282.0	394.4
3	202.6	279.7	301.9	452.0	614.9
4	259.9	353.9	376.3	562.7	751.1
5	280.2	382.6	401.6	600.4	795.8
x	$y = 5$				
0.0	0	0	0	0	0
1.2	89.5	105.1	102.4	133.8	156.6
2.4	201.9	251.2	250.4	344.9	422.4
3.6	259.7	339.3	346.7	398.5	635.6
4.8	277.5	374.6	390.2	577.5	757.6

Consider an orthotropic shell with the above geometrical parameters under a uniform transverse surface load $q_z = q_0 = \text{const}$. All the four sides of the shell are clamped:

$$u = \nu = w = \frac{\partial w}{\partial x} = 0 \quad \text{at} \quad x = 0 \text{ and } x = a,$$

$$u = \nu = w = \frac{\partial w}{\partial y} = 0 \quad \text{at} \quad y = 0 \text{ and } y = b. \tag{2.11}$$

Table 3 summarizes the deflections of the shell for $x = 6,\ 0 \le y \le 5$ and $y = 5,\ 0 \le x \le 6$ for the five sets of material constants (2.10). It can be seen that with decrease in the elastic modulus E_y, the deflection at the center ($x = 6,\ y = 5$) of the shell increases by a factor of 1.3, 1.4, 2.1, 2.8 compared with the deflection of the shell with the first set of elastic constants.

Figures 4 and 5 show the variation of the stresses σ_x^+, σ_x^-, σ_y^+, σ_y^- along the *OX*-axis for $y = 5$ and along the *OY*-axis for $x = 6$, respectively, for the fifth set of elastic constants. The stress σ_x^- is maximum on the short sides of the shell. Figure 6 shows the distribution of the maximum stress σ_x^- for the five sets of elastic constants (indicated by numerals). As the elastic modulus E_y decreases, the maximum stress σ_x^- increases by a factor of 1.16, 1.24, 1.44, and 1.64.

3. Statics of Noncircular Cylindrical Shells of Complex Shape (Classical Formulation). Along with circular cylindrical shells, it is of great interest to analyze the stress–strain state of noncircular cylindrical shells of low and high eccentricity, which are widely used in aerospace and mechanical engineering applications [100].

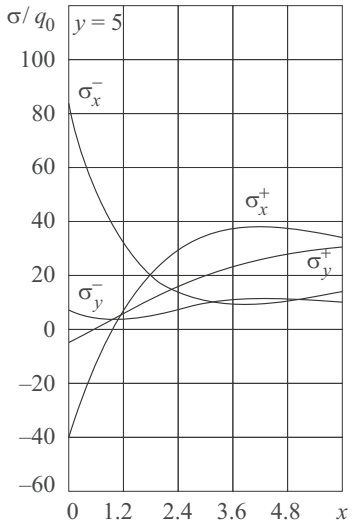

Fig. 4

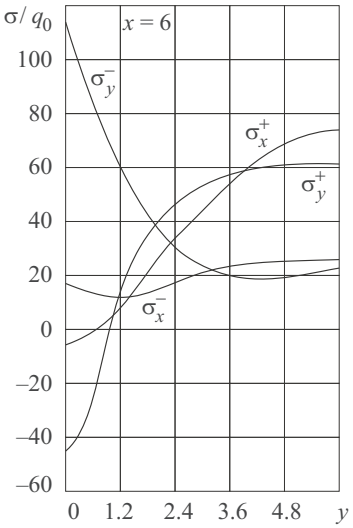

Fig. 5

In this connection, there is a need for effective methods of solving boundary-value problems for such shells, including problems for cylindrical shells whose cross-section is described analytically. Such problems include static problems for elliptic and corrugated cylindrical shells [77–79, 92–95].

In what follows, we will outline an approach to solving more complicated problems for corrugated elliptic cylindrical shells. We start with the equations of the Donnell–Mushtari–Vlasov theory of shells.

1. The first quadratic form for the mid-surface of a noncircular cylindrical shell is given by

$$dS^2 = ds^2 + \gamma^2(\theta)d\theta^2, \quad \gamma d\theta = dt, \tag{3.1}$$

where s is the longitudinal coordinate; θ is the azimuth angle; t is the circumferential coordinate; $\gamma(\theta)$ is the transformation coefficient between t and θ.

In polar coordinates, the directrix of the mid-surface (Fig. 7) is defined by

$$r(\theta) = \frac{a}{(1-e^2\cos^2\theta)^{1/2}} + \alpha\cos k\theta \quad (0 \le \theta \le 2\pi), \tag{3.2}$$

$$e = \sqrt{1-(a/b)^2} = 2\sqrt{\Delta}/(1+\Delta) \quad (\Delta = (b-a)/(b+a)), \tag{3.3}$$

where a, b, e are the semi-axes and eccentricity ($a < b$); α is the corrugation amplitude; k is the number of corrugations; the point O ($r = 0$) is at the intersection of the ellipse axes. Curve (3.2) describes an ellipse when $\alpha = 0$ and a wavy circle when $a = b$.

In the chosen polar coordinate system, the cross-sectional radius of curvature is defined by

$$R_\theta = R(\theta) = \frac{[r^2 + (r')^2]^{3/2}}{r^2 + 2(r')^2 - rr''}, \qquad r' = -\left[\frac{ae^2\sin 2\theta}{2(1-e^2\cos^2\theta)^{3/2}} + \alpha k\sin k\theta\right],$$

$$r'' = -\left\{\frac{ae^2}{2}\left[\frac{2\cos 2\theta}{(1-e^2\cos^2\theta)^{3/2}} - \frac{3e^2\sin^2\theta}{2(1-e^2\cos^2\theta)^{5/2}}\right] + \alpha k^2\cos k\theta\right\}. \tag{3.4}$$

The governing system of partial differential equations in coordinates s and θ is

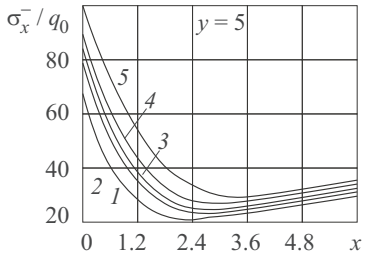

Fig. 6

$$\frac{\partial^2 u}{\partial \theta^2} = a_{11}\frac{\partial^2 u}{\partial s^2} + a_{12}\frac{\partial u}{\partial s} + a_{13}\frac{\partial u}{\partial \theta} + a_{14}\frac{\partial \nu}{\partial s} + a_{15}\frac{\partial^2 \nu}{\partial s \partial \theta} + a_{16}\frac{\partial \nu}{\partial \theta} + a_{17}w + a_{18}\frac{\partial w}{\partial s},$$

$$\frac{\partial^2 \nu}{\partial \theta^2} = a_{21}\frac{\partial u}{\partial s} + a_{22}\frac{\partial u}{\partial \theta} + a_{23}\frac{\partial^2 u}{\partial s \partial \theta} + a_{24}\frac{\partial^2 \nu}{\partial s^2} + a_{25}\frac{\partial v}{\partial s} + a_{26}\frac{\partial v}{\partial \theta} + a_{27}w + a_{28}\frac{\partial w}{\partial \theta},$$

$$\frac{\partial^4 w}{\partial \theta^4} = a_{31}\frac{\partial u}{\partial} + a_{32}\frac{\partial v}{\partial \theta} + a_{33}w + a_{34}\frac{\partial^2 w}{\partial s^2} + a_{35}\frac{\partial^3 w}{\partial s^3} + a_{36}\frac{\partial^4 w}{\partial s^4} + a_{37}\frac{\partial^2 w}{\partial s \partial \theta}$$

$$+ a_{38}\frac{\partial^3 w}{\partial s^2 \partial \theta} + a_{39}\frac{\partial w}{\partial \theta} + a_{3,10}\frac{\partial^3 w}{\partial s \partial \theta^2} + a_{3,11}\frac{\partial^4 w}{\partial s^2 \partial \theta^2} + a_{3,12}\frac{\partial^2 w}{\partial \theta^2} + a_{3,13}\frac{\partial^3 w}{\partial \theta^3} + b_1, \tag{3.5}$$

where u, v, w are the longitudinal, circumferential, and normal displacements of the mid-surface; the coefficients a_{ij} and b_1 can be found in [79].

The ends $s = 0$ and $s = l$ of the shell are clamped:

$$u = v = w = \vartheta_s = 0 \quad \text{at} \quad s = 0, l, \tag{3.6}$$

where ϑ_s is the angle of rotation of the normal.

The boundary-value problem is solved using spline-approximation with respect to the longitudinal coordinate to reduce it to a one-dimensional problem whose solution with respect to the circumferential coordinate is found using the stable numerical discrete-orthogonalization method.

The solution of the boundary-value problem (3.5), (3.6) is represented as

$$u(s,\theta) = \sum_{i=0}^{N} u_i(\theta)\psi_{1i}(s),$$

$$v(s,\theta) = \sum_{i=0}^{N} v_i(\theta)\psi_{2i}(s),$$

$$w(s,\theta) = \sum_{i=0}^{N} w_i(\theta)\psi_{3i}(s), \tag{3.7}$$

where $u_i(\theta), v_i(\theta), w_i(\theta)\,(i = \overline{0,N})$ are unknown functions; $\psi_{ni}(s)\ (n = 1, 2, 3)$ are linear combinations of cubic (for $n = 1, 2$) and quintic (for $n = 3$) B-splines such that certain boundary conditions can be satisfied exactly. Satisfying the boundary conditions (3.6), we derive the following expressions for the B-splines in (3.7):

$$\psi_{10}(s) = -4B_3^{-1}(s) + B_3^0(s), \qquad \psi_{11}(s) = B_3^{-1}(s) - 0.5B_3^0(s) + B_3^1(s),$$

$$\psi_{1j}(s) = B_3^j(s) \quad (j = \overline{2, N-2}), \qquad \psi_{1N-1}(s) = B_3^{N+1}(s) - 0.5B_3^N(s) + B_3^{N-1}(s),$$

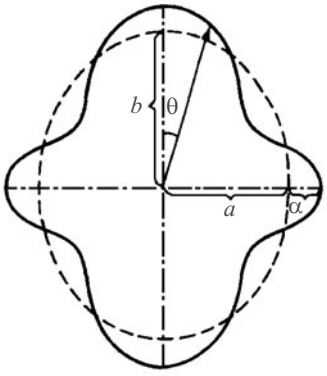

Fig. 7

$$\psi_{1N}(s)=-4B_3^{N+1}(s)+B_3^N(s),\qquad \psi_{20}(s)=-4B_3^{-1}(s)+B_3^0(s),$$

$$\psi_{21}(s)=B_3^{-1}(s)-0.5B_3^0(s)+B_3^1(s),\qquad \psi_{2j}(s)=B_3^j(s)\quad (j=\overline{2,N-2}),$$

$$\psi_{2N-1}(s)=B_3^{N+1}(s)-0.5B_3^N(s)+B_3^{N-1}(s),\qquad \psi_{2N}(s)=-4B_3^{N+1}(s)+B_3^N(s),$$

$$\psi_{30}(s)=\frac{165}{4}B_5^{-2}(s)-\frac{33}{8}B_5^{-1}(s)+B_5^0(s),\qquad \psi_{31}(s)=B_5^{-1}(s)-\frac{26}{33}B_5^0(s)+B_5^1(s),$$

$$\psi_{32}(s)=B_5^{-2}(s)-\frac{1}{33}B_5^0(s)+B_5^2(s),\qquad \psi_{3i}(s)=B_5^i(s)\quad (i=\overline{3,N-3}),$$

$$\psi_{3,N-2}(s)=B_5^{N+2}(s)-\frac{1}{33}B_5^N(s)+B_5^{N-2}(s),\qquad \psi_{3,N-1}(s)=B_5^{N+1}(s)-\frac{26}{33}B_5^N(s)+B_5^{N-1}(s),$$

$$\psi_{3,N}(s)=\frac{165}{4}B_5^{N+2}(s)-\frac{33}{8}B_5^{N+1}(s)+B_5^N(s), \tag{3.8}$$

where B_3^j $(j=\overline{-1,N+1})$ are cubic B-splines; B_5^j $(j=\overline{-2,N+2})$ are quintic splines over a uniform partition.

Substituting (3.7) into the differential equations (3.5), requiring them to be satisfied at the collocation points $s=s_m$ $(m=\overline{0,N})$, i.e., in $N+1$ sections, and performing some transformations, we obtain the following system of ordinary differential equations:

$$\frac{d\overline{U}}{d\theta}=A(\theta)\overline{U}+\bar{f}(\theta)\quad (0\le\theta\le 2\pi) \tag{3.9}$$

$$\left(\overline{U}=\{\overline{u},\overline{u}',\overline{v},\overline{v}',\overline{w},\overline{w}',\overline{w}'',\overline{w}'''\}^T=\{\overline{u}_1,\overline{u}_2,\overline{u}_3,\overline{u}_4,\overline{u}_5,\overline{u}_6,\overline{u}_7,\overline{u}_8\}^T,\ \overline{u}_p=\{u_{p_0},u_{p_1},\dots u_{p_N}\}^T,\ p=\overline{1,8}\right).$$

Periodicity or symmetry conditions are formulated if the shell is circumferentially closed, and boundary conditions at the rectilinear edges are prescribed if the shell is circumferentially open.

The boundary-value problem for the system of equations (3.9) with appropriate conditions for θ is solved using the discrete-orthogonalization method. Substituting the functions $u_i(\theta), v_i(\theta), w_i(\theta)$ $(i=\overline{0,N})$ into (3.7), we obtain the solution of the initial–boundary-value problem for displacements and then use them to determine the stress–strain state of the shell.

2. This approach was used to analyze the stress–strain state of corrugated cylindrical shells with elliptical cross-section depending on degree of ellipticity, corrugation parameters, and thickness.

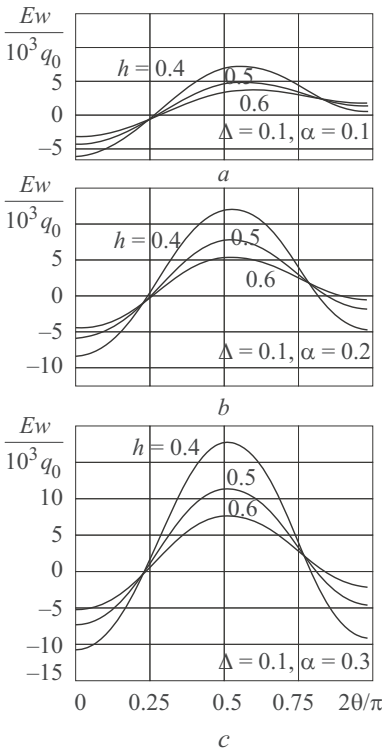

Fig. 8

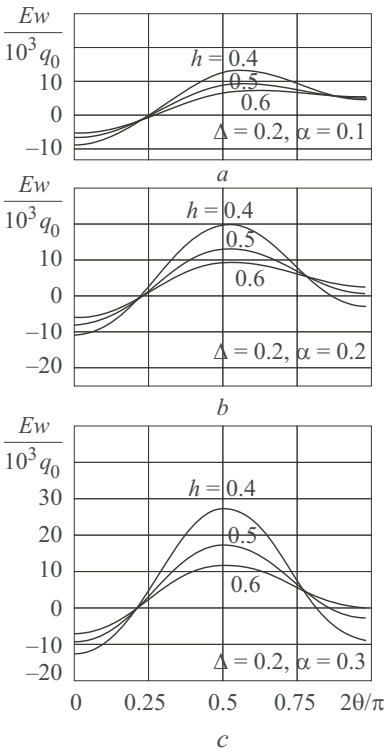

Fig. 9

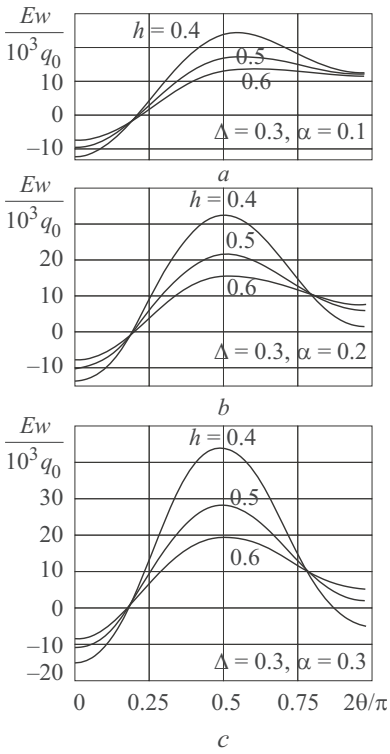

Fig. 10

Let us determine the stress–strain state of a closed shell with clamped ends under uniform pressure $q_\gamma = q_0$. For cylindrical shells with the cross-sectional perimeter of the mid-surface equal to the length of a circle of radius R, the following equalities hold:

$$\pi(a+b)f = 2\pi R, \qquad f = 1+\frac{\Delta^2}{4}+\frac{\Delta^4}{64}+\frac{\Delta^6}{256}+\ldots,$$

$$a = \frac{R}{f}(1-\Delta), \qquad b = \frac{R}{f}(1+\Delta). \tag{3.10}$$

The input data are $R = 20$, $l = 30$, $k = 4$ (Δ, α and h have the values indicated in Figs. 8–10 and Table 4). Figures 8*a*, *b*, *c* show the distribution of the deflection w over the interval $0 \le \theta \le \pi/2$ in the middle section $s = 15$ of a shell with $\Delta = 0.1$ (b/a = 11/9), $\alpha = 0.1$, 0.2, 0.3, and $h = 0.4$, 0.5, 0.6. From Fig. 8*a*, it follows that the shell with low ellipticity and low amplitude of corrugations ($\alpha/R = 0.005$) deflects at $\theta = 0$ (major vertex) in the opposite direction to the applied load, the deflection being maximum at $\theta \approx 0.28\pi$ (the center of the interval). The deflections at $\theta = 0$ and $\theta \approx 0.28\pi$ are approximately equal in absolute magnitude. When $\theta = \pi/2$ (minor vertex), the shell deflects in the direction of the load due to ellipticity, the deflection being very small. From Fig. 8*b*, it follows that as the corrugation amplitude is increase to $\alpha = 0.2$ ($\alpha/R = 0.010$), while Δ and h are kept constant, the maximum deflection at $\theta \approx 0.28\pi$ increases almost twice as that at $\alpha = 0.1$; the deflection at $\theta = 0$ is opposite to the applied load and is slightly smaller than that at $\theta \approx 0.28\pi$; the deflection at $\theta = \pi/2$ is less than that at $\theta = 0$ and is also opposite to the load. In this case, the effect of corrugation become stronger. Figure 8*c* demonstrates that for $\alpha = 0.3$ ($\alpha/R = 0.015$) and the same values of Δ and h, the maximum deflection at $\theta \approx 0.28\pi$ is greater by a factor of almost 1.5 that the deflection at $\alpha = 0.2$ and the deflection at $\theta = 0$ and $\theta = \pi/2$ is opposite to the load and is less by a factor of 1.5 than the maximum deflection (at $\theta \approx 0.28\pi$).

Thus, corrugation with amplitude $\alpha = 0.3$ has a stronger effect on the deformation of the shell than ellipticity does, even if α/R is very small.

Figure 9*a*, *b*, *c* shows the deflection of the shell within $0 \le \theta \le \pi/2$ in the middle section $s = l/2 = 15$ for $\Delta = 0.2$ (b/a = 3/2), $\alpha = 0.1$, 0.2, 0.3, and $h = 0.4$, 0.5, 0.6.

From Fig. 9*a*, it follows that when $\alpha = 0.1$ ($\alpha/R = 0.005$) the deflection is maximum at $\theta \approx 0.28\pi$ and is somewhat less and has opposite sign at $\theta = 0$. The deflection at $\theta = \pi/2$ is in the same direction as the applied load and is half the deflection at $\theta = 0$. In this case, ellipticity has a stong effect.

Figure 9*b* demonstrates that when $\alpha = 0.2$ ($\alpha/R = 0.01$), the maximum deflection at $\theta \approx 0.28\pi$ is almost twice that at $\alpha = 0.1$, while the deflection at $\theta = 0$ is almost half that at $\alpha = 0.1$ and is opposite. When $\theta = \pi/2$, the shell deflects in the same direction in which the load acts for $h = 0.5, 0.6$ and in the opposite direction for $h = 0.4$.

In this case, the effect of corrugation is noticeable. From Fig. 9*c*, it follows that when $\alpha = 0.3$ ($\alpha/R = 0.015$), the maximum deflections at $\theta \approx 0.28\pi$ and $\theta = 0$ are, respectively, much greater than and half that at $\alpha = 0.2$.

At $\theta = 0$, the shell deflects in the opposite direction. The deflection at $\theta = \pi/2$ is somewhat different from the deflection at $\theta = 0$, but has the same direction.

Figure 10*a* demonstrates that when $\alpha = 0.1$ ($\alpha/R = 0.005$), the deflection is maximum at $\theta \approx 0.28\pi$, is half as great and has opposite sign at $\theta = 0$, and at $\theta = \pi/2$, has the same magnitude as the deflection at $\theta = 0$ and the same sign as the maximum deflection.

It follows from Fig. 10*b* that the maximum deflection at $\alpha = 0.2$ ($\alpha/R = 0.01$) is greater by a factor of 1.5 than at $\alpha = 0.1$ when $\theta \approx 0.28\pi$ and is less by a factor of 3 than the maximum deflection and has opposite sign when $\theta = 0$.

Figure 10*c* shows that the maximum deflection at $\alpha = 0.3$ ($\alpha/R = 0.015$) is double that at $\alpha = 0.1$ when $\theta \approx 0.28\pi$ and greater by a factor of 4/3 than the deflection at $\alpha = 0.2$. When $\theta = 0$, the deflection is less by a factor of 4 than the maximum deflection and has opposite sign. When $\theta = \pi/2$, the deflection has the same direction as that of the load for $h = 0.5, 0.6$ and has opposite direction for $h = 0.4$. Figure 10 indicates that when $\theta = 0$, the deflections are similar in both magnitude and direction for all values of α.

Compared with Fig. 10, the maximum deflections increase by a factor of 1.5 to 2. This is because the effect of ellipticity is weaker than the effect of corrugation amplitude.

The stress–strain state of some noncircular cylindrical shells was determined in [77–79].

Table 4 gives the stresses σ_θ^+ and σ_θ^- within $0 \le \theta \le \pi/2$ on the outside and inside surfaces, respectively, of the shell for $\alpha = 0.1, 0.3$ and the values of Δ and h specified above. It can be seen which stresses correspond to the deflections in Figs. 8–10. The stress σ_θ^+ is minimum at $\Delta = 0.1$ and $\theta = 0$ and is much greater and opposite in sign (compression) at $\Delta \ge 0.2$. When $\theta = \pi/2$, the stress σ_θ^+ is positive (tension) at $\Delta = 0.1, 0.2$ and reverses sign at $\Delta \ge 0.3$. The stress σ_θ^+ is maximum at $\theta \approx 0.6\pi/2$ (tension).

The pattern is similar for $h = 0.5, 0.6$. The stress σ_θ^- is mainly tensile. It may become compressive only at $\theta \approx 0.6\pi/2$. The stress σ_θ^- is higher than σ_θ^+.

4. Free Vibrations of Rectangular Plates with Variable Thickness (Classical Formulation). Basic Equations. Consider a freely vibrating rectangular orthotropic plate of variable thickness $h(x, y)$ described in a rectangular coordinate system (the plane Oxy is the midsurface of the plate) [39].

To formulate the problem, we will use the Kirchhoff–Love theory. Based on the assumptions of this theory, the vibrations of the plate can be described by the following equation [4]:

$$\frac{\partial Q_x}{\partial x} + \frac{\partial Q_y}{\partial y} = \rho h \frac{\partial^2 w}{\partial t^2},$$

$$\frac{\partial M_x}{\partial x} + \frac{\partial M_{xy}}{\partial y} = Q_x,$$

$$\frac{\partial M_y}{\partial y} - \frac{\partial M_{xy}}{\partial x} = Q_y, \tag{4.1}$$

where x and y are Cartesian coordinates ($0 \le x \le a$, $0 \le y \le b$); t is time; w is the deflection of the plate; ρ is the density of the material.

TABLE 4

σ	h	$2\theta / \pi$	$\alpha = 0.1$			$\alpha = 0.3$		
			$\Delta = 0.1$	$\Delta = 0.2$	$\Delta = 0.3$	$\Delta = 0.1$	$\Delta = 0.2$	$\Delta = 0.3$
σ_θ^+	0.4	0	1.36	–20.54	–55.2	–45.71	–55.82	–86.12
		0.2	19.44	3.65	–2.14	–8.11	–33.28	–50.13
		0.4	75.83	96.66	146.61	135.21	172.5	261.07
		0.6	105.61	149.8	211.2	192.75	279.01	381.79
		0.8	57.49	74.26	87.7	38.46	19	–12.16
		1	16.72	8.45	–12.96	–99.34	–179.99	–311.68
	0.5	0	–2.8	–25.06	–58.22	–44.27	–61.03	–94.31
		0.2	15.64	0.08	0.11	–2.24	–17.21	–23.66
		0.4	61.07	77.51	115.25	109.07	137.47	199.91
		0.6	81.64	114.07	159.97	143.16	196.56	275.76
		0.8	47.66	64.04	80.55	22.49	21.79	7.23
		1	19.58	20.82	15.68	–65.48	–111.79	–189.47
	0.6	0	–3.99	–25.48	–56.52	–38.41	–56.97	–89.34
		0.2	12.82	2.5	–0.56	0.4	–10.26	–13.29
		0.4	50.12	63.51	93.8	88.54	110.88	158.15
		0.6	66.06	91.95	129.13	111.57	150.52	204.53
		0.8	41.46	57.42	75.16	21.5	24.37	192.86
		1	21.18	27.23	30.38	–43.43	–71.06	–119.16
σ_θ^-	0.4	0	70.31	72.77	92.86	113.19	104.61	120.71
		0.2	62.5	71.68	83.65	92.03	113.41	139.53
		0.4	26.47	21.72	8.44	–24.95	–45.25	–97.36
		0.6	12.76	0	–11.02	–70.31	–128.82	–183.33
		0.8	69.34	92.26	133.98	84.87	141.16	225.14
		1	112.61	163.23	241.06	221.46	342.56	529.05

TABLE 4 (continued)

σ	h	$2\theta/\pi$	$\alpha = 0.1$			$\alpha = 0.3$		
			$\Delta = 0.1$	$\Delta = 0.2$	$\Delta = 0.3$	$\Delta = 0.1$	$\Delta = 0.2$	$\Delta = 0.3$
σ_{θ}^{-}	0.5	0	61.02	67.98	89.8	100.51	102.66	124.96
		0.2	50.03	58.16	64.4	69.32	80.48	93
		0.4	19.93	15.97	7.01	–23.52	–39.02	–73
		0.6	12.47	5.23	–0.61	–46.99	–77.07	–119.34
		0.8	54.05	69.46	96.92	76.87	107.49	164.62
		1	84.55	117.16	167.25	165.24	244.05	365.74
	0.6	0	53.13	62.07	83.91	86.71	93.36	116.84
		0.2	42	47.56	53.95	55.49	62.53	69.79
		0.4	16.88	13.61	6.78	–18.85	–30.91	–55
		0.6	11.98	6.94	2.82	–32.51	–51.91	–74
		0.8	43.39	53.79	7.23	61.72	83.89	124.44
		1	65.92	87.92	121.85	127.74	182.42	267.06

The moments M_x, M_y, M_{xy} and the shearing forces Q_x, Q_y are related by

$$M_x = -\left(D_{11}\frac{\partial^2 w}{\partial x^2} + D_{12}\frac{\partial^2 w}{\partial y^2} \right), \quad Q_x = -\left[D_{11}\frac{\partial^3 w}{\partial x^3} + (D_{12} + 2D_{66})\frac{\partial^3 w}{\partial x \partial y^2} \right],$$

$$M_y = -\left(D_{12}\frac{\partial^2 w}{\partial x^2} + D_{22}\frac{\partial^2 w}{\partial y^2} \right), \quad Q_y = -\left[D_{22}\frac{\partial^3 w}{\partial y^3} + (D_{12} + 2D_{66})\frac{\partial^3 w}{\partial x^2 \partial y} \right],$$

$$M_{xy} = -2D_{66}\frac{\partial^2 w}{\partial x \partial y}. \tag{4.2}$$

The stiffnesses D_{ij} of the plate are defined by the formulas

$$D_{ij} = \frac{B_{ij}h^3(x,y)}{12}, \quad B_{11} = \frac{E_1}{1-\nu_1\nu_2}, \quad B_{12} = \frac{\nu_2 E_1}{1-\nu_1\nu_2} = \frac{\nu_1 E_2}{1-\nu_1\nu_2},$$

$$B_{22} = \frac{E_2}{1-\nu_1\nu_2}, \quad B_{66} = G_{12},$$

where $E_1, E_2, G_{12}, \nu_1, \nu_2$ are the elastic and shear moduli and Poisson's ratios.

From the system of equations (4.1), (4.2), we derive an equivalent differential equation for the deflection *w*:

$$D_{11}\frac{\partial^4 w}{\partial x^4}+D_{22}\frac{\partial^4 w}{\partial y^4}+2(D_{12}+2D_{22})\frac{\partial^4 w}{\partial x^2\partial y^2}+2\frac{\partial D_{11}}{\partial x}\frac{\partial^3 w}{\partial x^3}+2\frac{\partial D_{22}}{\partial y}\frac{\partial^3 w}{\partial y^3}$$

$$+2\frac{\partial}{\partial y}(D_{12}+2D_{66})\frac{\partial^3 w}{\partial x^2\partial y}+2\frac{\partial}{\partial x}(D_{12}+2D_{66})\frac{\partial^3 w}{\partial x\partial y^2}$$

$$+\left(\frac{\partial^2 D_{11}}{\partial x^2}+\frac{\partial^2 D_{12}}{\partial y^2}\right)\frac{\partial^2 w}{\partial x^2}+\left(\frac{\partial^2 D_{12}}{\partial x^2}+\frac{\partial^2 D_{22}}{\partial y^2}\right)\frac{\partial^2 w}{\partial y^2}+4\frac{\partial^2 D_{66}}{\partial x\partial y}\frac{\partial^2 w}{\partial x\partial y}+\rho h\frac{\partial^2 w}{\partial t^2}=0. \tag{4.3}$$

Boundary conditions for the deflection are prescribed on the edges $x = 0$, $x = a$, $y = 0$, $y = b$. At $y = \text{const}$, the following boundary conditions are specified:

(i) both edges are clamped:

$$w=0,\quad \frac{\partial w}{\partial y}=0 \quad \text{at} \quad y=0,\quad y=b, \tag{4.4}$$

(ii) both edges are hinged:

$$w=0,\quad \frac{\partial^2 w}{\partial y^2}=0 \quad \text{at} \quad y=0,\quad y=b, \tag{4.5}$$

(iii) one edge is hinged, the other is clamped:

$$w=0,\quad \frac{\partial^2 w}{\partial y^2}=0 \quad \text{at} \quad y=0,$$

$$w=0,\quad \frac{\partial w}{\partial y}=0 \quad \text{at} \quad y=b. \tag{4.6}$$

Similar conditions can be specified on the edges $x = \text{const}$.

Problem-Solving Method. The solution of Eq. (4.3) can be represented as

$$w=\sum_{i=0}^{N} w_i(x)\,\psi_i(y), \tag{4.7}$$

where $w_i(x)(i=\overline{1,N})$ are unknown functions; $\psi_i(y)$ are functions set up using quintic B-splines ($N \geq 6$) to satisfy the boundary conditions at $y = \text{const}$:

$$\psi_0(y)=\alpha_{11}B_5^{-2}(y)+\alpha_{12}B_5^{-1}(y)+B_5^0(y),$$

$$\psi_1(y)=\alpha_{21}B_5^{-1}(y)+\alpha_{22}B_5^0(y)+B_5^1(y),$$

$$\psi_2(y)=\alpha_{31}B_5^{-2}(y)+\alpha_{32}B_5^0(y)+B_5^2(y), \quad i=3,4,\ldots,N-3,$$

$$\psi_{N-2}(y)=\beta_{31}B_5^{N+2}(y)+\beta_{32}B_5^N(y)+B_5^{N+2}(y),$$

$$\psi_{N-1}(y)=\beta_{21}B_5^{N+1}(y)+\beta_{22}B_5^N(y)+B_5^{N-1}(y),$$

$$\psi_N(y)=\beta_{11}B_5^{N+2}(y)+\beta_{12}B_5^{N+1}(y)+B_5^N(y), \tag{4.8}$$

where $B_5^i(y)$ ($i = -2, \ldots, N+2$, i is the spline number) are splines over a uniform partition Δ with spacing h_y: $y_{-5} < y_{-4} < \ldots < y_N < y_{N+5} < \ldots < y_{N+5}$; $y_0 = 0$; $y_N = b$:

$$B_5^i(y) = \frac{1}{120}\begin{cases} 0, & \infty < y < y_{i-3}, \\ z^5, & y_{i-3} \le y < x_{i-2}, \\ -5z^5 + 5z^4 + 10z^3 + 10z^2 + 5z + 1, & y_{i-2} \le y < y_{i-1}, \\ 10z^5 - 20z^4 - 20z^3 + 20z^2 + 50z + 26, & y_{i-1} \le y < y_i, \\ -10z^5 + 30z^4 - 60z^2 + 66, & y_i \le y < y_{i+1}, \\ 5z^5 - 20z^4 + 20z^3 + 20z^2 - 50z + 26, & y_{i+1} \le y < y_{i+2}, \\ (1-z)^5, & y_{i+2} \le y < y_{i+3}, \\ 0, & y_{i+3} \le y < \infty, \end{cases}$$

where $z = (y - y_k)/h_y$ on the interval $[y_k, y_{k+1}], k = \overline{i-3, i+2}$, $i = \overline{-3, N+2}$, $h_y = y_{k+1} - y_k = \text{const}$; α_{ij} and β_{ij} ($i = 1, 2, 3$, $j = 1, 2$) are constant coefficients depending on the boundary conditions on the edges $y = 0$ and $y = b$, respectively.

Denote

$$A_\alpha = \begin{bmatrix} \alpha_{11} & \alpha_{12} \\ \alpha_{21} & \alpha_{22} \\ \alpha_{31} & \alpha_{32} \end{bmatrix}, \quad A_\beta = \begin{bmatrix} \beta_{11} & \beta_{12} \\ \beta_{21} & \beta_{22} \\ \beta_{31} & \beta_{32} \end{bmatrix}.$$

If the edges $y = 0$, $y = b$ are clampled, then

$$A_\alpha = A_\beta = \begin{bmatrix} 165/4 & -33/8 \\ 1 & -26/33 \\ 1 & -1/33 \end{bmatrix}.$$

If the edges $y = 0$, $y = b$ are hinged, then

$$A_\alpha = A_\beta = \begin{bmatrix} 12 & -3 \\ -1 & 0 \\ -1 & 0 \end{bmatrix}.$$

If one edge is clamped and the other is hinged, then

$$A_\alpha = \begin{bmatrix} 165/4 & -33/8 \\ 1 & -26/33 \\ 1 & -1/33 \end{bmatrix}, \quad A_\beta = \begin{bmatrix} 12 & -3 \\ -1 & 0 \\ -1 & 0 \end{bmatrix}.$$

Let us represent Eq. (4.3) in the form

$$\frac{\partial^4 w}{\partial x^4} = a_1 \frac{\partial^3 w}{\partial x^3} + a_2 \frac{\partial^4 w}{\partial x^2 \partial y^2} + a_3 \frac{\partial^3 w}{\partial x^2 \partial y} + a_4 \frac{\partial^2 w}{\partial x^2}$$

$$+ a_5 \frac{\partial^3 w}{\partial x \partial y^2} + a_6 \frac{\partial^2 w}{\partial x \partial y} + a_7 \frac{\partial^4 w}{\partial y^4} + a_8 \frac{\partial^3 w}{\partial y^3} + a_9 \frac{\partial^2 w}{\partial y^2} + a_{10} w, \tag{4.9}$$

where $a_i = a_i(x, y)$, $i = 1, 2, \ldots, 9$, $a_{10} = a_{10}(x, y, \omega)$.

Substituting (4.7) into Eq. (4.9), we require it to hold at the collocation points $\xi_k \in [0, b]$, $k = 0, N$. Let the partition have an even number of knots, i.e., $N = 2n + 1 (n \ge 3)$, and the collocation points be such that $\xi_{2i} \in [y_{2i}, y_{2i+1}]$, $\xi_{2i+1} \in [y_{2i}, y_{2i+1}]$,

$(i = 0, 1, \ldots, n)$. Then there are two collocation points within the interval $[y_{2i}, y_{2i+1}]$ and no collocation points within the adjacent intervals $[y_{2i+1}, y_{2i+2}]$. The collocation points within each interval $[y_{2i}, y_{2i+1}]$ are chosen so that $\xi_{2i} = x_{2i} + z_1 h_y$, $\xi_{2i+1} = y_{2i} + z_2 h_y$ $(i = 0, 1, 2, \ldots, n)$, where z_1 and z_2 are the roots of a Legendre quadratic on the interval [0, 1]: $z_1 = 1/2 - \sqrt{3}/6$, $z_2 = 1/2 + \sqrt{3}/6$. This choice of collocation points is optimal and significantly improves the accuracy of approximation. We obtain a system of $N+1$ linear differential equations for w_i. If

$$\Psi_j = [\psi_i^{(j)}(\xi_k)]\,(k, i = 0, \ldots, N;\ j = 0, \ldots, 4),$$

$$\overline{w} = \{w_0, w_1, \ldots, w_N\}^T, \qquad \overline{a}_r^T = \{a_r(x, \xi_0),\ a_r(x, \xi_1),\ \ldots,\ a_r(x, \xi_N)\} \qquad (r = 1, \ldots, 9),$$

$$\overline{a}_{10}^T = \{a_{10}(x,\ \xi_0,\ \omega),\quad a_r(x,\ \xi_1,\ \omega),\ \ldots,\ a_r(x,\ \xi_N,\ \omega)\},$$

and the matrix $[c_i a_{ij}]$ is denoted by $\overline{c} * A$, where $A = [a_{ij}]\,\{i, j = 0, \ldots, N\}$, the system of differential equations becomes

$$\overline{w}^{IV} = \Psi_0^{-1}(\overline{a}_7 * \Psi_4 + \overline{a}_8 * \Psi_3 + \overline{a}_9 * \Psi_2 + \overline{a}_{10} * \Psi)\overline{w}$$

$$+\Psi_0^{-1}(\overline{a}_5 * \Psi_2 + \overline{a}_6 * \Psi_1)\overline{w}' + \Psi_0^{-1}(\overline{a}_2 * \Psi_3 + \overline{a}_3 * \Psi_1$$

$$+ \overline{a}_4 * \Psi_0)\overline{w}'' + \Psi_0^{-1}(\overline{a}_1 * \Psi_0)\overline{w}'''. \tag{4.10}$$

This system can be reduced to the normal form

$$\frac{d\overline{Y}}{dx} = A(x, \omega)\overline{Y} \qquad (0 \le x \le a) \tag{4.11}$$

$\overline{Y} = \{w_1, w_2, \ldots, w_{N+1}, w_1', w_2', \ldots, w_{N+1}', w_1'', w_2'', \ldots, w_{N+1}'', w_1''', w_2''', \ldots, w_{N+1}'''\}^T$; $w_K^{(I)} = w^{(I)}(x, \xi_K)$, $K = 1, \ldots, N+1$, $I = 1, 2, 3$; $A(x, \omega)$ is an $(N+1)\times(N+1)$-matrix.

The boundary conditions for this system are given by

$$B_1\overline{Y}(0) = \overline{b}_1, \quad B_2\overline{Y}(a) = \overline{b}_2, \tag{4.12}$$

where $\overline{b}_1$, $\overline{b}_2$ are zero vectors.

Analysis of the Numerical Results. The eigenvalue problem for the system of ordinary differential equations (4.11) with the boundary conditions (4.12) is solved with the discrete-orthogonalization and incremental search methods [21, 76].

The approach was used to analyze the spectrum of natural vibrations of a square plate of variable thickness with various boundary conditions. The thickness of the plate varies as $h(x) = [\alpha(6x^2 - 6x + 1) + 1]h_0$. The cross-sections of the plate are shown below:

The plate is made of orthotropic fibreglass cloth with Young's moduli $E_1 = 4.76 \cdot 10^4$ MPa and $E_2 = 2.07 \cdot 10^4$ MPa, shear modulus $G_{12} = 0.531 \cdot 10^4$ MPa, and Poisson's ratios $\nu_1 = 0.149$ and $\nu_1 = 0.0647$. The values of the dimensionless frequency $\overline{\omega} = \omega a^2 (\rho h / D_0)^{1/2}$, $D_0 = (h_0^3 / 12) \cdot 10^4$ MPa, of a clamped plate determined with the splines-collocation method with different number of collocation points (N = 10, 12, 14, 16, 18, 20, 22) differ insignificantly (Table 5).

Tables 6 and 7 summarize dimensionless frequencies $\overline{\omega}_i$ $(i = 1, 2, 3)$ (ordered by value) of an orthotropic square plate for $\alpha \le 0$ and $\alpha > 0$, respectively, and the following boundary conditions:

TABLE 5

α	ω	N						
		10	12	14	16	18	20	22
0	ω_1	61.139	61.132	61.129	61.127	61.127	61.127	61.127
	ω_2	107.188	107.066	107.016	106.994	106.982	106.976	106.972
	ω_3	142.550	142.537	142.532	142.530	142.529	142.528	142.528
0.3	ω_1	62.108	62.102	62.099	62.099	62.098	62.098	62.098
	ω_2	97.737	97.637	97.598	97.580	97.570	97.566	97.562
	ω_3	145.289	145.276	145.271	145.269	145.268	145.268	145.267

(i) all edges are clamped (boundary conditions of type A):

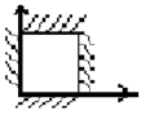

$$w = 0, \quad \frac{\partial w}{\partial y} = 0 \quad \text{at} \quad y = 0, \quad y = a,$$

$$w = 0, \quad \frac{\partial w}{\partial x} = 0 \quad \text{at} \quad x = 0, \quad x = a;$$

(ii) three edges are clamped and one edge is hinged (boundary conditions of type B):

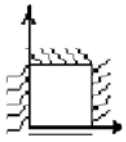

$$w = 0, \quad \frac{\partial w}{\partial y} = 0 \quad \text{at} \quad y = a,$$

$$w = 0, \quad \frac{\partial w}{\partial x} = 0 \quad \text{at} \quad x = 0, \quad x = a,$$

$$w = 0, \quad \frac{\partial^2 w}{\partial y^2} = 0 \quad \text{at} \quad y = 0;$$

and boundary conditons of type C:

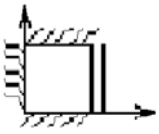

$$w = 0, \quad \frac{\partial w}{\partial y} = 0 \quad \text{at} \quad y = 0, \quad y = a,$$

$$w = 0, \quad \frac{\partial w}{\partial x} = 0 \quad \text{at} \quad x = 0,$$

$$w = 0, \quad \frac{\partial^2 w}{\partial x^2} = 0 \quad \text{at} \quad x = a;$$

(iii) two edges are clamped and the other two are hinged (boundary conditions of type D):

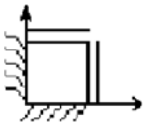

$$w = 0, \quad \frac{\partial w}{\partial y} = 0 \quad \text{at} \quad y = 0,$$

TABLE 6

Boundary conditions	ω	α					
		–0.5	–0.4	–0.3	–0.2	–0.1	0
A	ω_1	58.375	59.012	59.605	60.159	60.674	61.139
	ω_2	121.526	119.010	116.240	113.311	110.281	107.188
	ω_3	124.339	129.656	134.030	137.585	140.405	142.550
B	ω_1	50.227	51.605	52.905	54.129	54.270	56.320
	ω_2	102.334	100.723	98.953	97.083	95.147	93.166
	ω_3	121.396	126.863	131.384	135.083	138.045	140.330
C	ω_1	52.733	52.211	51.624	50.995	50.337	49.659
	ω_2	109.151	112.403	110.490	107.334	104.080	100.783
	ω_3	116.222	113.496	114.497	116.613	117.777	118.403
D	ω_1	43.939	44.009	43.998	43.923	43.790	43.607
	ω_2	97.299	95.178	92.905	90.549	88.155	85.755
	ω_3	105.958	109.322	111.879	113.750	115.019	115.748
E	ω_1	48.701	47.412	46.059	4.676	43.289	41.918
	ω_2	95.664	97.177	97.994	98.235	97.985	96.671
	ω_3	113.313	110.306	107.049	103.676	100.170	97.306
G	ω_1	45.045	46.929	48.698	50.354	51.893	53.306
	ω_2	85.738	85.046	84.248	83.378	82.453	81.479
	ω_3	119.425	124.989	129.605	133.396	136.448	138.819

$$w = 0, \quad \frac{\partial^2 w}{\partial y^2} = 0 \quad \text{at} \quad y = a,$$

$$w = 0, \quad \frac{\partial w}{\partial x} = 0 \quad \text{at} \quad x = 0,$$

$$w = 0, \quad \frac{\partial^2 w}{\partial x^2} = 0 \quad \text{at} \quad x = a;$$

boundary conditions of type E:

TABLE 7

Boundary conditions	ω	α				
		0.1	0.2	0.3	0.4	0.5
A	ω_1	61.542	61.871	62.108	62.237	62.238
	ω_2	104.058	100.904	97.737	94.557	91.364
	ω_3	144.062	144.968	145.289	145.035	144.212
B	ω_1	57.266	58.096	58.791	59.339	59.724
	ω_2	91.149	89.104	87.026	84.911	82.749
	ω_3	144.977	143.017	143.469	138.723	131.720
C	ω_1	48.965	48.257	47.535	46.801	46.051
	ω_2	97.477	94.187	90.928	87.713	84.546
	ω_3	118.535	118.208	117.477	116.269	114.688
D	ω_1	43.376	43.098	42.744	42.402	41.982
	ω_2	83.369	81.013	78.694	76.420	74.190
	ω_3	115.981	115.752	115.085	113.998	112.506
E	ω_1	40.583	39.297	38.077	36.933	35.878
	ω_2	93.185	89.743	86.364	38.065	79.858
	ω_3	96.249	94.852	93.149	91.160	88.934
G	ω_1	54.586	55.718	56.642	57.495	58.109
	ω_2	80.460	79.389	78.258	77.055	75.765
	ω_3	140.291	134.815	129.283	123.717	118.135

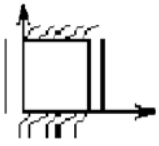

$$w = 0, \quad \frac{\partial w}{\partial y} = 0 \quad \text{at} \quad y = 0, \quad y = a,$$

$$w = 0, \quad \frac{\partial^2 w}{\partial x^2} = 0 \quad \text{at} \quad x = 0, \quad x = a;$$

and boundary conditions of type G:

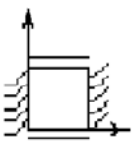

$$w = 0, \quad \frac{\partial^2 w}{\partial y^2} = 0 \quad \text{at} \quad y = 0, \quad y = a,$$

$$w = 0, \quad \frac{\partial w}{\partial x} = 0 \quad \text{at} \quad x = 0, \quad x = a.$$

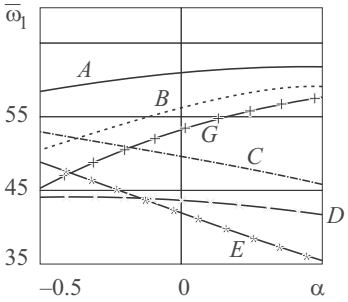

Fig. 11

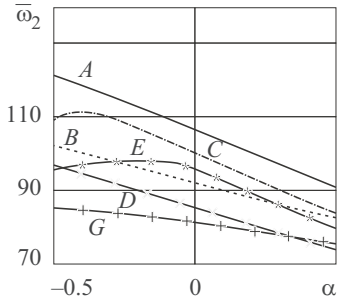

Fig. 12

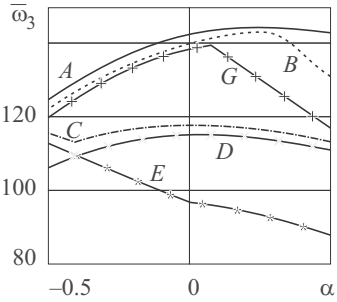

Fig. 13

The number of collocation points $N = 10$. Figures 11–13 show the dimensionless frequency $\overline{\omega}_i$ of vibrations of a square orthotropic plate with various boundary conditions for various values of the parameter α.

The maxima and minima of the frequencies $\overline{\omega}_2$ and $\overline{\omega}_3$ are the points of change of mode shape. The frequency of the clamped plate is maximum for all boundary conditions and all values of α. The first frequency for type D boundary conditions changes a little compared with the other boundary conditions. Figure 14 shows natural modes of vibrations of a plate with boundary conditions of type G.

Problems of the free vibrations of plates and shallow shells with variable thickness were solved using the proposed approach and the classical theory in [12, 34, 35, 50].

5. Free Vibrations of Conical Shells with Variable Parameters (Classical Formulation). Problem Formulation. Consider a freely vibrating isotropic conical shell of variable thickness $h(x, y)$ described in a curvilinear orthogonal coordinate system (s, θ), where s is the meridional coordinate; θ is the azimuth angle. The Lame parameters $A = 1$, $B = r$; the radii of principal curvatures $R_s = 0$, $R_\theta = r / \sin\varphi$, where r is radius of a parallel circle; φ is the angle between the normal to the mid-surface and the axis of revolution.

The Kirchhoff–Love theory of thin shells employs the following equations to describe the free vibrations of conical shells [8]:

$$\frac{\partial}{\partial s}(rN_s) + \frac{\partial S}{\partial \theta} - \cos\varphi N_\theta = r\rho h \frac{\partial^2 u(s,\theta,t)}{\partial t^2},$$

$$\frac{\partial N_\theta}{\partial \theta} + \frac{\partial}{\partial s}(rS) + \cos\varphi S + \sin\varphi\left(Q_\theta + \frac{\partial H}{\partial s}\right) = r\rho h \frac{\partial^2 v(s,\theta,t)}{\partial t^2},$$

$$\frac{\partial}{\partial s}(rQ_s) + \frac{\partial Q_\theta}{\partial \theta} - \sin\varphi N_\theta = r\rho h \frac{\partial^2 w(s,\theta,t)}{\partial t^2},$$

$$\frac{\partial}{\partial s}(rM_s) + \frac{\partial H}{\partial \theta} - \cos\varphi M_\theta - rQ_s = 0,$$

$$\frac{\partial}{\partial s}(rH) + \frac{\partial M_\theta}{\partial \theta} + \cos\varphi H - rQ_\theta = 0, \qquad (5.1)$$

where s, θ are the curvilinear orthogonal coordinates of a point on the midsurface ($s_0 \le s \le s_a$, $0 \le \theta \le b$); t is time; u, v, w are the displacements of the mid-surface; ρ is the density of the material; Strains and displacements are related by

$$\varepsilon_s = \frac{\partial u}{\partial s}, \qquad \varepsilon_\theta = \frac{1}{r}\frac{\partial v}{\partial \theta} + \frac{\cos\varphi}{r}u + \frac{\sin\varphi}{r}w,$$

$$\varepsilon_{s\theta} = \frac{1}{r}\frac{\partial u}{\partial \theta} + \frac{\partial v}{\partial s} - \frac{\cos\varphi}{r}v, \qquad \chi_s = -\frac{\partial^2 w}{\partial s^2},$$

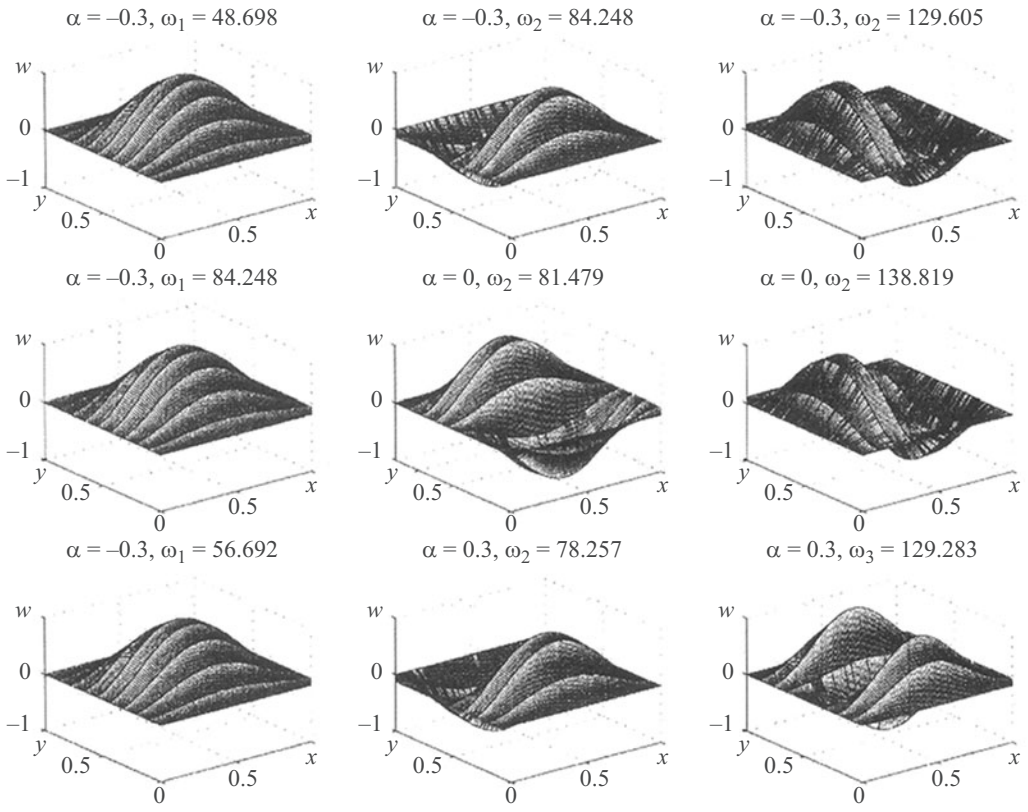

Fig. 14

$$\chi_\theta = -\frac{1}{r^2}\frac{\partial^2 w}{\partial\theta^2} - \frac{\cos\varphi}{r}\frac{\partial w}{\partial s}, \qquad \chi_{s\theta} = \frac{\cos\varphi}{r^2}\frac{\partial w}{\partial\theta} - \frac{1}{r}\frac{\partial^2 w}{\partial s\partial\theta}. \tag{5.2}$$

If the material of the shells is isotropic, the normal and shearing forces N_s, N_θ, S, bending and twisting moments M_s, M_θ, and H are expressed in terms of strains as

$$N_s = D_N(\varepsilon_s + \nu\varepsilon_\theta), \qquad N_\theta = D_N(\nu\varepsilon_s + \varepsilon_\theta), \qquad S = \frac{1-\nu}{2}D_N\varepsilon_{s\theta},$$

$$M_s = D_M(\chi_s + \nu\chi_\theta), \qquad M_\theta = D_M(\nu\chi_s + \chi_\theta), \qquad H = D_M(1-\nu)\chi_{s\theta}. \tag{5.3}$$

The stiffnesses of the shell are given by

$$D_N = Eh/(1-\nu), \qquad D_M = Eh^3/[12(1-\nu)],$$

where E and v are, respectively, the elastic modulus and Poisson's ratio of the shell material.

The mid-surface undergoes small vibrations, the displacements $u(s, \theta, t)$, $v(s, \theta, t)$, $w(s, \theta, t)$ can be represented by harmonic functions:

$$u(s,\theta,t) = u(s,\theta)e^{-i\omega t}, \qquad v(s,\theta,t) = v(s,\theta)e^{-i\omega t}, \qquad w(s,\theta,t) = w(s,\theta)e^{-i\omega t}, \tag{5.4}$$

where ω is the natural frequency.

From the system of equations (5.1)–(5.3) with (5.4), we derive three equivalent differential equations for the displacements *u*, *v*, *w*:

$$\frac{\partial^2 u}{\partial \theta^2} = F_u\left(u,\ \frac{\partial u}{\partial s},\ \frac{\partial^2 u}{\partial s^2},\ \frac{\partial u}{\partial \theta},\ v,\ \frac{\partial v}{\partial s},\ \frac{\partial v}{\partial \theta},\ \frac{\partial^2 v}{\partial s \partial \theta},\ w,\ \frac{\partial w}{\partial s},\ \omega\right),$$

$$\frac{\partial^2 v}{\partial \theta^2} = F_v\left(u, \frac{\partial u}{\partial s}, \frac{\partial u}{\partial \theta}, \frac{\partial^2 u}{\partial s \partial \theta}, v, \frac{\partial v}{\partial s}, \frac{\partial v}{\partial \theta}, \frac{\partial^2 v}{\partial s^2}, w, \frac{\partial w}{\partial s}, \frac{\partial w}{\partial \theta}, \frac{\partial^2 w}{\partial s^2}, \frac{\partial^2 w}{\partial \theta^2}, \frac{\partial^2 w}{\partial s \partial \theta}, \frac{\partial^3 w}{\partial s^2 \partial \theta}, \frac{\partial^3 w}{\partial \theta^3}, \omega\right),$$

$$\frac{\partial^4 w}{\partial \theta^4} = F_w\left(u, \frac{\partial u}{\partial s}, \frac{\partial v}{\partial \theta}, w, \frac{\partial w}{\partial s}, \frac{\partial w}{\partial \theta}, \frac{\partial^2 w}{\partial s^2}, \frac{\partial^2 w}{\partial \theta^2}, \frac{\partial^2 w}{\partial s \partial \theta}, \frac{\partial^3 w}{\partial s^3}, \frac{\partial^3 w}{\partial \theta^3}, \frac{\partial^3 w}{\partial s \partial \theta^2}, \frac{\partial^3 w}{\partial s^2 \partial \theta}, \frac{\partial^4 w}{\partial s^4}, \frac{\partial^4 w}{\partial s^2 \partial \theta^2}, \omega\right), \tag{5.5}$$

where F_u, F_υ, F_w are linear differential operators.

Boundary conditions for displacements are prescribed on the edges $s = s_0, s_a$ and $\theta = 0, b$. The following boundary conditions can be specified on the edges $s = \text{const}$:

(i) clamped edge:

$$u = v = w = \frac{\partial w}{\partial s} \quad \text{at} \quad s = s_0, \quad s = s_a; \tag{5.6}$$

(ii) hinged edge:

$$v = \frac{\partial u}{\partial s} = w = \frac{\partial^2 w}{\partial s^2} \quad \text{at} \quad s = s_0, \quad s = s_a. \tag{5.7}$$

Similar conditions can be specified on the edges θ = const:

(i) clamped edge:

$$u = v = w = \frac{\partial w}{\partial \theta} \quad \text{at} \quad \theta = 0, \quad \theta = b; \tag{5.8}$$

(ii) hinged edge:

$$u = \frac{\partial v}{\partial \theta} = w = \frac{\partial^2 w}{\partial \theta^2} \quad \text{at} \quad \theta = 0, \quad \theta = b. \tag{5.9}$$

Problem-Solving Method. The solution of the system of equations (5.5) is represented in the form

$$u = \sum_{i=0}^{N} u_i(\theta)\varphi_i(s), \qquad v = \sum_{i=0}^{N} v_i(\theta)\chi_i(s), \qquad w = \sum_{i=0}^{N} w_i(\theta)\psi_i(s), \tag{5.10}$$

where $u_i(\theta), v_i(\theta), w_i(\theta) (i = 0, \ldots, N)$ are unknown functions; $\varphi_i(s), \chi_i(s)$ are functions set up using cubic *B*-splines ($N \geq 4$); $\psi_i(s)$ are functions set up using quintic *B*-splines ($N \geq 6$). The functions $\varphi_i(s), \chi_i(s), \psi_i(s)$ are chose so as to satisfy the boundary conditions at $s = \text{const}$ using linear combinations of cubic and quintic *B*-splines, respectively.

We rearrange the system of equations (5.5) as

$$\frac{\partial^2 u}{\partial \theta^2} = a_{11}\frac{\partial u}{\partial \theta} + a_{12}\frac{\partial^2 u}{\partial s^2} + a_{13}\frac{\partial u}{\partial s} + a_{14}u + a_{15}\frac{\partial^2 v}{\partial s \partial \theta} + a_{16}\frac{\partial v}{\partial \theta} + a_{17}\frac{\partial v}{\partial s}$$

$$+ a_{18}\ v + a_{19}\frac{\partial w}{\partial s} + a_{110}w + a_{111}(\omega)u,$$

$$\frac{\partial^2 v}{\partial \theta^2} = a_{21}\frac{\partial^2 u}{\partial s \partial \theta} + a_{22}\frac{\partial u}{\partial \theta} + a_{23}\frac{\partial u}{\partial s} + a_{24}u + a_{25}\frac{\partial v}{\partial \theta} + a_{26}\frac{\partial^2 v}{\partial s^2} + a_{27}\frac{\partial v}{\partial s} + a_{28}v + a_{29}\frac{\partial^3 w}{\partial \theta^3}$$

$$+a_{210}\frac{\partial^2 w}{\partial\theta^2}+a_{211}\frac{\partial^3 w}{\partial s^2\partial\theta}+a_{212}\frac{\partial^2 w}{\partial s\partial\theta}+a_{213}\frac{\partial w}{\partial\theta}+a_{214}\frac{\partial^2 w}{\partial s^2}+a_{215}\frac{\partial w}{\partial s}+a_{216}\,w+a_{217}(\omega)v,$$

$$\frac{\partial^4 w}{\partial\theta^4}=a_{31}\frac{\partial u}{\partial s}+a_{32}\,u+a_{33}\frac{\partial v}{\partial\theta}+a_{34}\frac{\partial^3 w}{\partial\theta^3}+a_{35}\frac{\partial^4 w}{\partial s^2\partial\theta^2}+a_{36}\frac{\partial^3 w}{\partial s\partial\theta^2}+a_{37}\frac{\partial^2 w}{\partial\theta^2}$$

$$+a_{38}\frac{\partial^3 w}{\partial s^2\partial\theta}+a_{39}\frac{\partial^2 w}{\partial s\partial\theta}+a_{310}\frac{\partial w}{\partial\theta}+a_{311}\frac{\partial^4 w}{\partial s^4}+a_{312}\frac{\partial^3 w}{\partial s^3}+a_{313}\frac{\partial^2 w}{\partial s^2}+a_{314}\frac{\partial w}{\partial s}+a_{315}w+a_{316}(\omega)w, \qquad (5.11)$$

where $a_{1n}=a_{1n}(s,\theta)$, $a_{2m}=a_{2m}(s,\theta)$, $a_{3k}=a_{3k}(s,\theta)$, $n=1,\dots,10$, $m=1,\dots,16$, $k=1,\dots,15$, $a_{111}=a_{111}(s,\theta,\omega)$, $a_{217}=a_{217}(s,\theta,\omega)$, $a_{316}=a_{316}(s,\theta,\omega)$.

Substituting (5.10) into Eqs. (5.11), we require that they hold at given collocation points $\xi_k\in[s_a,s_b]$, $k=0,\dots,N$. If the number of knots ($N=2n+1$, $n\ge 3$) is even and $\xi_{2i}\in[s_{2i},s_{2i+1}]$, $\xi_{2i+1}\in[s_{2i},s_{2i+1}]$ ($i=0,\dots,n$), there are two collocation points within the interval $[s_{2i},s_{2i+1}]$ and no collocation points with the adjacent intervals $[s_{2i+1},s_{2i+2}]$. The collocation points within each interval $[s_{2i},s_{2i+1}]$ are chosen so that $\xi_{2i}=s_{2i}+z_1h$, $\xi_{2i+1}=s_{2i}+z_2h$ ($i=0,\dots,n$), where h is the mesh spacing; z_1 and z_2 are the roots of a Legendre quadratic on the interval [0, 1], $z_1=1/2-\sqrt{3}/6$ and $z_2=1/2+\sqrt{3}/6$. This choice of collocation points is optimal and significantly improves the accuracy of approximation. After all transformations, we obtain a system of $N+1$ linear differential equations for u_i, v_i, w_i. If

$$\Phi_l=[\varphi_i^{(l)}(\xi_k)],\quad \mathrm{X}_l=[\chi_i^{(l)}(\xi_k)],\quad \Psi_m=[\psi_i^{(m)}(\xi_k)]$$

$$(i,k=0,\dots,N,\ l=0,\dots,2,\ m=0,\dots,4),$$

$$\bar u^T=\{u_0,\dots,u_N\},\quad \bar v^T=\{v_0,\dots,v_N\},\quad \bar w^T=\{w_0,\dots,w_N\},$$

$$\bar a_{1r}^T=\{a_{1r}(\theta,\xi_0),\dots,a_{1r}(\theta,\xi_N)\}\ \ (r=1,\dots,10),$$

$$\bar a_{2r}^T=\{a_{2r}(\theta,\xi_0),\dots,a_{2r}(\theta,\xi_N)\}\ \ (r=1,\dots,16),$$

$$\bar a_{3r}^T=\{a_{3r}(\theta,\xi_0),\dots,a_{3r}(\theta,\xi_N)\}\ \ (r=1,\dots,15),$$

$$\bar a_{111}^T=\{a_{111}(\theta,\xi_0,\omega),\dots,a_{111}(\theta,\xi_N,\omega)\},$$

$$\bar a_{217}^T=\{a_{217}(\theta,\xi_0,\omega),\dots,a_{217}(\theta,\xi_N,\omega)\},$$

$$\bar a_{316}^T=\{a_{316}(\theta,\xi_0,\omega),\dots,a_{111}(\theta,\xi_N,\omega)\},$$

and the matrix $[c_ia_{ij}]$ is denoted by $\bar c\cdot A$, where $A=[a_{ij}]$ ($i,j=0,\dots,N$), and $\bar c=\{c_0,\dots,c_N\}$, the system of differential equations (5.11) becomes

$$\bar u''=\Phi_0^{-1}\{(\bar a_{12}\cdot\Phi_2+\bar a_{13}\cdot\Phi_1+\bar a_{14}\cdot\Phi_0+\bar a_{111}\cdot\Phi_0)\bar u+(\bar a_{11}\cdot\Phi_0)\bar u'+(\bar a_{17}\cdot\mathrm{X}_1+\bar a_{18}\cdot\mathrm{X}_0)\bar v$$

$$+(\bar a_{15}\cdot\mathrm{X}_1+\bar a_{16}\cdot\mathrm{X}_0)\bar v'+(\bar a_{19}\cdot\Psi_1+\bar a_{110}\cdot\Psi_0)\bar w\},$$

$$\bar v''=\mathrm{X}_0^{-1}\{(\bar a_{23}\cdot\Phi_1+\bar a_{24}\cdot\Phi_0)\bar u+(\bar a_{21}\cdot\Phi_1+\bar a_{22}\cdot\Phi_0)\bar u'$$

$$+(\bar a_{26}\cdot\mathrm{X}_2+\bar a_{27}\cdot\mathrm{X}_1+\bar a_{28}\cdot\mathrm{X}_0+\bar a_{217}\cdot\mathrm{X}_0)\bar v+(\bar a_{25}\cdot\mathrm{X}_0)\bar v'$$

$$+(\bar a_{214}\cdot\Psi_2+\bar a_{215}\cdot\Psi_1+\bar a_{216}\cdot\Psi_0)\bar w+(\bar a_{2111}\cdot\Psi_2+\bar a_{212}\cdot\Psi_1+\bar a_{213}\cdot\Psi_0)\bar w'$$

$$+(\bar a_{210}\cdot\Psi_0)\bar w''+(\bar a_{29}\cdot\Psi_0)\bar w'''\}$$

$$\bar w^{\mathrm{IV}}=\Psi_0^{-1}\{(\bar a_{31}\cdot\Phi_1+\bar a_{32}\cdot\Phi_0)\bar u+(\bar a_{33}\cdot\mathrm{X}_0)\bar v'+(\bar a_{311}\cdot\Psi_4+\bar a_{312}\cdot\Psi_3+\bar a_{313}\cdot\Psi_2+\bar a_{314}\cdot\Psi_1$$

TABLE 8

L, m	R_1, m	R_2, m	h_0, m	b, rad	β_k, deg	Notation
0.12	0.09	0.09	0.004	π/2	0	C1
0.12	0.0875	0.0925	0.004	π/2	2.5	K2.5
0.12	0.085	0.095	0.004	π/2	5	K5
0.12	0.08	0.1	0.004	π/2	10	K10
0.12	0.075	0.105	0.004	π/2	15	K15
0.12	0.07	0.11	0.004	π/2	20	K20
0.12	0.065	0.115	0.004	π/2	25	K25
0.12	0.06	0.12	0.004	π/2	30	K30

$$+\bar{a}_{315}\cdot\Psi_0+\bar{a}_{316}\cdot\Psi_0)\overline{w}+(\bar{a}_{38}\cdot\Psi_2+\bar{a}_{39}\cdot\Psi_1+\bar{a}_{310}\cdot\Psi_0)\overline{w}'$$

$$+(\bar{a}_{35}\cdot\Psi_2+\bar{a}_{36}\cdot\Psi_1+\bar{a}_{37}\cdot\Psi_0)\overline{w}''+(\bar{a}_{34}\cdot\Psi_0)\overline{w}'''\},\qquad(5.12)$$

where $u_i^{(k)}=u^{(k)}(\theta,\xi_i)$, $v_i^{(k)}=v^{(k)}(\theta,\xi_i)$, $w_i^{(l)}=w^{(l)}(\theta,\xi_i)$ $(k=0,\dots,1,\ l=0,\dots,3,\ i=0,\dots,N)$.

This system of ordinary differential equations can be represented in normal form:

$$\frac{d\overline{Y}}{d\theta}=A(\theta,\omega)\overline{Y}\qquad(0\le\theta\le b),\qquad(5.13)$$

where $Y^T=\{u_0,\dots,u_N,u_0',\dots,u_N',v_0,\dots,v_N,v_0',\dots,v_N',w_0,\dots,w_N,w_0',\dots,w_N',w_0'',\dots,w_N'',w_0''',\dots,w_N'''\}$, $A(\theta,p)$ is a $8(N+1)\times 8(N+1)$ matrix.

The boundary conditions (5.6)–(5.9) for system (5.13) can be represented as

$$B_1\overline{Y}(0)=\overline{0},\quad B_2\overline{Y}(b)=\overline{0}.\qquad(5.14)$$

The eigenvalue problem for the system of ordinary differential equations (5.13) with the boundary conditions (5.14) is solved with the discrete-orthogonalization and incremental search methods.

This approach was used to analyze the natural frequency spectrum of isotropic conical panels.

Analysis of the Numerical Results. Consider non-closed isotropic conical shells (panels) defined by eight sets of geometrical parameters collected in Table 8, where L is the length of the generatrix; R_1 and R_2 are the radii of the bases; b is the cone angle; β_k is the taper angle. The thickness of the shells varies as

$$h=h_0(1+\alpha\cos\theta)\qquad(-0.5\le\alpha\le 0.5),\qquad(5.15)$$

where h_0 is the thickness of a shell of constant thickness and equivalent mass. The shells are made of steel with the following material characteristics: $E=2.14\cdot10^{11}$ Pa, $\nu=0.2588$, $\rho=7850$ kg/m^3.

The conical panels are subject to the following boundary conditions (5.6)–(5.9):

G_1: all the edges are clamped (conditions (5.6), (5.8));

G_2: three edges are clamped (conditions (5.6) both (5.8) at $\theta=b$) and the fourth edge is hinged (condition (5.7) at $\theta=0$);

G_3: the edges $s=$const are clamped (conditions (5.6)) and the edges $\theta=$const are hinged (conditions (5.9)).

TABLE 9

i	A	B	E, %	C	E, %	D	E, %
1	3501.92	3489.15	0.36	3485.65	0.46	3480.40	0.61
2	5176.39	5167.92	0.16	5166.65	0.19	5162.83	0.26
3	5479.31	5474.13	0.09	5469.52	0.18	5456.79	0.41
4	7082.30	7081.76	0.01	7079.53	0.04	7070.94	0.16

TABLE 10

i	α					
	–0.2			–0.1		
	A	C	E, %	A	C	E, %
1	3146.49	3142.51	0.13	3261.88	3258.22	0.11
2	4464.61	4463.34	0.03	4779.10	4777.83	0.03
3	5107.28	5102.03	0.10	5110.15	5104.74	0.11
4	6553.05	6550.98	0.03	6767.75	6765.68	0.03
i	0.1			0.2		
	A	C	E, %	A	C	E, %
1	3494.41	3491.22	0.09	3612.02	3609.16	0.08
2	5114.44	5109.19	0.10	5117.15	5111.90	0.10
3	5394.24	5392.81	0.03	5695.68	5694.25	0.03
4	7141.92	7140.17	0.02	7319.22	7317.79	0.02

The frequencies obtained using the spline-collocation method with different number of collocation points ($N = 10, N = 12, N = 14, N = 16$) differ by no greater than 3%. Since the frequencies calculated using $N \geq 12$ collocation points differ a little, we will discuss the values obtained with $N = 12$.

The reliability of the results is tested by comparing the frequencies of free bending vibrations of a cylindrical shell of constant thickness (C1 in Table 8) and conical shells of equivalent mass (K2.5 and K5 in Table 8) hinged at all edges. With such a problem formulation, it is possible to derive analytic expressions for the frequencies of a cylindrical panel.

Table 9 summarizes the frequencies ω_i, Hz of flexural vibrations of a cylindrical shell and conical shells of equivalent mass with all edges hinged calculated analytically (A) and with the spline-collocation method (B, C, D). Here the frequencies of the cylindrical shell (C1) obtained analytically are in column A; the frequencies for the cylindrical shell (C1) calculated with the spline-collocation method are in column B; the frequencies of the conical shells K2.5 and K5 obtained with the spline-collocation method are in columns C and D, respectively; the relative difference between analytic and numerical results

TABLE 11

Boundary conditions	i	α					
		–0.5	–0.4	–0.3	–0.2	–0.1	0
G_1	1	4.583	4.821	5.019	5.203	5.380	5.554
	2	4.740	5.074	5.410	5.732	6.035	6.317
	3	7.063	7.526	7.908	8.249	8.573	8.889
	4	7.158	7.620	8.049	8.444	8.789	9.077
	i	0.1	0.2	0.3	0.4	0.5	0
	1	5.726	5.896	6.067	6.237	6.407	—
	2	6.577	6.815	7.031	7.225	7.398	—
	3	9.197	9.468	9.682	9.890	10.10	—
	4	9.308	9.543	9.825	10.07	10.29	—
G_2	i	–0.5	–0.4	–0.3	–0.2	–0.1	0
	1	3.963	4.074	4.202	4.313	4.425	4.536
	2	4.425	4.759	5.061	5.364	5.634	5.889
	3	6.127	6.557	6.812	6.971	7.098	7.242
	4	6.875	7.226	7.480	7.703	7.910	8.117
	i	0.1	0.2	0.3	0.4	0.5	0
	1	4.647	4.743	4.854	4.966	5.077	—
	2	6.096	6.271	6.414	6.525	6.637	—
	3	7.417	7.608	7.846	8.101	8.372	—
	4	8.308	8.499	8.674	8.849	9.008	—
G_3	i	–0.5	–0.4	–0.3	–0.2	–0.1	0
	1	3.470	3.629	3.772	3.915	4.058	4.186
	2	3.979	4.299	4.617	4.939	5.258	5.523
	3	5.379	5.411	5.443	5.459	5.491	5.575
	4	5.777	6.382	6.907	7.257	7.576	7.846
	i	0.1	0.2	0.3	0.4	0.5	0
	1	4.313	4.456	4.584	4.711	4.838	—
	2	5.539	5.570	5.602	5.634	5.682	—
	3	5.890	6.201	6.511	6.818	7.127	—
	4	8.101	8.340	8.563	8.769	8.960	—

are given in column E. As is seen, the maximum difference between numerical and analytic results does not exceed 0.4%, which is indicative of the adequate accuracy of the numerical approach.

The natural frequencies of hinged cylindrical and conical shells with thickness varying as in (5.15) were determined as a test problem. The calculated results are collected in Table 10, where the frequencies of the cylindrical panel are in column A; the frequencies of the conical panel are in column C; the relative difference between the frequencies of columns A and C are in column E. The difference between the frequencies of the cylindrical and conical panels does not exceed 0.15%.

The natural frequencies of conical shells of variable thickness are summarized in Table 11 for a cone angle of 10° (K10 in Table 1), in Table 5 for a cone angle of 20° (K20 in Table 1), and in Table 6 for a cone angle of 30° (K30 in Table 1). Various boundary conditions were examined.

Tables 11–13 show how the thickness affects the dynamic characteristics of conical shells and allow analyzing the difference of the natural frequencies of conical shells with variable thickness and constant thickness. This difference increases with increase in the parameter α and in the frequencies.

The frequency is strongly dependent on the parameter α. For example, the frequencies of shells of variable thickness with $|\alpha| = 0.5$ differ from that of a shell of constant thickness and equivalent mass by 12% to 25%, depending on the type of boundary conditions. Thus, minor alterations of the thickness may cause considerable changes in the dynamic characteristics of shells comparable (in order of magnitude) with the effect of boundary conditions.

Tables 11–13 show how the boundary conditions affect the spectrum of natural frequencies. It can be seen that the more edges are clamped, the higher the frequency. The boundary conditions of type G_3 (edges $s = \text{const}$ are clamped and edges $\theta = \text{const}$ are hinged), the second and third frequencies approach each other as the mid-surface shape tends to that of the conical shell of constant thickness.

For all boundary conditions, the natural frequency of the shell decreases with increasing cone angle. Note that the effect of these changes is an order of magnitude weaker than the effect of the thickness of the shell and the type of boundary conditions. The frequencies of shells with cone angles of 10 and 30° differ by 5–7%. The greater the cone angle, the sharper the change of the natural frequencies.

Figures 15–18 show mode shapes corresponding to four natural frequencies of shells with one edge hinged and three edges clamped. As can be seen, the first natural frequency corresponds to two circumferential half-waves and one longitudinal half-wave; the second frequency to three circumferential half-waves and one longitudinal half-wave; the third frequency to one longitudinal half-wave and four circumferential half-waves; and the fourth frequency corresponds to two circumferential half-waves and two meridional half-waves.

These results are indicative of the high efficiency of the spline-collocation method when applied to analyze the natural frequency spectrum of thin conical shells (panels) with arbitrarily varying thickness. The free vibrations of conical shells with thickness varying in one or two directions are analyzed in more detail using the classical theory in [13, 14, 46].

6. Stress–Strain State of Noncircular Cylindrical Shells (Refined Formulation). Consider nonthin orthotropic noncircular cylindrical shells. We will use the refined theory of shells based on the straight-line hypothesis [21, 31].

To describe the coordinate surface of the shell, we will use an orthogonal coordinate system s, t, where s and t are the longitudinal and circumferential coordinates, and γ is the normal to this surface. From the general equations presented in [21], we derive the kinematic equations

$$\varepsilon_s = \frac{\partial u}{\partial s}, \quad \varepsilon_t = \frac{\partial v}{\partial t} + k(t)w, \quad \varepsilon_{st} = \frac{\partial u}{\partial t} + \frac{\partial v}{\partial s},$$

$$\kappa_s = \frac{\partial \psi_s}{\partial s}, \quad \kappa_t = \frac{\partial \psi_t}{\partial t} - k(t)\left(\frac{\partial v}{\partial t} + k(t)w\right), \quad 2\kappa_{st} = \frac{\partial \psi_s}{\partial t} + \frac{\partial \psi_t}{\partial s} - k(t)\frac{\partial u}{\partial t},$$

$$\gamma_s = \psi_s - \vartheta_s, \quad \gamma_t = \psi_t - \vartheta_t, \quad \vartheta_s = -\frac{\partial w}{\partial s}, \quad \vartheta_t = -\frac{\partial w}{\partial t} + k(t)v, \tag{6.1}$$

where $\varepsilon_s, \varepsilon_t, \varepsilon_{st}$ are the tangential strains of the coordinate surface; $\kappa_s, \kappa_t, \kappa_{st}$ are the bending strains of the coordinate surface; u, v, w are displacements; φ_s, φ_t are the complete angles of rotation of the normal; $k(t)$ is the curvature of the directrix; ϑ_s, ϑ_t are the angles of rotation of the normal without the effect of transverse shear; γ_s, γ_t are the angles of rotation of the normal caused by transverse shear.

TABLE 12

Boundary conditions	i	α					
		–0.5	–0.4	–0.3	–0.2	–0.1	0
	1	4.498	4.724	4.921	5.107	5.287	5.464
	2	4.678	5.019	5.351	5.665	5.958	6.228
	3	6.927	7.367	7.745	8.095	8.430	8.713
	4	6.995	7.523	7.970	8.321	8.536	8.760
G_1	i	0.1	0.2	0.3	0.4	0.5	0
	1	5.639	5.813	5.987	6.160	6.334	—
	2	6.474	6.695	6.893	7.069	7.225	—
	3	8.899	9.097	9.308	9.532	9.763	—
	4	9.083	9.403	9.685	9.908	10.12	—
	i	–0.5	–0.4	–0.3	–0.2	–0.1	0
	1	3.883	4.011	4.122	4.234	4.345	4.456
	2	4.377	4.711	5.013	5.300	5.570	5.793
	3	5.984	6.382	6.605	6.764	6.891	7.051
	4	6.812	7.114	7.353	7.576	7.783	7.990
G_2	i	0.1	0.2	0.3	0.4	0.5	0
	1	4.568	4.679	4.791	4.902	5.013	—
	2	5.984	6.143	6.271	6.398	6.494	—
	3	7.242	7.464	7.703	7.974	8.260	—
	4	8.196	8.372	8.563	8.722	8.897	—
	i	–0.5	–0.4	–0.3	–0.2	–0.1	0
	1	3.390	3.565	3.708	3.852	3.979	4.122
	2	3.947	4.265	4.584	4.919	5.239	5.348
	3	5.188	5.236	5.268	5.284	5.316	5.556
	4	5.682	6.271	6.780	7.130	7.433	7.719
G_3	i	0.1	0.2	0.3	0.4	0.5	0
	1	4.265	4.393	4.536	4.663	4.806	—
	2	5.379	5.411	5.443	5.475	5.523	—
	3	5.857	6.175	6.478	6.780	7.082	—
	4	7.990	8.228	8.451	8.658	8.849	—

TABLE 13

Boundary conditions	i	α					
		–0.5	–0.4	–0.3	–0.2	–0.1	0
	1	4.326	4.543	4.742	4.931	5.116	5.299
	2	4.566	4.906	5.226	5.523	5.792	6.035
	3	6.631	7.065	7.416	7.669	7.873	8.078
	4	6.831	7.346	7.594	7.880	8.211	8.549
G_1	i	0.1	0.2	0.3	0.4	0.5	0
	1	5.480	5.660	5.839	6.018	6.197	—
	2	6.249	6.437	6.602	6.747	6.875	—
	3	8.296	8.528	8.775	9.031	9.292	—
	4	8.885	9.149	9.363	9.573	9.786	—
	i	–0.5	–0.4	–0.3	–0.2	–0.1	0
	1	3.746	3.868	3.987	4.106	4.225	4.342
	2	4.290	4.617	4.920	5.194	5.431	5.626
	3	5.748	6.053	6.238	6.388	6.550	6.743
	4	6.605	6.872	7.110	7.343	7.566	7.776
G_2	i	0.1	0.2	0.3	0.4	0.5	0
	1	4.458	4.571	4.682	4.788	4.891	—
	2	5.782	5.911	6.024	6.128	6.231	—
	3	6.971	7.228	7.504	7.790	8.082	—
	4	7.972	8.157	8.333	8.504	8.673	—
	i	–0.5	–0.4	–0.3	–0.2	–0.1	0
	1	3.263	3.422	3.581	3.724	3.867	4.011
	2	3.899	4.218	4.552	4.870	4.997	5.029
	3	4.854	4.902	4.934	4.966	5.188	5.507
	4	5.539	6.112	6.557	6.891	7.210	7.512
G_3	i	0.1	0.2	0.3	0.4	0.5	0
	1	4.154	4.297	4.440	4.584	4.711	—
	2	5.061	5.093	5.141	5.188	5.236	—
	3	5.825	6.127	6.430	6.732	7.035	—
	4	7.799	8.053	8.260	8.451	8.626	—

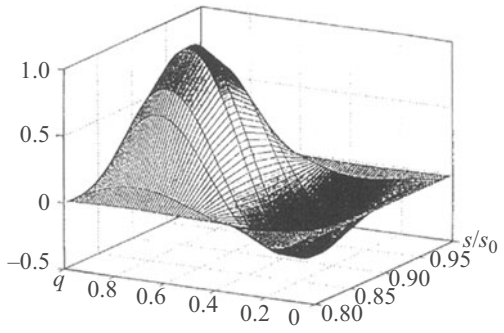

Fig. 15

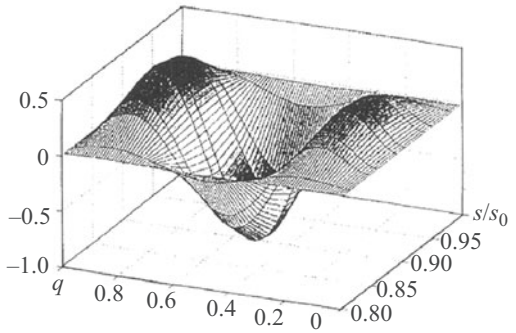

Fig. 16

The equilibrium equations are

$$\frac{\partial N_s}{\partial s}+\frac{\partial N_{ts}}{\partial t}+q_s=0, \qquad \frac{\partial N_t}{\partial t}+\frac{\partial N_{st}}{\partial s}+k(t)Q_t+q_t=0,$$

$$\frac{\partial Q_s}{\partial s}+\frac{\partial Q_t}{\partial t}-k(t)N_t+q_\gamma=0, \qquad \frac{\partial M_s}{\partial s}+\frac{\partial M_{ts}}{\partial t}-Q_s=0,$$

$$\frac{\partial M_t}{\partial t}+\frac{\partial M_{st}}{\partial s}-Q_t=0, \qquad N_{st}-k(t)M_{ts}-N_{ts}=0, \tag{6.2}$$

where N_s, N_t, N_{st}, N_{ts} are the tangential forces; Q_s, Q_t are the shearing forces; M_s, M_t, M_{st}, M_{ts} are the bending and twisting moments; q_s, q_t, q_γ are the components of the surface load.

The constitutive equations for orthotropic shells symmetric about the chosen coordinate surface are

$$N_s=C_{11}\varepsilon_s+C_{12}\varepsilon_t, \qquad N_t=C_{12}\varepsilon_s+C_{22}\varepsilon_t,$$

$$N_{st}=C_{66}\varepsilon_{st}+2k(t)D_{66}\kappa_{st}, \qquad N_{ts}=C_{66}\varepsilon_{st},$$

$$M_s=D_{11}\kappa_s+D_{12}\kappa_t, \qquad M_t=D_{12}\kappa_s+D_{22}\kappa_t, \qquad M_{ts}=M_{st}=2D_{66}\kappa_{st},$$

$$Q_s=K_1\gamma_s, \qquad Q_t=K_2\gamma_t, \tag{6.3}$$

where

$$C_{11}=\frac{E_s h}{1-\nu_s\nu_t}, \qquad C_{12}=\nu_t C_{11}, \qquad C_{22}=\frac{E_t h}{1-\nu_s\nu_t}, \qquad C_{66}=G_{st}h,$$

$$D_{11}=\frac{E_s h^3}{12(1-\nu_s\nu_t)}, \qquad D_{12}=\nu_t D_{11}, \qquad D_{22}=\frac{E_t h^3}{12(1-\nu_s\nu_t)}, \qquad D_{66}=\frac{G_{st}h^3}{12},$$

$$K_1=\frac{5}{6}hG_{s\gamma}, \qquad K_2=\frac{5}{6}hG_{t\gamma}, \tag{6.4}$$

where E_s, E_t, ν_s, ν_t are the elastic moduli and Poisson's ratios in the directions s and t; G_{st}, $G_{s\gamma}$, $G_{t\gamma}$ are the shear moduli; $h = h(s, t)$ is the thickness of the shell.

To solve such a two-dimensional boundary-value problem, we will approximate the candidate solution by spline functions in one coordinate direction and will solve the resulting one-dimensional boundary-value problem with the stable numerical discrete-orthogonalization method. This approach allows solving problems for various boundary conditions on each edge of the shell. The governing system of equations is

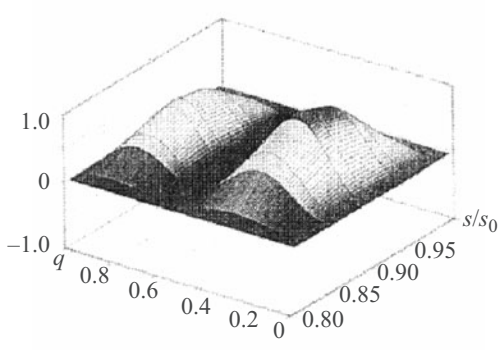

Fig. 17

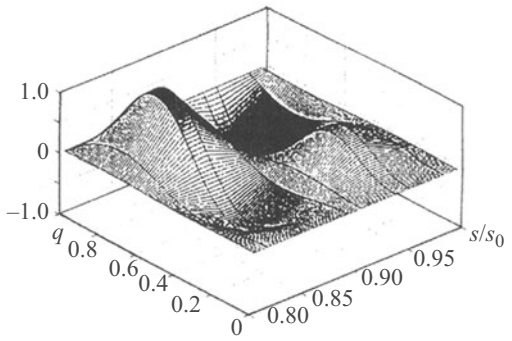

Fig. 18

$$\frac{\partial^2 u}{\partial t^2} = a_{11}\frac{\partial^2 u}{\partial s^2} + a_{12}\frac{\partial u'}{\partial s} + a_{13}\frac{\partial w}{\partial s} + a_{14}\frac{\partial v}{\partial s} + a_{15}\frac{\partial u}{\partial s} + a_{16}v' + a_{17}w + a_{18}u' + a_{19}q_s,$$

$$\frac{\partial^2 v}{\partial t^2} = a_{21}\frac{\partial u'}{\partial s} + a_{22}v + a_{23}\frac{\partial^2 v}{\partial s^2} + a_{24}w + a_{25}w' + a_{26}\frac{\partial \psi'_s}{\partial s} + a_{27}\psi_t + a_{28}\frac{\partial^2 \psi_t}{\partial s^2}$$

$$+ a_{29}\frac{\partial \psi_t}{\partial s} + a_{2,10}\frac{\partial u}{\partial s} + a_{2,11}v' + a_{2,12}u' + a_{2,13}\frac{\partial v}{\partial s} + a_{2,14}\psi'_s + a_{2,15}q_t,$$

$$\frac{\partial^2 w}{\partial t^2} = a_{31}\frac{\partial u}{\partial s} + a_{32}v + a_{33}v' + a_{34}w + a_{35}\frac{\partial^2 w}{\partial s^2} + a_{36}\frac{\partial \psi_s}{\partial s} + a_{37}\psi'_t + a_{38}\psi_t$$

$$+ a_{39}\psi_s + a_{3,10}\frac{\partial w}{\partial s} + a_{3,11}w' + a_{3,12}q_\gamma,$$

$$\frac{\partial^2 \psi_s}{\partial t^2} = a_{41}u' + a_{42}\frac{\partial^2 u}{\partial s^2} + a_{43}\frac{\partial v'}{\partial s} + a_{44}\frac{\partial w}{\partial s} + a_{45}\psi_s + a_{46}\frac{\partial^2 \psi_s}{\partial s^2} + a_{47}\frac{\partial \psi'_t}{\partial s} + a_{48}\frac{\partial \psi_t}{\partial s}$$

$$+ a_{49}\frac{\partial u}{\partial s} + a_{4,10}v' + a_{4,11}w + a_{4,12}\frac{\partial v}{\partial s} + a_{4,13}\frac{\partial \psi_s}{\partial s} + a_{4,14}\psi'_t + a_{4,15}\psi'_s + a_{4,16}q_s,$$

$$\frac{\partial^2 \psi_t}{\partial t^2} = a_{51}\frac{\partial u'}{\partial s} + a_{52}v + a_{53}v' + a_{54}\frac{\partial^2 v}{\partial s^2} + a_{55}w + a_{56}w' + a_{57}\frac{\partial \psi'_s}{\partial s} + a_{58}\psi_t + a_{59}\frac{\partial^2 \psi_t}{\partial s^2}$$

$$+ a_{5,10}\psi'_t + a_{5,11}\frac{\partial u}{\partial s} + a_{5,12}u' + a_{5,13}\frac{\partial v}{\partial s} + a_{5,14}\psi'_s + a_{5,15}\frac{\partial \psi_t}{\partial s} + a_{5,16}\frac{\partial \psi_s}{\partial s} + a_{5,17}q_t. \qquad (6.5)$$

The expressions for the coefficients a_{ij} can be found in [87].

Supplementing the system of governing equations (6.5) with boundary conditions on all edges for open shells and with boundary conditions on the curved edges and periodicity conditions along the circumference for closed shells, we arrive at a two-dimensional boundary-value problem.

The system of equations (6.5) includes no higher than 2nd-order derivatives of the unknown functions with respect to s. On this basis, we can use cubic splines to approximate the solutions with respect to the coordinate s. Then the candidate solution of the boundary-value problem for the system of equations (6.5) can be represented as

$$u(s,t) = \sum_{i=o}^{N} u_i(t)\varphi_{1i}(s), \qquad v(s,t) = \sum_{i=o}^{N} v_i(t)\varphi_{2i}(s), \qquad w(s,t) = \sum_{i=o}^{N} w(t)_i\,\varphi_{3i}(s),$$

$$\psi_s(s,t)=\sum_{i=o}^{N}\psi_{si}(t)\varphi_{4i}(s),\qquad \psi_t(s,t)=\sum_{i=o}^{N}\psi_{ti}(t)\varphi_{5i}(s), \tag{6.6}$$

where $u_i(t)$, $v_i(t)$, $w_i(t)$, $\psi_{si}(t)$, $\psi_{ti}(t)$ are the unknown functions of variable t; $\varphi_{ji}(s)$ ($j=\overline{1,5}$) are linear combinations of cubic B-splines over a uniform partition Δ: $0=s_0<s_1<\ldots<s_N=L$ that satisfy the boundary conditions on the curved edges $s=0$ and $s=L$.

The following boundary conditions are prescribed on the curved edges s = const:

(i) edge is clamped:

$$u=v=w=\psi_s=\psi_t=0; \tag{6.7}$$

(ii) edge is hinged and is free in the longitudinal direction:

$$N_s=v=w=M_s=\psi_t=0 \quad \text{or} \quad \frac{\partial u}{\partial s}=v=w=\frac{\partial \psi_s}{\partial s}=\psi_t=0; \tag{6.8}$$

(iii) edge is clamped and is free in the normal direction:

$$u=N_{st}=Q_s=\psi_s=M_{st}=0 \quad \text{or} \quad u=\frac{\partial v}{\partial s}=\frac{\partial w}{\partial s}=\psi_s=\frac{\partial \psi_t}{\partial s}=0; \tag{6.9}$$

(iv) edge is hinged:

$$u=v=w=M_s=Q_t=0 \quad \text{or} \quad u=v=w=\frac{\partial \psi_s}{\partial s}=\psi_t=0. \tag{6.10}$$

Since the boundary conditions (6.7)–(6.10) contain only unknown functions and their first derivatives, which are equated to zero, on the edge s = const they can be represented in terms of B-splines:

(a) if the unknown function is equal to zero, then

$$\varphi_{j0}(s)=-4B_3^{-1}(s)+B_3^0(s),$$

$$\varphi_{j1}(s)=B_3^{-1}(s)-\frac{1}{2}B_3^0(s)+B_3^1(s),$$

$$\varphi_{ji}(s)=B_3^i(s) \quad (i=2,3,\ldots,N-2); \tag{6.11}$$

(b) if the derivative of the unknown function with respect to s is equal to zero, then

$$\varphi_{j0}(s)=B_3^0(s),$$

$$\varphi_{j1}(s)=B_3^{-1}(s)-\frac{1}{2}B_3^0(s)+B_3^1(s),$$

$$\varphi_{ji}(s)=B_3^i(s) \quad (i=2,3,\ldots,N-2). \tag{6.12}$$

The functions $\varphi_{j,\,N-1}(s)$ and $\varphi_{j,N}(s)$ are represented in a similar way.

Substituting solution (6.6) into the governing system of equations (6.5) and requiring them to be satisfied on $N+1$ lines $s=\xi_i$ ($i=\overline{1,N+1}$), according to the spline-collocation method, we obtain a system of ordinary differential equations of order $10(N+1)$:

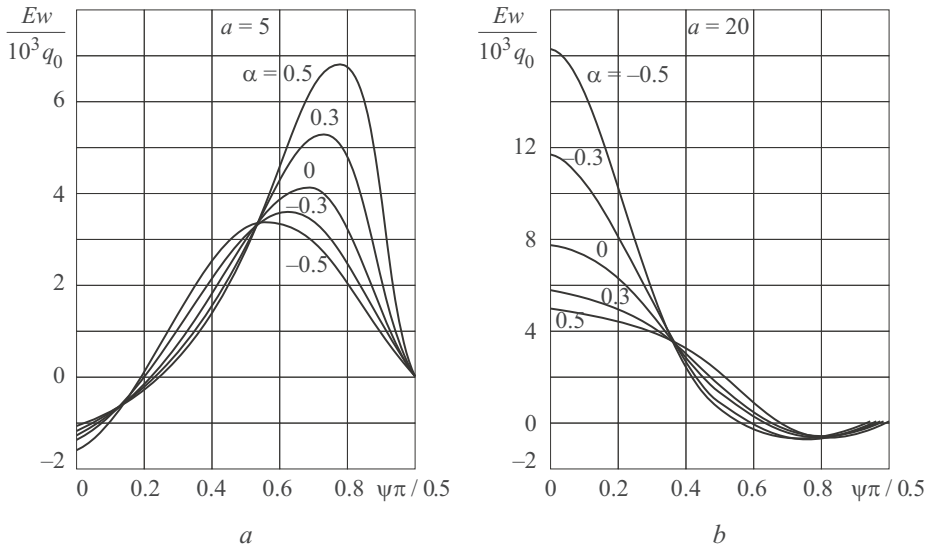

Fig. 19

$$\frac{d\bar{R}}{dt} = A\bar{R} + \bar{f} \tag{6.13}$$

$$(\bar{R} = \{u_0, \ldots, u_N,\ u'_0, \ldots, u'_N,\ v_0, \ldots, v_N,\ v'_0, \ldots, v'_N,\ w_0, \ldots, w_N,\ w'_0, \ldots, w'_N,$$

$$\psi_{s0}, \ldots, \psi_{sN},\ \psi'_{s0}, \ldots, \psi'_{sN},\ \psi_{t0}, \ldots, \psi_{tN},\ \psi'_{t0}, \ldots, \psi'_{tN}\}^T),$$

where $\bar{R}$ is a vector function of t; $\bar{f}$ is the vector of right-hand sides; A is a square matrix whose elements depend on t.

The boundary conditions on the straight edges t_1 and t_2 of longitudinally open shells are

$$A_1\bar{R}(t_1) = \bar{a}_1, \qquad A_2\bar{R}(t_2) = \bar{a}_2. \tag{6.14}$$

The resulting one-dimensional boundary-value problem (6.13), (6.14) is solved by the stable numerical discrete-orthogonalization method.

Let us use this approach to determine the stress–strain state of an open transversely isotropic elliptic cylindrical shell with thickness varying in the longitudinal direction under a uniform normal load $q_\gamma = q_0 = \text{const}$. The shell is clamped along the entire boundary. The cross-section of the coordinate surface of the shell is defined parametrically:

$$x = b\cos\psi, \qquad z = a\sin\psi \qquad (-\pi/2 \le \psi \le \pi/2), \tag{6.15}$$

where a and b are the ellipse semiaxes; ψ is the angle. The coordinate t is transformed into the coordinate θ for the function $v(t(\theta))$ as follows:

$$\frac{dt}{d\theta} = \sqrt{\left(\frac{dx}{d\theta}\right)^2 + \left(\frac{dz}{d\theta}\right)^2} = \omega(\theta), \qquad \frac{\partial v}{\partial t} = \frac{1}{\omega(\theta)}\frac{\partial v}{\partial \theta}, \qquad \frac{\partial v}{\partial \theta} = \frac{\partial v}{\partial t}\frac{\partial t}{\partial \theta}. \tag{6.16}$$

It is assumed that the ellipse area remains invariable and equals the area of a circle of radius R, i.e., $ab = R^2 = \text{const}$. The thickness of the shell varies in the circumferential direction as $h(\psi) = h_0(1 + \alpha\cos 2\psi)$ so that the weight of the shell remains constant with variation in α. The transverse shear modulus of the shell material is given by $G' = E / d$, where E is the elastic modulus in the isotropy plane.

We will study the influence of the variation in the thickness (the weight being kept constant) of the shell with the following parameters on the circumferential distribution of deflection and stress: $L = 30$, $h_0 = 1$, $R = 10$, $a = 5, 20$, $d = 40$, $\nu = 0.3$, $\alpha = 0, \pm 0.3, \pm 0.5$.

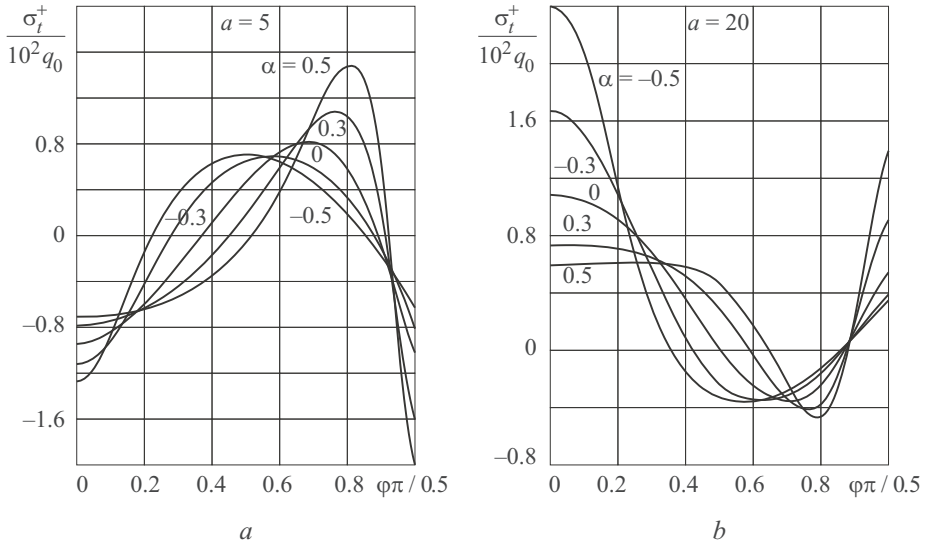

Fig. 20

This problem is described by the system of partial differential equations with variable coefficients (6.5). The boundary conditions (6.7)–(6.10) are prescribed on the edges of the shell.

Figures 19–21 show the deflections and stresses on the lateral surfaces of the shell in the section $s = L/2$ depending on its thickness. From Fig. 19*a* it follows that for an ellipse with $a = 5$ the deflection is maximum near the straight edge and increases with α (by a factor of more than 1.5 at $\alpha = 0.5$), i.e., with the thickness near the major vertex of the ellipse. As this thickness decreases, the deflection decreases insignificantly. The stiffer vertex shifts in the opposite direction to the applied load. Figure 19*b* demonstrates that the pattern is very different when $a = 20$: the maximum deflection is near the minor vertex of the ellipse and increases (by a factor of more than 2 at $\alpha = -0.5$) with decrease in α, i.e., the thickness of the shell near this vertex. As this thickness increases ($\alpha = 0.3, 0.5$), the deflection decreases insignificantly.

Figure 20 shows how the stresses on the outside surface of the shell vary with its thickness. It is seen from Fig. 20*a* that the maximum value of σ_t^+ increases with α (its value at $\alpha = 0.5$ is almost double that at $\alpha = 0$). Figure 20*b* shows that the stress is maximum at the minor vertex of the ellipse. The stress at $\alpha = -0.5$ is more than double that at $\alpha = 0$.

The stress pattern on the inside surface of the shell with $a = 5$ in Fig. 21*a* is qualitatively similar to that in Fig. 20*a*, but has opposite sign. Quantitatively, the maximum stress σ_t^- is more than twice as high as the stress σ_t^+. It can be seen from Fig. 21*b* that at $a = 20$, the stress σ_t^- is almost half the stress σ_t^+. The stress σ_t^- is maximum near the straight edge of the shell with $a = 5$.

Thus, by changing the thickness of a shell keeping its weight constant, it is possible to influence the distribution of displacements and stresses.

The static behavior of nonthin noncircular shells was studied in [88–91].

7. Stress State of Conical Shells of Variable Thickness (Refined Formulation). Let us determine the stress state of nonthin orthotropic conical shells under distributed surface and local loads, using a refined theory based on the straight-line hypothesis [21]. To describe the shell, we will use an orthogonal coordinate system s, θ, γ, where s = const and θ = const are the lines of curvature of the coordinate surface, and γ is the normal coordinate to the coordinate surface.

The coordinate surface of the conical shell is described by the first quadratic form $dS^2 = ds^2 + r^2 d\theta^2$, where r is the radius given by $r = r_0 + \cos\varphi \cdot s$, r_0 is the radius of the datum plane, φ is the angle between the normal and the axis of revolution, φ is the radius of curvature $R_\theta = r/\sin\varphi$.

From the general equations presented in [24], we derive the kinematic equations

$$\varepsilon_s = \frac{\partial u}{\partial s}, \quad \varepsilon_\theta = \frac{1}{r}\left(\frac{\partial v}{\partial \theta} + u\cos\varphi + w\sin\varphi\right), \quad \varepsilon_{s\theta} = \frac{1}{r}\frac{\partial u}{\partial \theta} + r\frac{\partial}{\partial s}\left(\frac{v}{r}\right),$$

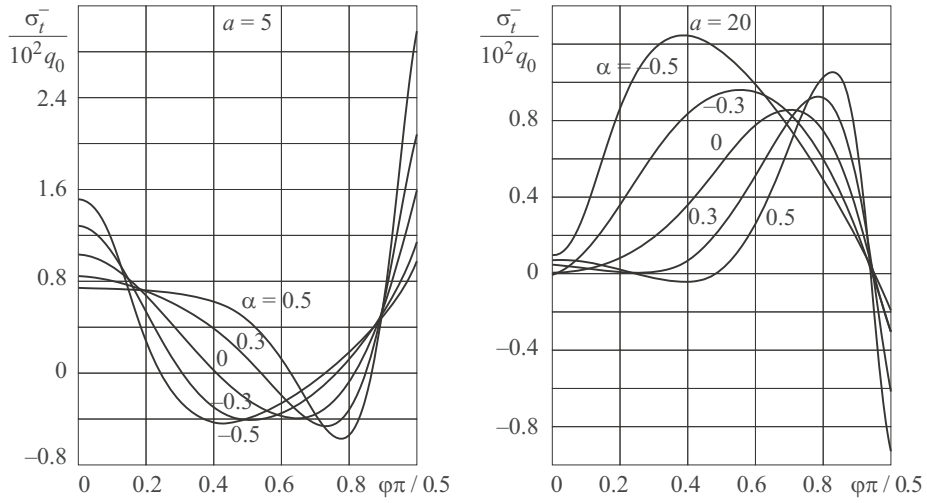

Fig. 21

$$\kappa_s = \frac{\partial \psi_s}{\partial s}, \quad \kappa_\theta = \frac{1}{r}\left\{ \frac{\partial \psi_\theta}{\partial \theta} + \psi_s \cos\varphi - \frac{\sin\varphi}{r}\left(\frac{\partial v}{\partial \theta} + u\cos\varphi + w\sin\varphi \right) \right\},$$

$$2\kappa_{s\theta} = \frac{1}{r}\frac{\partial \psi_s}{\partial \theta} + r\frac{\partial}{\partial s}\left(\frac{\psi_\theta}{r} \right) - \frac{\sin\varphi}{r^2}\left(\frac{\partial u}{\partial \theta} - v\cos\varphi \right),$$

$$\gamma_s = \psi_s - \vartheta_s, \quad \gamma_\theta = \psi_\theta - \vartheta_\theta, \quad \vartheta_s = -\frac{\partial w}{\partial s}, \quad \vartheta_\theta = -\frac{1}{r}\frac{\partial w}{\partial \theta} + \frac{v\sin\varphi}{r}, \tag{7.1}$$

where ε_s, ε_θ, $\varepsilon_{s\theta}$ are the tangential strains of the coordinate surface; κ_s, κ_θ, $\kappa_{s\theta}$ are the bending strains of the coordinate surface; ϑ_s, ϑ_θ are the angles of rotation of the normal without the effect of transverse shear; γ_s, γ_θ are the angles of rotation of the normal caused by transverse shear; u, v, w are the displacements; ψ_s, ψ_θ are the complete angles of rotation of the normal.

The equilibrium equations are

$$\cos\varphi N_s + r\frac{\partial N_s}{\partial s} - \cos\varphi N_\theta + \frac{\partial N_{\theta s}}{\partial \theta} + rq_s = 0,$$

$$\frac{\partial N_\theta}{\partial \theta} + \cos\varphi N_{s\theta} + r\frac{\partial N_{s\theta}}{\partial s} + \cos\varphi N_{\theta s} + \sin\varphi Q_\theta + rq_\theta = 0,$$

$$\cos\varphi Q_s + r\frac{\partial Q_s}{\partial s} + \frac{\partial Q_\theta}{\partial \theta} - \sin\varphi N_\theta + rq_\gamma = 0,$$

$$r\frac{\partial M_s}{\partial s} + \cos\varphi M_s - \cos\varphi M_\theta + \frac{\partial M_{\theta s}}{\partial \theta} - rQ_s = 0,$$

$$\frac{\partial M_\theta}{\partial \theta} + (M_{s\theta} + M_{\theta s})\cos\varphi + r\frac{\partial M_{s\theta}}{\partial s} - rQ_\theta = 0, \tag{7.2}$$

where N_s, N_θ, $N_{s\theta}$, $N_{\theta s}$ are the tangential forces; Q_s, Q_θ are the shearing forces; M_s, M_θ, $M_{s\theta}$, $M_{\theta s}$ are the bending and twisting moments; q_s, q_θ, q_γ are the components of the surface load.

The constitutive equations are

$$N_s = C_{11}\varepsilon_s + C_{12}\varepsilon_\theta, \quad N_\theta = C_{12}\varepsilon_s + C_{22}\varepsilon_\theta, \quad N_{s\theta} = C_{66}\varepsilon_{s\theta} + \frac{2\sin\varphi}{r}D_{66}\kappa_{s\theta},$$

$$N_{\theta s} = C_{66}\varepsilon_{s\theta}, \quad M_s = D_{11}\kappa_s + D_{12}\kappa_\theta, \quad M_\theta = D_{12}\kappa_s + D_{22}\kappa_\theta,$$

$$M_{\theta s} = M_{s\theta} = 2D_{66}\kappa_{s\theta}, \quad Q_s = K_1\gamma_s, \quad Q_\theta = K_2\gamma_\theta, \tag{7.3}$$

$$\left(C_{11} = \frac{E_s h}{1-\nu_s\nu_\theta}, \quad C_{12} = \nu_\theta C_{11}, \quad C_{22} = \frac{E_\theta h}{1-\nu_s\nu_\theta}, \quad C_{66} = G_{s\theta}h, \quad D_{11} = \frac{E_s h^3}{12(1-\nu_s\nu_\theta)}, \right.$$

$$\left. D_{12} = \nu_\theta D_{11}, \quad D_{22} = \frac{E_\theta h^3}{12(1-\nu_s\nu_\theta)}, \quad D_{66} = \frac{G_{s\theta}h^3}{12}, \quad K_1 = \frac{5}{6}hG_{s\gamma}, \quad K_2 = \frac{5}{6}hG_{\theta\gamma} \right), \tag{7.4}$$

where E_s, E_θ, ν_s, ν_θ are the elastic moduli and Poisson's ratios in the directions s and θ; $G_{s\theta}$, $G_{s\gamma}$, $G_{\theta\gamma}$ are the shear moduli; $h = h(s, \theta)$ is the thickness of the shell.

From formulas (7.1)–(7.4), we derive a governing system of partial differential equations for displacements describing the stress–strain state of conical shells of variable thickness:

$$\frac{\partial^2 u}{\partial\theta^2} = b_{11}u + b_{12}\frac{\partial u}{\partial s} + b_{13}\frac{\partial u}{\partial\theta} + b_{14}\frac{\partial^2 u}{\partial s^2} + b_{15}v + b_{16}\frac{\partial v}{\partial s} + b_{17}\frac{\partial v}{\partial\theta} + b_{18}\frac{\partial^2 v}{\partial s\partial\theta} + b_{19}w + b_{1,10}\frac{\partial w}{\partial s} + b_{1,11}q_s,$$

$$\frac{\partial^2 v}{\partial\theta^2} = b_{21}u + b_{22}\frac{\partial u}{\partial s} + b_{23}\frac{\partial u}{\partial\theta} + b_{24}\frac{\partial^2 u}{\partial s\partial\theta} + b_{25}v + b_{26}\frac{\partial v}{\partial s} + b_{27}\frac{\partial v}{\partial\theta} + b_{28}\frac{\partial^2 v}{\partial s^2}$$

$$+ b_{29}w + b_{2,10}\frac{\partial w}{\partial\theta} + b_{2,11}\frac{\partial\psi_s}{\partial\theta} + b_{2,12}\frac{\partial^2\psi_s}{\partial s\partial\theta} + b_{2,13}\psi_\theta + b_{2,14}\frac{\partial\psi_\theta}{\partial s} + b_{2,15}\frac{\partial^2\psi_\theta}{\partial s^2} + b_{2,16}q_\theta,$$

$$\frac{\partial^2 w}{\partial\theta^2} = b_{31}u + b_{32}\frac{\partial u}{\partial s} + b_{33}v + b_{34}\frac{\partial v}{\partial\theta} + b_{35}w + b_{36}\frac{\partial w}{\partial s} + b_{37}\frac{\partial w}{\partial\theta}$$

$$+ b_{38}\frac{\partial^2 w}{\partial s^2} + b_{39}\psi_s + b_{3,10}\frac{\partial\psi_s}{\partial s} + b_{3,11}\psi_\theta + b_{3,12}\frac{\psi_\theta}{\partial\theta} + b_{3,13}q_\gamma,$$

$$\frac{\partial^2\psi_s}{\partial\theta^2} = b_{41}u + b_{42}\frac{\partial u}{\partial s} + b_{43}\frac{\partial u}{\partial\theta} + b_{44}\frac{\partial^2 u}{\partial s^2} + b_{45}v + b_{46}\frac{\partial v}{\partial s} + b_{47}\frac{\partial v}{\partial\theta} + b_{48}\frac{\partial^2 v}{\partial s\partial\theta}$$

$$+ b_{49}w + b_{4,10}\frac{\partial w}{\partial s} + b_{4,11}\psi_s + b_{4,12}\frac{\partial\psi_s}{\partial s} + b_{4,13}\frac{\partial\psi_s}{\partial\theta} + b_{4,14}\frac{\partial^2\psi_s}{\partial s^2} + b_{4,15}\psi_\theta$$

$$+ b_{4,16}\frac{\partial\psi_\theta}{\partial s} + b_{4,17}\frac{\partial\psi_\theta}{\partial\theta} + b_{4,18}\frac{\partial^2\psi_\theta}{\partial s\partial\theta} + b_{4,19}q_s,$$

$$\frac{\partial^2\psi_\theta}{\partial\theta} = b_{51}u + b_{52}\frac{\partial u}{\partial s} + b_{53}\frac{\partial u}{\partial\theta} + b_{54}\frac{\partial^2 u}{\partial s\partial\theta} + b_{55}v + b_{56}\frac{\partial v}{\partial s} + b_{57}\frac{\partial v}{\partial\theta} + b_{58}\frac{\partial^2 v}{\partial s^2}$$

$$+ b_{59}w + b_{5,10}\frac{\partial w}{\partial\theta} + b_{5,11}\psi_s + b_{5,12}\frac{\partial\psi_s}{\partial s} + b_{5,13}\frac{\partial\psi_s}{\partial\theta} + b_{5,14}\frac{\partial^2\psi_s}{\partial s\partial\theta} + b_{5,15}\psi_\theta$$

$$+ b_{5,16}\frac{\partial\psi_\theta}{\partial s} + b_{5,17}\frac{\partial\psi_\theta}{\partial\theta} + b_{5,18}\frac{\partial^2\psi_\theta}{\partial s^2} + b_{5,19}q_\theta \qquad (0 \le s \le L, 0 \le \theta \le 2\pi). \tag{7.5}$$

The expressions for the coefficients b_{ij} can be found in [69].

To solve such a problem, we will approximate the candidate solution by cubic spline functions in one coordinate direction and will solve the resulting one-dimensional boundary-value problem with the stable numerical discrete-orthogonalization method.

To determine the arbitrary constants in the general solution of system (7.4), it is necessary to prescribe five boundary conditions on each edge of the shell. There may be clamped, hinged, symmetry, etc. boundary conditions set on straight and curved edges.

Thus, the stress–strain state of nonthin conical shells of variable thickness is described by a system of partial differential equations (7.5) with appropriate boundary conditions.

For example, the following boundary conditions can be set on the curved and straight edges of the shell:

(a) clamping:

$$u = v = w = 0, \quad \overline{\overline{\psi}}_s = \overline{\overline{\psi}}_\theta = 0, \tag{7.6}$$

(b) hinging:

$$\frac{\partial u}{\partial s} = 0, \quad v = w, \quad \frac{\partial \overline{\overline{\psi}}_s}{\partial s} = 0, \quad \overline{\overline{\psi}}_\theta = 0 \quad \text{(curved edges)}, \tag{7.7}$$

$$u = 0, \quad \frac{\partial v}{\partial \theta} = 0, \quad w = 0, \quad \frac{\partial \overline{\overline{\psi}}_\theta}{\partial \theta} = 0 \quad \text{(straight edges)}. \tag{7.8}$$

Let us use the above approach to analyze the displacement and stress fields in nonthin conical shells with circumferentially varying thickness. Let the thickness of conical shells vary as (5.15), i.e., $h(\theta) = h_0(1 + \alpha \cos\theta)$.

Let us show that the weight of the shell is independent of the parameter α.

The quantity $\overline{h} = \int_0^L \int_0^{2\pi} h(s,\theta)\, ds\, d\theta$ remains constant because the expression $1 + \alpha\cos\theta$ does not depend on s, i.e.,

$$\int_0^{2\pi} (1 + \alpha\cos\theta)\, d\theta = 2\pi = \text{const}.$$

Let us determine the stress–strain state of an isotropic closed nonthin conical shell with circumferentially varying thickness under uniform normal pressure $q_\gamma = q_0 = \text{const}$. The shell ends $s = 0$ and $s = L$ are clamped. Input data: $L = 30$, $r_0 = 12.5$, $E_s = E_\theta = E$, $\nu = 0.3$. Half the cone angle $\psi = \pi/6$.

Let us analyze the effect of the parameters of h_0 and α on the stress–strain state of conical shells of constant weight. Since the shell is mechanically and geometrically symmetric about the boundaries $\theta = 0$ and $\theta = \pi$, we will consider half the shell: $\theta \in [0, \pi]$. The following symmetry conditions are set on the boundaries $\theta = 0$ and $\theta = \pi$:

$$\frac{\partial u}{\partial t} = \frac{\partial w}{\partial t} = 0, \quad v = 0, \quad \frac{\partial \Psi_s}{\partial t} = 0, \quad \Psi_t = 0.$$

According to the spline-approximation method, a candidate solution can be represented as

$$u(s,\theta) = \sum_{i=0}^{N} u_i(\theta)\varphi_{1i}(s), \quad v(s,\theta) = \sum_{i=0}^{N} v_i(\theta)\varphi_{2i}(s), \quad w(s,\theta) = \sum_{i=0}^{N} w_i(\theta)\varphi_{3i}(s),$$

$$\psi_s(s,\theta) = \sum_{i=0}^{N} \psi_{si}(\theta)\varphi_{4i}(s), \quad \psi_\theta(s,\theta) = \sum_{i=0}^{N} \psi_{\theta i}(\theta)\varphi_{5i}(s). \tag{7.9}$$

If the edges $s = \text{const}$ are clamped, then

$$\varphi_{10}(s) = -4B_3^{-1}(s) + B_3^0(s), \quad \varphi_{11}(s) = B_3^{-1}(s) - 0.5B_3^0(s) + B_3^1(s),$$

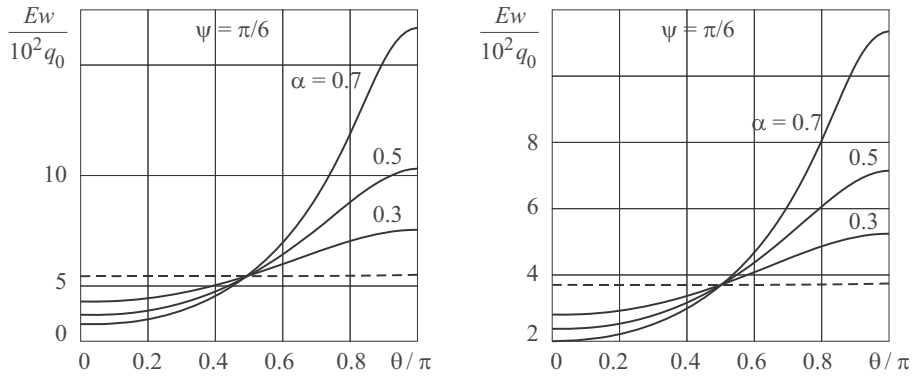

Fig. 22

$$\varphi_{1i}(s)=B_3^i(s) \quad (i=2,3,\ldots,N-2),$$

$$\varphi_{1,N-1}(s)=B_3^{N+1}(s)-0.5B_3^N(s)+B_3^{N-1}(s), \qquad \varphi_{1N}(s)=-4B_3^{N+1}(s)+B_3^N(s),$$

$$\varphi_{20}(s)=-4B_3^{-1}(s)+B_3^0(s), \qquad \varphi_{21}(s)=B_3^{-1}(s)-0.5B_3^0(s)+B_3^1(s),$$

$$\varphi_{2i}(s)=B_3^i(s) \quad (i=2,3,\ldots,N-2),$$

$$\varphi_{2,N-1}(s)=B_3^{N+1}(s)-0.5B_3^N(s)+B_3^{N-1}(s), \qquad \varphi_{2N}(s)=-4B_3^{N=1}(s)+B_3^N(s),$$

$$\varphi_{30}(s)=-4B_3^{-1}(s)+B_3^0(s), \qquad \varphi_{31}(s)=B_3^{-1}(s)-0.5B_3^0(s)+B_3^1(s),$$

$$\varphi_{3i}(s)=B_3^i(s) \quad (i=2,3,\ldots,N-2),$$

$$\varphi_{3,N-1}(s)=B_3^{N+1}(s)-0.5B_3^N(s)+B_3^{N-1}(s), \qquad \varphi_{3N}(s)=-4B_3^{N=1}(s)+B_3^N(s),$$

$$\varphi_{40}(s)=-4B_3^{-1}(s)+B_3^0(s), \qquad \varphi_{41}(s)=B_3^{-1}(s)-0.5B_3^0(s)+B_3^1(s),$$

$$\varphi_{4i}(s)=B_3^i(s) \quad (i=2,3,\ldots,N-2),$$

$$\varphi_{4,N-1}(s)=B_3^{N+1}(s)-0.5B_3^N(s)+B_3^{N-1}(s), \qquad \varphi_{4N}(s)=-4B_3^{N=1}(s)+B_3^N(s),$$

$$\varphi_{50}(s)=-4B_3^{-1}(s)+B_3^0(s), \qquad \varphi_{51}(s)=B_3^{-1}(s)-0.5B_3^0(s)+B_3^1(s),$$

$$\varphi_{5i}(s)=B_3^i(s) \quad (i=2,3,\ldots,N-2),$$

$$\varphi_{5,N-1}(s)=B_3^{N+1}(s)-0.5B_3^N(s)+B_3^{N-1}(s), \qquad \varphi_{5N}(s)=-4B_3^{N=1}(s)+B_3^N(s). \tag{7.10}$$

Substituting solution (7.4) into the governing system of equations (7.2) and requiring them to be satisfied on $N+1$ lines $s=\xi_i$ ($i=\overline{1,N+1}$), according to the spline-collocation method, we obtain a system of ordinary differential equations of order $10(N+1)$:

$$\frac{d\bar{R}}{d\theta}=A\bar{R}+\bar{f}, \tag{7.11}$$

$$\bar{R}=\{u_0,\ldots,u_N,\ u_0',\ldots,u_N',\ v_0,\ldots,v_N,\ v_0',\ldots,v_N',\ w_0,\ldots,w_N,\ w_0',\ldots,w_N',$$

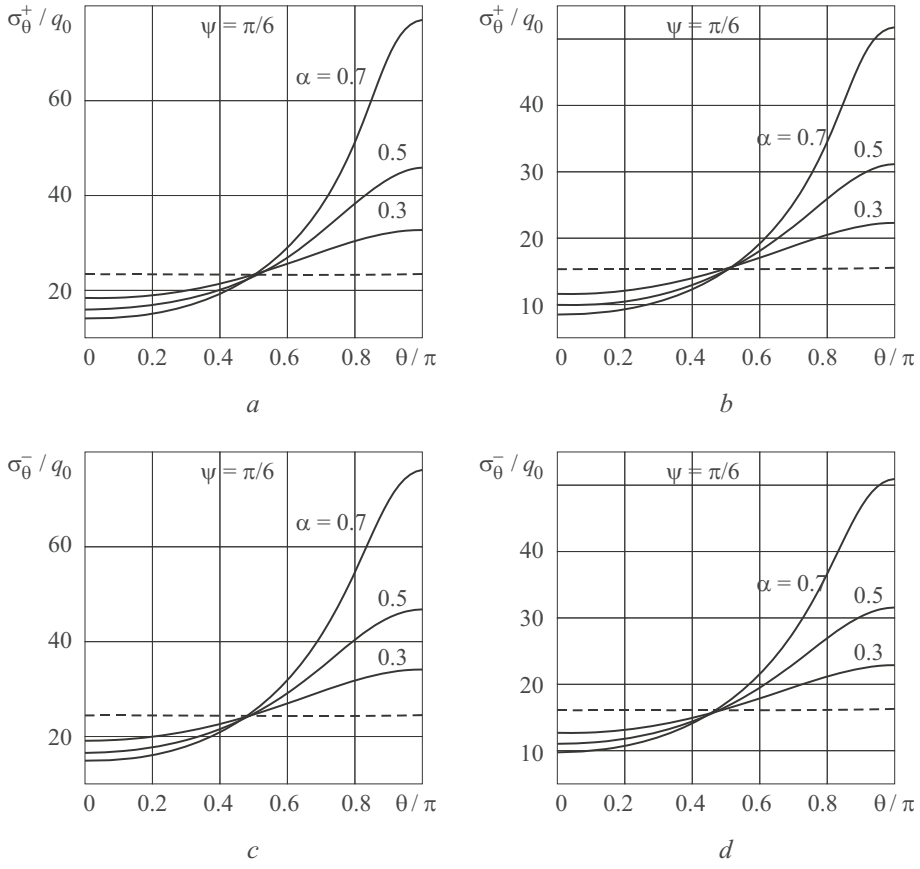

Fig. 23

$$\psi_{s0},\ldots,\psi_{sN},\ \psi'_{s0},\ldots,\psi'_{sN},\ \psi_{t0},\ldots,\psi_{\theta N},\ \psi'_{\theta 0},\ldots,\psi'_{\theta N}\}^T$$

is a vector function of θ; $\bar{f}$ is the vector of right-hand sides; A is a square matrix whose elements depend on θ. The symmetry conditions on the straight edges are

$$A_1\bar{R}(\theta_1)=\bar{a}_1,\qquad A_2\bar{R}(\theta_2)=\bar{a}_2. \tag{7.12}$$

The resulting one-dimensional boundary-value problem (7.11), (7.12) is solved by the stable numerical discrete-orthogonalization method.

Figure 22*a* shows the circumferential distribution of the deflection w within $0 \le \theta \le \pi$ in the section $s = L/2$ for $h_0 = 1$ (Fig. 22*a*), $h_0 = 1.5$ (Fig. 22*b*), and $\alpha = 0, 0.3, 0.5, 0.7$. The values of the parameter α are indicated in the figures. The dashed line corresponds to the shell of constant thickness with $\alpha = 0$. It can be seen that as h_0 is increased from 1 to 1.5, the maximum deflection decreases by a factor of 1.5. The maximum deflections at $\alpha = 0, 0.3, 0.5, 0.7$ are in a ratio of 1:2:3:5.

Figures 22*a*, *b*, *c* show the circumferential distribution of the stresses $\sigma_\theta^{\pm}$ within $0 \le \theta \le \pi$ in the section $s = L/2$ for $h_0 = 1$ (Fig. 23*a*, *c*), $h_0 = 1.5$ (Fig. 23*b*, *d*), and $\alpha = 0, 0.3, 0.5, 0.7$. The dashed line corresponds to the shell of constant thickness with $\alpha = 0$. It can be seen that the curves for stresses are similar to those for deflections.

Thus, varying the values of the parameters h_0 and α in (5.15) and keeping the weight of the shell constant, we can find the rational distributions of the deflection and stresses.

Let us analyze the stress–strain state of closed conical shells under a localized load defined by

TABLE 14

β	a	Ew/q_0		
		$\psi = 0$	$\psi = \pi/6$	$\psi = \pi/4$
$\pi/4$	2	–0.8818	–1.0053	–1.1963
	4	–0.812	–0.92993	–1.1127
	8	–0.6542	–0.75287	–0.90693
$\pi/6$	2	–1.3308	–1.4723	–1.6891
	4	–1.2269	–1.3619	–1.5691
	8	–0.99073	–1.1029	–1.2768
$\pi/12$	2	–1.9601	–2.112	–2.3441
	4	–1.7863	–1.9311	–2.1527
	8	–1.4213	–1.5417	–1.7277

$$-q_\gamma = \begin{cases} q_0(\cos\theta - \cos\beta), & 0 \le \theta \le \beta,\ L/2 - a \le s \le L/2 + a, \\ 0, & \beta \le \theta \le \pi - \beta, \\ -q_0(\cos\theta - \cos\beta), & \pi - \beta \le \theta \le \pi + \beta,\ L/2 - a \le s \le L/2 + a, \\ 0, & \pi + \beta \le \theta \le 2\pi - \beta, \\ q_0(\cos\theta - \cos\beta), & 2\pi - \beta \le \theta \le 2\pi,\ L/2 - a \le s \le L/2 + a. \end{cases}$$

The shells are made of transversely isotropic and orthotropic materials and clamped at the ends. The values of the cone angle ψ and the parameters α and β are variable. The value q_0 is selected so that the load remains the same (equal to $q^* = q_0(\pi/12)$) for different values of α and β. It is shown that increasing the interval of application of the load leads to a decrease in w and σ_θ in the zone of maximum load at $\theta = 0$.

Table 14 summarizes the maximum deflections for $\theta = 0$, different degrees of localization of the load, and different cone angles. The input data: $G_{s\gamma} = G_{\theta\gamma} = 0.2E, G_{s\theta} = 0.4E, E_s = 5E, E_\theta = 1.25E, \nu_s = 0.45, \nu_\theta = 0.18, L = 30, r_0 = R_0 - L/2\sin\psi, R_0 = 20$. The shells have constant thickness ($h = 1.5$).

Thus, by varying the parameters of localization of the load on the shell, it is possible to influence the distribution of displacements and stresses.

The above results on the displacement and stress fields in nonthin conical shells of variable thickness are of theoretical and practical value in the strength and reliability design of structural members. The stress–strain state of shallow conical and spherical shells with variable thickness was analyzed using a refined theory in [32, 55–62, 70, 71].

8. Numerical Solution of Problems. Free Vibrations of Shallow Shells with Variable Parameters (Refined Formulation).

Starting Equations. Consider a shallow orthotropic shell with rectangular planform and variable (in two directions) thickness $h(x, y)$ undergoing free vibrations. We will use a refined problem formulation and the straight-element hypothesis. The planform geometry is approximately identified with the geometry of the midsurface, while the principal curvatures are such that $k_1 \cdot k_2 \approx 0$.

According to the straight-element hypothesis, the displacements are given by

$$u_x(x, v, z, t) = u(x, y, t) + z\psi_x(x, y, t),$$

$$u_y(x, v, z, t) = v(x, y, t) + z\psi_y(x, y, t),$$

$$u_z(x, v, z, t) = w(x, y, t), \tag{8.1}$$

where x, y, z are coordinates; u_x, u_y, u_z are the respective displacements; u, v, w are the displacements of the coordinate surface along the x-, y-, and z-axes, respectively; ψ_x, ψ_y are the complete angles of rotation of the straight-line element.

The expressions for strains below follow from (8.1):

$$e_x(x, y, z, t) = \varepsilon_x(x, y, t) + z\chi_x(x, y, t),$$

$$e_y(x, y, z, t) = \varepsilon_y(x, y, t) + z\chi_y(x, y, t),$$

$$e_{xy}(x, y, z, t) = \varepsilon_{xy}(x, y, t) + z2\chi_{xy}(x, y, t),$$

$$e_{xz}(x, y, z, t) \cong \gamma_x(x, y, t),$$

$$e_{yz}(x, y, z, t) \cong \gamma_x(x, y, t), \tag{8.2}$$

where γ_x and γ_y are the angles of rotation caused by transverse shear; ε_x, ε_y, and ε_{xy} are the shear strains that determine the internal geometry of the coordinate surface; χ_x, χ_y, $2\chi_{xy}$ are the flexural strains characterizing the bending and twisting of the coordinate surface.

The strains and displacements are related by

$$\varepsilon_x = \frac{\partial u}{\partial x} + k_1 w, \qquad \varepsilon_y = \frac{\partial v}{\partial y} + k_2 w, \qquad \varepsilon_{xy} = \frac{\partial u}{\partial y} + \frac{\partial v}{\partial x},$$

$$\chi_x = \frac{\partial \psi_x}{\partial x} + k_1^2 w, \qquad \chi_y = \frac{\partial \psi_y}{\partial y} + k_2^2 w, \qquad 2\chi_{xy} = \frac{\partial \psi_x}{\partial y} + \frac{\partial \psi_y}{\partial x},$$

$$\psi_x = \gamma_x + \vartheta_x, \qquad \psi_y = \gamma_y + \vartheta_y,$$

$$\vartheta_x = -\frac{\partial w}{\partial x} + k_1 u, \qquad \vartheta_y = -\frac{\partial w}{\partial y} + kv, \tag{8.3}$$

where ϑ_x and ϑ_y are the angles of rotation of the normal without the effect of transverse shear; k_1 and k_2 are curvatures.

The free transverse vibrations of shallow shells are described by the following refined equations:

$$\frac{\partial N_x}{\partial x} + \frac{\partial N_{yx}}{\partial y} = 0, \qquad \frac{\partial N_{xy}}{\partial x} + \frac{\partial N_y}{\partial y} = 0,$$

$$\frac{\partial Q_x}{\partial x} + \frac{\partial Q_y}{\partial y} - k_1 N_x - k_2 N_y + \rho h \frac{\partial^2 w}{\partial t^2} = 0,$$

$$\frac{\partial M_x}{\partial x} + \frac{\partial M_{yx}}{\partial y} - Q_x + \rho \frac{h^3}{12} \frac{\partial^2 \psi_x}{\partial t^2} = 0,$$

$$\frac{\partial M_{xy}}{\partial x} + \frac{\partial M_y}{\partial y} - Q_y + \rho \frac{h^3}{12} \frac{\partial^2 \psi_y}{\partial t^2} = 0, \tag{8.4}$$

where x and y are the Cartesian coordinates of a point on the midsurface ($0 \le x \le a,\ 0 \le y \le b$); t is time; w is deflection; ρ is the density of the material.

The normal and shearing forces N_x, N_y, N_{xy}, N_{yx}, the bending and twisting moments M_x, M_y, M_{xy}, M_{yx}, and the transverse forces Q_x, Q_y are given by

$$N_x = C_{11}\varepsilon_x + C_{12}\varepsilon_y, \quad N_y = C_{12}\varepsilon_x + C_{22}\varepsilon_y,$$

$$N_{xy} = C_{66}\varepsilon_{xy} + 2k_2 D_{66}\chi_{xy}, \quad N_{yx} = C_{66}\varepsilon_{xy} + 2k_1 D_{66}\chi_{xy},$$

$$M_x = D_{11}\chi_x + D_{12}\chi_y, \quad M_y = D_{12}\chi_x + D_{22}\chi_y, \quad M_{xy} = M_{yx} = 2D_{66}\chi_{xy},$$

$$Q_x = K_1\gamma_x, \quad Q_y = K_2\gamma_y, \tag{8.5}$$

where

$$C_{11} = \frac{E_x h}{1-\nu_x\nu_y}, \quad C_{12} = \nu_y C_{11}, \quad C_{22} = \frac{E_y h}{1-\nu_x\nu_y}, \quad C_{66} = G_{xy}h,$$

$$D_{11} = \frac{E_x h^3}{12(1-\nu_x\nu_y)}, \quad D_{12} = \nu_y D_{11}, \quad D_{22} = \frac{E_y h^3}{12(1-\nu_x\nu_y)}, \quad D_{66} = \frac{G_{xy}h^3}{12},$$

$$K_1 = \frac{5}{6}hG_{xz}, \quad K_2 = \frac{5}{6}hG_{yz}, \tag{8.6}$$

E_x, E_y are the elastic moduli, G_{xy}, G_{xz}, G_{yz} are the shear moduli; ν_x, ν_y are Poisson's ratios; $h = h(x, y)$ is the thickness.

The system of equations (8.4)–(8.5) yields five equivalent differential equations for the three displacements u, v, w and the two angles ψ_x, ψ_y:

$$C_{11}\frac{\partial^2 u}{\partial x^2} + \frac{\partial C_{11}}{\partial x}\frac{\partial u}{\partial x} + \frac{\partial C_{66}}{\partial y}\frac{\partial u}{\partial y} + C_{66}\frac{\partial^2 u}{\partial y^2} + \frac{\partial C_{66}}{\partial y}\frac{\partial v}{\partial x} + \frac{\partial C_{12}}{\partial x}\frac{\partial v}{\partial y}$$

$$+(C_{12} + C_{66})\frac{\partial^2 v}{\partial x\partial y} + \left(k_1\frac{\partial C_{11}}{\partial x} + k_2\frac{\partial C_{12}}{\partial x}\right)w + (k_1 C_{11} + k_2 C_{12})\frac{\partial w}{\partial x}$$

$$+k_1\frac{\partial D_{66}}{\partial y}\frac{\partial \psi_x}{\partial y} + k_1 D_{66}\frac{\partial^2 \psi_x}{\partial y^2} + k_1\frac{\partial D_{66}}{\partial y}\frac{\partial \psi_y}{\partial x} + k_1 D_{66}\frac{\partial^2 \psi_y}{\partial x\partial y} = 0,$$

$$C_{66}\frac{\partial^2 v}{\partial x^2} + \frac{\partial C_{12}}{\partial y}\frac{\partial u}{\partial x} + \frac{\partial C_{66}}{\partial x}\frac{\partial u}{\partial y} + (C_{12} + C_{66})\frac{\partial^2 u}{\partial x\partial y} - k_2^2 K_2 v + \frac{\partial C_{66}}{\partial x}\frac{\partial v}{\partial x} + \frac{\partial C_{22}}{\partial y}\frac{\partial v}{\partial y}$$

$$+C_{22}\frac{\partial^2 v}{\partial y^2} - \left(k_1\frac{\partial C_{12}}{\partial y} + k_2\frac{\partial C_{22}}{\partial y} + k_1^2 k_2\frac{\partial D_{12}}{\partial y} + k_2^3\frac{\partial D_{22}}{\partial y}\right)w$$

$$+(k_1 C_{12} + k_2 C_{22} + k_2 K_2 + k_1^2 k_2 D_{12} + k_2^3 D_{22})\frac{\partial w}{\partial y}$$

$$-k_2\frac{\partial D_{12}}{\partial y}\frac{\partial \psi_x}{\partial x} - k_2 D_{12}\frac{\partial^2 \psi_x}{\partial x\partial y} + k_2 K_2 \psi_y - k_2\frac{\partial D_{22}}{\partial y}\frac{\partial \psi_y}{\partial y} + k_2 D_{22}\frac{\partial^2 \psi_y}{\partial y^2} = 0,$$

$$K_1\frac{\partial^2 w}{\partial x^2} - k_1\frac{\partial K_1}{\partial x}u - (K_1 k_1 + k_2 C_{11} + k_2 C_{12})\frac{\partial u}{\partial x} - k_2\frac{\partial K_2}{\partial y}v$$

$$-(K_2 k_2 + k_1 C_{12} + k_2 C_{22})\frac{\partial v}{\partial y} - (k_1^2 C_{11} + 2k_1 k_2 C_{12} + k_2^2 C_{22} - \rho h\omega^2)w$$

$$+\frac{\partial K_1}{\partial x}\frac{\partial w}{\partial x} + \frac{\partial K_2}{\partial y}\frac{\partial w}{\partial y} + K_2\frac{\partial^2 w}{\partial y^2} + \frac{\partial K_1}{\partial x}\psi_x + K_1\frac{\partial \psi_x}{\partial x} + \frac{\partial K_2}{\partial y}\psi_y + K_2\frac{\partial \psi_y}{\partial y} = 0,$$

$$D_{11}\frac{\partial^2\psi_x}{\partial x^2}+K_1k_1u-\left(k_1^2\frac{\partial D_{11}}{\partial x}+k_2^2\frac{\partial D_{12}}{\partial x}\right)w-(k_1^2D_{11}+k_2^2D_{12}+K_1)\frac{\partial w}{\partial x}$$

$$-\left(K_1-\rho\frac{h^3}{12}\omega^2\right)\psi_x+\frac{\partial D_{11}}{\partial x}\frac{\partial\psi_x}{\partial x}+\frac{\partial D_{66}}{\partial y}\frac{\partial\psi_x}{\partial y}+D_{66}\frac{\partial^2\psi_x}{\partial y^2}$$

$$+\frac{\partial D_{66}}{\partial y}\frac{\partial\psi_y}{\partial x}+\frac{\partial D_{12}}{\partial x}\frac{\partial\psi_y}{\partial y}+(D_{12}+D_{66})\frac{\partial^2\psi_y}{\partial x\partial y}=0,$$

$$D_{66}\frac{\partial^2\psi_y}{\partial x^2}+K_2k_2v-\left(k_1^2\frac{\partial D_{12}}{\partial y}+k_2^2\frac{\partial D_{22}}{\partial y}\right)w-(k_1^2D_{12}+k_2^2D_{22}+K_2)\frac{\partial w}{\partial y}$$

$$+\frac{\partial D_{12}}{\partial y}\frac{\partial\psi_x}{\partial x}+\frac{\partial D_{66}}{\partial x}\frac{\partial\psi_x}{\partial y}+(D_{12}+D_{66})\frac{\partial^2\psi_x}{\partial x\partial y}$$

$$-\left(K_2-\rho\frac{h^3}{12}\omega^2\right)\psi_y+\frac{\partial D_{66}}{\partial x}\frac{\partial\psi_y}{\partial x}+\frac{\partial D_{22}}{\partial y}\frac{\partial\psi_y}{\partial y}+D_{22}\frac{\partial^2\psi_y}{\partial y^2}=0. \tag{8.7}$$

The following boundary conditions for the displacements and angles are prescribed on the edges $x=0$, a and $y=0$, b. At $x=\text{const}$, the following boundary conditions are specified:

(i) both edges are clamped:

$$u=v=w=\psi_x=\psi_y=0 \quad \text{at} \quad x=0,\quad x=a; \tag{8.8}$$

(ii) both edges are hinged:

$$\frac{\partial u}{\partial x}=v=w=\frac{\partial\psi_x}{\partial x}=\psi_y=0 \quad \text{at} \quad x=0,\quad x=a; \tag{8.9}$$

(iii) one edge is clamped, and the other is hinged:

$$u=v=w=\psi_x=\psi_y=0 \quad \text{at} \quad x=0,$$

$$\frac{\partial u}{\partial x}=v=w=\frac{\partial\psi_x}{\partial x}=\psi_y=0 \quad \text{at} \quad x=a. \tag{8.10}$$

Similar conditions can be specified on the edges $y=\text{const}$. To this end, it is necessary to replace x by y, u by v, and ψ_x by ψ_y in Eqs. (8.8)–(8.10).

Problem-Solving Method. The solution of the system of equations (8.7) is represented in the form

$$u(x,y)=\sum_{i=0}^{N}u_i(x)\varphi_{1,i}(y),\qquad v(x,y)=\sum_{i=0}^{N}v_i(x)\varphi_{2,i}(y),\qquad w(x,y)=\sum_{i=0}^{N}w_i(x)\varphi_{3,i}(y),$$

$$\psi_x(x,y)=\sum_{i=0}^{N}\psi_{x_i}(x)\varphi_{4,i}(y),\qquad \psi_y(x,y)=\sum_{i=0}^{N}\psi_{y_i}(x)\varphi_{5,i}(y), \tag{8.11}$$

where $u_i(x)$, $v_i(x)$, $w_i(x)$, $\psi_{x_i}(x)$, $\psi_{y_i}(x)\,(i=0,\ldots,N)$ are unknown functions; $\varphi_{ji}(y)\,(j=1,\ldots,5)$ are functions set up using cubic B-splines $N\geq 4$ that satisfy the boundary conditions at the edges $y=0$ and $y=b$ with the help of linear combinations of cubic B-splines.

We rearrange the system of equations (8.7) as

$$\frac{\partial^2 u}{\partial x^2} = a_1 \frac{\partial u}{\partial x} + a_2 \frac{\partial u}{\partial y} + a_3 \frac{\partial^2 u}{\partial y^2} + a_4 \frac{\partial v}{\partial x} + a_5 \frac{\partial v}{\partial y} + a_6 \frac{\partial^2 v}{\partial x \partial y} + a_7 w$$

$$+ a_8 \frac{\partial w}{\partial x} + a_9 \frac{\partial \psi_x}{\partial y} + a_{10} \frac{\partial^2 \psi_x}{\partial y^2} + a_{11} \frac{\partial \psi_y}{\partial x} + a_{12} \frac{\partial^2 \psi_y}{\partial x \partial y},$$

$$\frac{\partial^2 v}{\partial x^2} = b_1 \frac{\partial u}{\partial x} + b_2 \frac{\partial u}{\partial y} + b_3 \frac{\partial^2 u}{\partial x \partial y} + b_4 v + b_5 \frac{\partial v}{\partial x} + b_6 \frac{\partial v}{\partial y} + b_7 \frac{\partial^2 v}{\partial y^2}$$

$$+ b_8 w + b_9 \frac{\partial w}{\partial y} + b_{10} \frac{\partial \psi_x}{\partial x} + b_{11} \frac{\partial^2 \psi_x}{\partial x \partial y} + b_{12} \psi_y + b_{13} \frac{\partial \psi_y}{\partial y} + b_{14} \frac{\partial^2 \psi_y}{\partial y^2},$$

$$\frac{\partial^2 w}{\partial x^2} = c_1 u + c_2 \frac{\partial u}{\partial x} + c_3 v + c_4 \frac{\partial v}{\partial y} + c_5 w + c_6 \frac{\partial w}{\partial x} + c_7 \frac{\partial w}{\partial y}$$

$$+ c_8 \frac{\partial^2 w}{\partial y^2} + c_9 \psi_x + c_{10} \frac{\partial \psi_x}{\partial x} + c_{11} \psi_y + c_{12} \frac{\partial \psi_y}{\partial y},$$

$$\frac{\partial^2 \psi_x}{\partial x^2} = d_1 u + d_2 w + d_3 \frac{\partial w}{\partial x} + d_4 \psi_x + d_5 \frac{\partial \psi_x}{\partial x} + d_6 \frac{\partial \psi_x}{\partial y} + d_7 \frac{\partial^2 \psi_x}{\partial y^2}$$

$$+ d_8 \frac{\partial \psi_y}{\partial x} + d_9 \frac{\partial \psi_y}{\partial y} + d_{10} \frac{\partial^2 \psi_y}{\partial x \partial y},$$

$$\frac{\partial^2 \psi_y}{\partial x^2} = g_1 v + g_2 w + g_3 \frac{\partial w}{\partial y} + g_4 \frac{\partial \psi_x}{\partial x} + g_5 \frac{\partial \psi_x}{\partial y} + g_6 \frac{\partial^2 \psi_x}{\partial x \partial y} + g_7 \psi_y$$

$$+ g_8 \frac{\partial \psi_y}{\partial x} + g_9 \frac{\partial \psi_y}{\partial y} + g_{10} \frac{\partial^2 \psi_y}{\partial y^2} \tag{8.12}$$

$$(a_m = a_m(x, y) \quad (m = 1, \dots, 12), \quad b_p = b_p(x, y) \quad (p = 1, \dots, 14),$$
$$c_q = c_q(x, y) \quad (q = 1, \dots, 4, 6, \dots, 12), \quad c_5 = c_5(x, y, \omega),$$
$$d_r = d_r(x, y) \quad (r = 1, \dots, 3, 5, \dots, 10), \quad d_4 = d_4(x, y, \omega),$$
$$g_s = g_s(x, y) \quad (s = 1, \dots, 6, 8, 9, 10), \quad g_7 = g_7(x, y, \omega)). \tag{8.13}$$

Substituting (8.11) into Eqs. (8.12), we require that they hold at given collocation points $\xi_k \in [0, b]$, $k = 0, \dots, N$. This system of ordinary differential equations can be represented in normal form:

$$\frac{d\overline{Y}}{dx} = A(x, \omega)\overline{Y} \quad (0 \le x \le a), \tag{8.14}$$

where

$$\overline{Y} = [\overline{u}, \overline{u}', \overline{v}, \overline{v}', \overline{w}, \overline{w}', \overline{\psi}_x, \overline{\psi}'_x, \overline{\psi}_y, \overline{\psi}'_y]^T$$

$$= u_0, \dots, u_N, v_0, \dots, v_N, w_0, \dots, w_N, \psi_{x_0}, \dots, \psi_{x_N}, \psi_{y_0}, \dots, \psi_{y_N}]^T$$

is the column vector of unknown functions and their $10(N+1)$-order derivatives; $A(x, \omega)$ is a $10(N+1) \times 10(N+1)$-matrix.

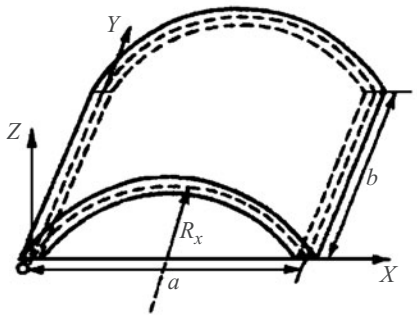

Fig. 24

The boundary conditions (8.8)–(8.10) for system (8.14) can be represented as

$$B_1\overline{Y}(0)=\overline{0}, \qquad B_2\overline{Y}(a)=\overline{0}. \tag{8.15}$$

The eigenvalue problem for the system of ordinary differential equations (8.14) with the boundary conditions (8.15) is solved with the discrete-orthogonalization and incremental search methods.

Calculated Results. We use the above procedure to examine the natural frequency spectrum of a shallow isotropic shell with variable thickness and square planform ($a=b=0.5$ m). The thickness of the shell varies as

$$h=h_0\left[1+\alpha(6\zeta^2-6\zeta+1)\right], \tag{8.16}$$

where $0\le\zeta\le 1, |\alpha|<1, \zeta=x/a; h_0=0.04$ m is the thickness of a shell with constant thickness and equivalent mass. For a shallow cylindrical shell, we have $k_1=1/R_x$ and $k_2=1/R_y=0$.

The number of collocation points $N=14$. The physical characteristics of the shell: $E=2.016\cdot 10^{11}$ Pa, $\nu=0.3$, $\rho=7800$ kg/m^3. Let $r_x=6.26000$, $r_x=1.60250$, $r_x=0.86125$, where $r_x=R_x/a$ is the dimensionless radius of curvature.

The following boundary conditions are considered:

(i) all edges are clamped (BC1):

$$u=v=w=\psi_x=\psi_y=0 \quad \text{for} \quad x=0, \quad x=a,$$

$$u=v=w=\psi_x=\psi_y=0 \quad \text{for} \quad y=0, \quad y=b;$$

(ii) three edges are clamped and the fourth edge is hinged (BC2):

$$u=v=w=\psi_x=\psi_y=0 \quad \text{for} \quad x=0, \quad x=a,$$

$$u=\frac{\partial v}{\partial y}=w=\psi_x=\frac{\partial\psi_y}{\partial y}=0 \quad \text{for} \quad y=0, \quad y=b;$$

(iii) two opposite edges are clamped and the other two edges are hinged (BC3):

$$u=v=w=\psi_x=\psi_y=0 \quad \text{for} \quad x=0, \quad x=a,$$

$$u=\frac{\partial v}{\partial y}=w=\psi_x=\frac{\partial\psi_y}{\partial y}=0 \quad \text{for} \quad y=0, \quad y=b;$$

(iv) two adjacent edges are clamped and the other two edges are hinged (BC4):

$$u=v=w=\psi_x=\psi_y=0 \quad \text{for} \quad x=0, \quad y=0,$$

TABLE 15

r_x	i	$\overline{\omega}_i = \omega_i a\sqrt{\rho(1-\nu^2)/E}$							
		N							
		8	10	12	14	16	18	20	22
6.26000	1	0.4606	0.4557	0.4537	0.4528	0.4523	0.4520	0.4518	0.4517
	2	1.0829	1.0810	1.0802	1.0799	1.0797	1.0796	1.0795	1.0795
	3	1.0829	1.0810	1.0802	1.0799	1.0797	1.0796	1.0795	1.0795
	4	1.1817	1.1294	1.1085	1.0986	1.0937	1.0908	1.0891	1.0881
1.60250	1	1.7392	1.7056	1.6926	1.6866	1.6835	1.6818	1.6808	1.6801
	2	0.5364	0.5322	0.5305	0.5297	0.5292	0.5290	0.5289	0.5289
	3	1.0810	1.0791	1.0783	1.0779	1.0777	1.0776	1.0775	1.0775
	4	1.2631	1.2140	1.1945	1.1854	1.1807	1.1781	1.1766	1.1757
0.86125	1	1.7559	1.7225	1.7095	1.7036	1.7005	1.6988	1.6978	1.6972
	2	0.6980	0.6947	0.6934	0.6928	0.6925	0.6923	0.6921	0.6921
	3	1.0760	1.0740	1.0732	1.0728	1.0726	1.0725	1.0724	1.0724
	4	1.4558	1.4131	1.3962	1.3883	1.3843	1.3821	1.3808	1.3800

$$\frac{\partial u}{\partial x} = v = w = \frac{\partial \psi_x}{\partial x} = \psi_y = 0 \quad \text{for} \quad x = a,$$

$$u = \frac{\partial v}{\partial y} = w = \psi_x = \frac{\partial \psi_y}{\partial y} = 0 \quad \text{for} \quad y = b;$$

(v) all edges are hinged (BC5):

$$\frac{\partial u}{\partial x} = v = w = \frac{\partial \psi_x}{\partial x} = \psi_y = 0 \quad \text{for} \quad x = 0, \quad x = a,$$

$$u = \frac{\partial v}{\partial y} = w = \psi_x = \frac{\partial \psi_y}{\partial y} = 0 \quad \text{for} \quad y = 0, \quad y = b.$$

The results obtained with different number N of collocation points are somewhat different. The absolute value of frequency and, hence, the accuracy of calculations increase with the number of collocation points. However, the difference is hardly noticeable at $N > 16$. For this reason, we performed calculations for $N = 18$, which ensured an error less than 1% (the difference between the calculated frequencies and those found analytically, by Fourier-series expansion).

Table 15 summarizes dimensionless resonant frequencies as functions of the number N of collocation points for shells with different curvature of the midsurface, constant thickness ($\alpha = 0$), and all hinged edges.

TABLE 16

i	$\overline{\omega}_i = \omega_i a\sqrt{\rho(1-\nu^2)/E}$								
	$r_x = 6.26000$			$r_x = 1.60250$			$r_x = 0.86125$		
	A	C	P, %	A	C	P, %	A	C	P, %
1	0.4516	0.4519	0.08	0.5287	0.5290	0.07	0.6920	0.6923	0.04
2	1.0794	1.0796	0.02	1.0775	1.0776	0.01	1.0724	1.0725	0.01
3	1.0860	1.0908	0.45	1.1737	1.1781	0.38	1.3783	1.3821	0.28
4	1.6788	1.6818	0.18	1.6959	1.6988	0.17	1.7400	1.7429	0.17

For validation purposes, we compare the natural frequencies of a shallow isotropic shell with square planform and hinged edges calculated with our approach and by using the following Fourier-series expansion:

$$u = \sum_{m=1,3,\ldots}^{\infty}\sum_{n=1,3,\ldots}^{\infty} a_{mn}\cos\frac{m\pi x}{a}\sin\frac{n\pi y}{b},$$

$$v = \sum_{m=1,3,\ldots}^{\infty}\sum_{n=1,3,\ldots}^{\infty} b_{mn}\sin\frac{m\pi x}{a}\cos\frac{n\pi y}{b},$$

$$w = \sum_{m=1,3,\ldots}^{\infty}\sum_{n=1,3,\ldots}^{\infty} c_{mn}\sin\frac{m\pi x}{a}\sin\frac{n\pi y}{b},$$

$$\psi_x = \sum_{m=1,3,\ldots}^{\infty}\sum_{n=1,3,\ldots}^{\infty} d_{mn}\cos\frac{m\pi x}{a}\sin\frac{n\pi y}{b},$$

$$\psi_y = \sum_{m=1,3,\ldots}^{\infty}\sum_{n=1,3,\ldots}^{\infty} e_{mn}\sin\frac{m\pi x}{a}\cos\frac{n\pi y}{b}. \qquad (8.17)$$

Table 16 compares the dimensionless frequencies obtained using expansion (8.17) (A) and our approach for $N = 18$ (B) and gives the difference in percent (P). As is seen, the maximum difference does not exceed 0.5%, which is indicative of the high accuracy of the approach that employs the spline-approximation of unknown functions.

Tables 17 and 18 summarize the first four resonant frequencies of shells of variable ($|\alpha| > 0$) and constant thickness ($\alpha = 0$) with radii of curvature $r_x = 6.26000$ and $r_x = 1.60250$, respectively.

Figure 25 shows the first four modes of an isotropic shell with variable thickness for $\alpha = 0.1$, BC1, and different values of the curvature of the midsurface.

Analyzing Tables 17 and 18, we conclude that the natural frequencies of isotropic shells are more strongly dependent on the number of clamped edges than on the parameter α. The fewer there are clamped edges, the lower the frequency. The geometry of the surfaces bounding the shell, which are symmetric about the midsurface, has a strong effect on the behavior of the natural frequencies. The greater the difference between the curvatures of the bounding surfaces and midsurface, the more the difference between the frequencies of the shells with variable and constant thickness. The first frequency varies linearly with the parameter α for all values of curvature and all boundary conditions. The dependence $\overline{\omega} = f(\alpha)$ is nonlinear at higher frequencies in all cases. The higher frequencies are more strongly dependent on the parameter α than the lower frequencies. An analysis of

TABLE 17

BC	i	$\overline{\omega}_i = \omega_i a\sqrt{\rho(1-\nu^2)/E}$										
		α										
		–0.5	–0.4	–0.3	–0.2	–0.1	0	0.1	0.2	0.3	0.4	0.5
1	1	0.7514	0.7591	0.7665	0.7739	0.7813	0.7889	0.7967	0.8048	0.8131	0.8218	0.8308
	2	1.3567	1.3969	1.4317	1.4620	1.4884	1.5116	1.5060	1.4866	1.4661	1.4447	1.4225
	3	1.5921	1.5827	1.5709	1.5570	1.5414	1.5244	1.5318	1.5491	1.5640	1.5764	1.5865
	4	2.0631	2.0911	2.1130	2.1297	2.1420	2.1503	2.1551	2.1566	2.1549	2.1502	2.1426
2	1	0.6370	0.6513	0.6652	0.6788	0.6924	0.7060	0.7196	0.7334	0.7473	0.7613	0.7754
	2	1.3080	1.3500	1.3766	1.3681	1.3581	1.3472	1.3352	1.3226	1.3092	1.2954	1.2810
	3	1.3884	1.3836	1.3863	1.4182	1.4461	1.4707	1.4923	1.5111	1.5273	1.5411	1.5526
	4	1.9362	1.9660	1.9896	2.0082	2.0226	2.0331	2.0402	2.0440	2.0450	2.0430	2.0381
3	1	0.5538	0.5733	0.5922	0.6107	0.6289	0.6470	0.6649	0.6828	0.7006	0.7185	0.7363
	2	1.1981	1.1987	1.1975	1.1950	1.1914	1.1870	1.1819	1.1763	1.1702	1.1637	1.1571
	3	1.2698	1.3132	1.3509	1.3839	1.4131	1.4388	1.4615	1.4815	1.4989	1.5138	1.5263
	4	1.8231	1.8547	1.8802	1.9009	1.9172	1.9299	1.9392	1.9453	1.9487	1.9493	1.9422
4	1	0.5847	0.5897	0.5943	0.5983	0.6022	0.6060	0.6098	0.6138	0.6179	0.6223	0.6271
	2	1.1978	1.2244	1.2460	1.2636	1.2774	1.2879	1.2854	1.2722	1.2580	1.2435	1.2287
	3	1.3532	1.3454	1.3359	1.3251	1.3133	1.3013	1.2987	1.3040	1.3077	1.3095	1.3094
	4	1.8469	1.8683	1.8845	1.8963	1.9045	1.9096	1.9119	1.9114	1.9085	1.9032	1.8957
5	1	0.4467	0.4485	0.4496	0.4503	0.4511	0.4519	0.4532	0.4551	0.4577	0.4610	0.4654
	2	1.0512	1.0649	1.0737	1.0786	1.0805	1.0796	1.0762	1.0707	1.0632	1.0540	1.0431
	3	1.1289	1.1229	1.1158	1.1078	1.0995	1.0908	1.0820	1.0733	1.0648	1.0564	1.0484
	4	1.6422	1.6569	1.6676	1.6750	1.6796	1.6818	1.6819	1.6802	1.6766	1.6716	1.6649

TABLE 18

BC	i	$\bar{\omega}_i = \omega_i a\sqrt{\rho(1-\nu^2)/E}$										
		α										
		–0.5	–0.4	–0.3	–0.2	–0.1	0	0.1	0.2	0.3	0.4	0.5
1	1	0.8914	0.9009	0.9098	0.9184	0.9269	0.9355	0.9440	0.9528	0.9617	0.9709	0.9804
	2	1.3757	1.4143	1.4479	1.4772	1.5028	1.5252	1.5448	1.5617	1.5554	1.5361	1.5159
	3	1.6692	1.6611	1.6505	1.6380	1.6239	1.6084	1.5917	1.5740	1.5762	1.5883	1.5980
	4	2.0956	2.1226	2.1434	2.1593	2.1708	2.1785	2.1827	2.1836	2.1816	2.1764	2.1683
2	1	0.7943	0.8092	0.8235	0.8373	0.8509	0.8645	0.8779	0.8914	0.9049	0.9185	0.9323
	2	1.3257	1.3662	1.4014	1.4322	1.4505	1.4412	1.4308	1.4200	1.4083	1.3963	1.3839
	3	1.4752	1.4717	1.4660	1.4589	1.4595	1.4834	1.5045	1.5228	1.5387	1.5523	1.5635
	4	1.9702	1.9987	2.0214	2.0391	2.0527	2.0624	2.0689	2.0723	2.0727	2.0702	2.0649
3	1	0.7272	0.7461	0.7641	0.7815	0.7987	0.8156	0.8324	0.8491	0.8657	0.8824	0.8990
	2	1.2858	1.2982	1.2983	1.2971	1.2949	1.2919	1.2883	1.2842	1.2796	1.2748	1.2698
	3	1.2963	1.3277	1.3644	1.3966	1.4251	1.4503	1.4725	1.4921	1.5092	1.5239	1.5363
	4	1.8586	1.8889	1.9133	1.9329	1.9483	1.9603	1.9689	1.9745	1.9773	1.9773	1.9748
4	1	0.6773	0.6842	0.6904	0.6962	0.7017	0.7069	0.7122	0.7174	0.7229	0.7284	0.7342
	2	1.2127	1.2387	1.2598	1.2770	1.2909	1.3019	1.3104	1.3165	1.3203	1.3218	1.3192
	3	1.4248	1.4193	1.4119	1.4033	1.3936	1.3832	1.3721	1.3608	1.3491	1.3378	1.3286
	4	1.8739	1.8945	1.9101	1.9214	1.9292	1.9339	1.9359	1.9351	1.9320	1.9266	1.9189
5	1	0.5082	0.5133	0.5175	0.5214	0.5251	0.5290	0.5332	0.5378	0.5430	0.5489	0.5557
	2	1.0496	1.0629	1.0716	1.0767	1.0785	1.0776	1.0744	1.0690	1.0618	1.0527	1.0421
	3	1.2014	1.1984	1.1942	1.1893	1.1839	1.1781	1.1723	1.1665	1.1608	1.1555	1.1504
	4	1.6582	1.6732	1.6840	1.6916	1.6963	1.6988	1.6992	1.6977	1.6944	1.6896	1.6832

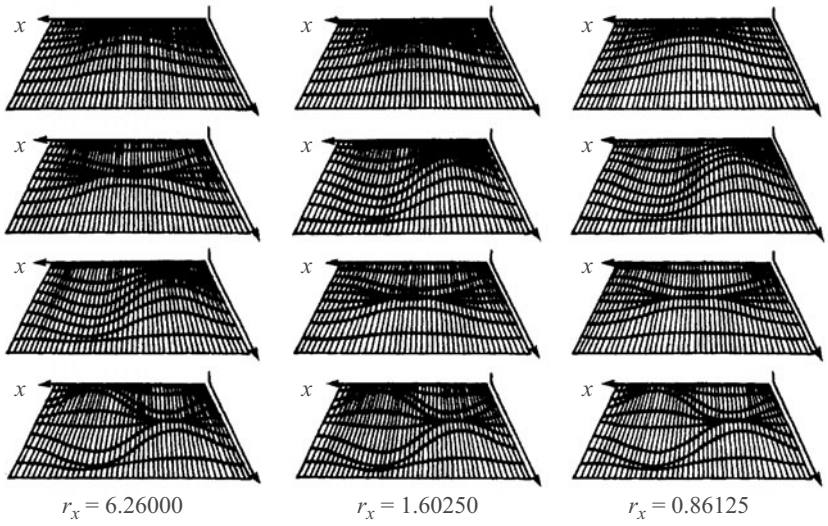

Fig. 25

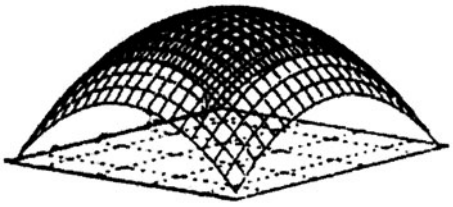

Fig. 26

formula (8.16) shows that the thickness of the shell is minimum at the point ($a/2$, y), which affects the vibration modes of the shell (Fig. 25) by slightly shifting the maximum amplitude toward the center when the number of half-waves along the *OX*-axis is odd.

We used the above procedure to examine the natural frequency spectrum of a shallow isotropic doubly curved shell with variable thickness and square planform ($a = b = 0.5$ m). The number of collocation points $N = 18$. The shell is made of orthogonally fiberglass-reinforced (2:1) plastic with the following characteristics: $E_1 = 3.68 \cdot 10^{10}$ Pa, $E_2 = 2.68 \cdot 10^{10}$ Pa, $G_{12} = 0.50 \cdot 10^{10}$ Pa, $G_{23} = 0.41 \cdot 10^{10}$ Pa, $G_{31} = 0.45 \cdot 10^{10}$ Pa, $\nu_1 = 0.077$, $\nu_2 = 0.105$, $\rho = 1870\,\text{kg/m}^3$.

Three cases are considered: $r_x = r_y = 12.5$, 3.125, 1.5625, where $r_x = R_x / a$ and $r_y = R_y / b$ are the dimensionless radii of curvature.

We used the spline-approximation method to determine the dimensionless frequencies for different number of collocation points ($N = 8$, 10, 12, 14, 16, 18, 20, 22). Tables 19 and 20 summarize these frequencies for shells with four clamped edges and $\alpha = -0.4$ and for shells with four hinged edges and $\alpha = 0.4$, respectively. For $N \geq 16$, the frequencies no longer significantly differ with increase in the number of collocation points for all boundary conditions and curvatures of the mid-surface.

Tables 21 and 22 summarize the first four resonant frequencies of orthotropic shells of variable ($|\alpha| > 0$) and constant ($\alpha = 0$) thickness with radii of curvature $r_x = r_y = 12.5$.

Figure 27 shows the first four natural modes of orthotropic shallow shells with double curvature and variable thickness for BC1 and $\alpha = 0.1$.

Tables 21 and 22 indicate that the natural frequencies of orthotropic shells are more strongly dependent on the boundary conditions than on the parameter α. The more there are clamped edges, the higher the frequency. The first frequency varies almost linearly with the parameter α for all values of curvature and all boundary conditions. The dependence $\overline{\omega} = f(\alpha)$ is nonlinear at higher frequencies. The higher frequencies are more strongly dependent on the parameter α than the lower

TABLE 19

$r_x = r_y$	i	$\overline{\omega}_i = \omega_i a^2 \sqrt{\rho h_0 / D_{11}}$							
		N							
		8	10	12	14	16	18	20	22
12.5	1	15.6808	15.6128	15.5885	15.5788	15.5739	15.5690	15.5690	15.5690
	2	38.9396	38.2883	37.9577	37.8168	37.7439	37.7098	37.6855	37.6758
	3	39.1875	38.9153	38.9056	38.9007	38.8959	38.8959	38.8959	38.8959
	4	55.0336	54.4163	54.1878	54.0906	54.0420	54.0177	54.0031	53.9934
3.125	1	17.3967	17.3384	17.3141	17.3043	17.2995	17.2995	17.2946	17.2946
	2	39.8583	39.2312	38.9007	38.7598	38.6917	38.6577	38.6334	38.6237
	3	40.1256	39.8291	39.8194	39.8194	39.8145	39.8145	39.8145	39.8145
	4	55.5537	54.9364	54.7079	54.6107	54.5621	54.5378	54.5232	54.5135
1.5625	1	22.0193	21.9658	21.9464	21.9415	21.9366	21.9318	21.9318	21.9318
	2	42.6629	42.1040	41.7831	41.6470	41.5790	41.5450	41.5207	41.5109
	3	42.9789	42.6338	42.6289	42.6241	42.6192	42.6192	42.6192	42.6192
	4	57.1869	56.5647	56.3363	56.2391	56.1905	56.1662	56.1516	56.1419

frequencies. From Fig. 27 it is seen that the sequence of natural modes is independent of the curvatures of the midsurface and these modes are the same as those of a plate with similar planform dimensions.

The results obtained here confirm the capability of our approach of determining the natural frequencies of shallow orthotropic doubly curved shells with different mechanical and geometrical parameters and different boundary conditions. This makes it possible to calculate the dynamic characteristics of such structures to determine their load-bearing capacity and ensure the required margin of safety.

Such problems are solved in [15, 48, 49, 58–62].

9. Free Vibrations of Closed Cylindrical Shells with Variable Parameters (Refined Formulation).

Problem Formulation. Consider closed circular cylindrical shells of variable thickness undergoing free vibrations. To determine the natural frequencies and vibration modes of such shells, it is necessary to use a refined theory. We will use the Timoshenko–Mindlin theory based on the straight-line hypothesis.

According to the accepted hypothesis, the small displacements of the shell can be represented in the mid-surface coordinate system $\theta\gamma z$ (γ is the normal coordinate to the mid-surface) as follows:

$$u_r(r,\theta,z) = w(\theta,z),$$

$$u_\theta(r,\theta,z) = v(\theta,z) + \gamma\Psi_\theta(\theta,z),$$

$$u_z(r,\theta,z) = u(\theta,z) + \gamma\Psi_z(\theta,z), \tag{9.1}$$

TABLE 20

$r_x = r_y$	i	$\overline{\omega}_i = \omega_i a^2 \sqrt{\rho h_0 / D_{11}}$							
		N							
		8	10	12	14	16	18	20	22
12.5	1	29.8111	29.6507	29.5826	29.5535	29.5389	29.5340	29.5292	29.5292
	2	50.3770	48.8993	48.3209	48.0584	47.9272	47.8542	47.8154	47.7911
	3	56.2099	56.1564	56.1370	56.1273	56.1224	56.1175	56.1175	56.1175
	4	71.9734	71.0936	70.7533	70.5978	70.5249	70.4811	70.4617	70.4471
3.125	1	33.8601	33.6851	33.6171	33.5879	33.5685	33.5636	33.5587	33.5539
	2	52.0539	50.5811	50.0076	49.7451	49.6138	49.5458	49.5020	49.4777
	3	57.2404	57.1821	57.1578	57.1432	57.1383	57.1383	57.1383	57.1334
	4	72.6587	71.7595	71.4144	71.2540	71.1762	71.1373	71.1130	71.1033
1.5625	1	44.2524	44.0337	43.9462	43.9073	43.8879	43.8781	43.8733	43.8684
	2	57.0654	55.5974	55.0287	54.7711	54.6447	54.5718	54.5329	54.5086
	3	60.4145	60.3270	60.2929	60.2784	60.2686	60.2686	60.2638	60.2638
	4	74.8023	73.8496	73.4802	73.3149	73.2372	73.1934	73.1691	73.1545

where $u(z,\theta)$, $v(z,\theta)$, $w(z,\theta)$ are the displacements of the coordinate surface; $\Psi_z(z,\theta)$, $\Psi_\theta(z,\theta)$ are functions describing the complete rotation of the normal ($-H/2 \le \gamma \le H/2$, $0 \le \theta \le 2\pi$, $0 \le z \le L$).

The kinematic equations are as follows:

$$e_\theta(r,\theta,z) = \varepsilon_\theta(\theta,z) + \gamma\kappa_\theta(\theta,z), \qquad e_z(r,\theta,z) = \varepsilon_z(\theta,z) + \gamma\kappa_z(\theta,z),$$

$$e_{\theta z}(r,\theta,z) = \varepsilon_{\theta z}(\theta,z) + 2\gamma\kappa_{\theta z}(\theta,z), \qquad e_{\gamma\theta}(r,\theta,z) = \gamma_\theta(\theta,z), \qquad e_{\gamma z}(r,\theta,z) = \gamma_z(\theta,z),$$

$$\varepsilon_z = \frac{\partial u}{\partial z}, \qquad \varepsilon_\theta = \frac{1}{R}\frac{\partial v}{\partial \theta} + \frac{1}{R}w, \qquad \varepsilon_{\theta z} = \frac{1}{R}\frac{\partial u}{\partial \theta} + \frac{\partial v}{\partial z}, \qquad \kappa_z = \frac{\partial \psi_z}{\partial z},$$

$$\kappa_\theta = \frac{1}{R}\frac{\partial \psi_\theta}{\partial \theta} - \frac{1}{R}\left(\frac{1}{R}\frac{\partial v}{\partial \theta} + \frac{1}{R}w\right), \qquad 2\kappa_{\theta z} = \frac{1}{R}\frac{\partial \psi_z}{\partial \theta} + \frac{\partial \psi_\theta}{\partial z} - \frac{1}{R^2}\frac{\partial u}{\partial \theta},$$

$$\gamma_\theta = \Psi_\theta + \frac{1}{R}\frac{\partial w}{\partial \theta} - \frac{1}{R}v, \qquad \gamma_z = \Psi_z + \frac{\partial w}{\partial z}, \tag{9.2}$$

where ε_θ, ε_z, $\varepsilon_{\theta z}$ are the tangential strains of the mid-surface; κ_θ, κ_z, $\kappa_{\theta z}$ are the bending strains; γ_θ, γ_z are the angles of rotation of the normal caused by transverse shear. The constitutive equations for orthotropic cylindrical shells of variable thickness are

TABLE 21

Boundary conditions	i	$\overline{\omega}_i = \omega_i a^2 \sqrt{\rho h_0 / D_{11}}$				
		α				
		–0.5	–0.4	–0.3	–0.2	–0.1
BC1	1	25.9322	26.2919	26.6516	27.0259	27.4050
	2	47.9612	49.4243	50.6832	50.5034	50.1339
	3	51.3491	51.1158	50.8339	51.7866	52.7539
	4	66.0967	67.1126	67.9438	68.6292	69.1833
BC2	1	22.1797	22.7387	23.3025	23.8712	24.4497
	2	45.8273	45.6523	45.4287	45.1760	44.9038
	3	46.4786	47.9903	49.2930	50.4402	51.4464
	4	62.5143	63.5740	64.4489	65.1732	65.7759
BC3	1	20.3277	20.4881	20.6242	20.7458	20.8624
	2	42.9886	44.0094	43.9851	43.5622	43.1101
	3	44.7336	44.3934	44.8600	45.5357	46.0801
	4	59.7972	60.5360	61.1047	61.5324	61.8435
BC4	1	19.4382	20.1819	20.9159	21.6547	22.3887
	2	40.2763	40.1985	40.0867	39.9604	39.8194
	3	45.3801	46.9307	48.2771	49.4534	50.4985
	4	59.1847	60.2929	61.2165	61.9942	62.6456
BC5	1	15.6225	15.5690	15.4864	15.3795	15.2628
	2	38.1327	37.7098	37.2529	36.7766	36.2905
	3	38.3271	38.8959	39.2653	39.4743	39.5375
	4	53.5656	54.0177	54.3142	54.4892	54.5572

TABLE 22

Boundary conditions	i	$\overline{\omega}_i = \omega_i a^2 \sqrt{\rho h_0 / D_{11}}$					
		α					
		0	0.1	0.2	0.3	0.4	0.5
BC1	1	27.7987	28.2070	28.6348	29.0722	29.5340	30.0104
	2	49.7354	49.3028	48.8410	48.3598	47.8542	47.3341
	3	53.6094	54.3628	55.0287	55.6120	56.1175	56.5550
	4	69.6305	69.9756	70.2284	70.3985	70.4811	70.4860
BC2	1	25.0329	25.6357	26.2433	26.8655	27.5022	28.1536
	2	44.6073	44.2962	43.9754	43.6448	43.3143	42.9886
	3	52.3407	53.1330	53.8379	54.4600	55.0044	55.4808
	4	66.2668	66.6654	66.9716	67.1952	67.3459	67.4188
BC3	1	20.9693	21.0763	21.1735	21.2756	21.3728	21.4700
	2	42.6386	42.1526	41.6519	41.1512	40.6506	40.1548
	3	46.5175	46.8529	47.1057	47.2758	47.3730	47.4022
	4	62.0525	62.1692	62.2032	62.1546	62.0331	61.8387
BC4	1	23.1324	23.8761	24.6246	25.3829	26.1461	26.9141
	2	39.6736	39.5229	39.3819	39.2458	39.1194	39.0125
	3	51.4220	52.2484	52.9775	53.6288	54.2073	54.7128
	4	63.1900	63.6420	64.0114	64.2982	64.5170	64.6579
BC5	1	15.1413	15.0198	14.9128	14.8156	14.7427	14.6990
	2	35.7947	35.3037	34.8225	34.3608	33.9136	33.5004
	3	39.4791	39.3042	39.0271	38.6528	38.1910	37.6369
	4	54.5281	54.4211	54.2413	53.9934	53.6823	53.3129

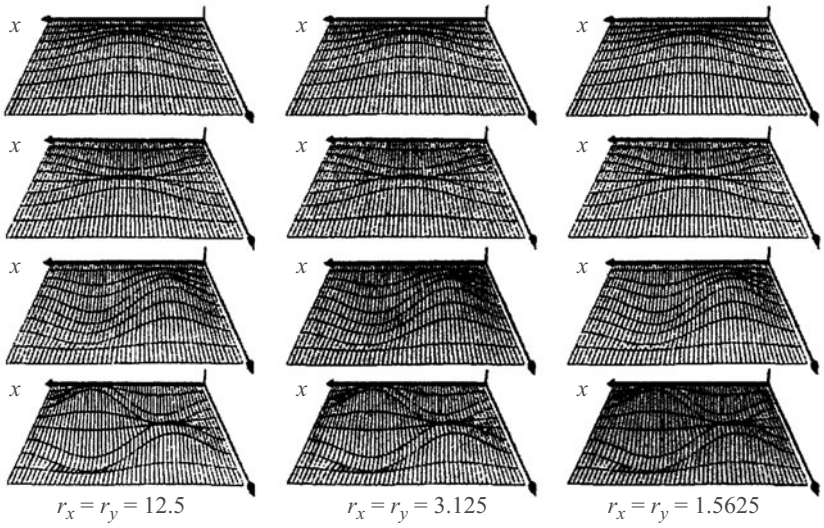

Fig. 27

$$N_z = C_{11}\varepsilon_z + C_{12}\varepsilon_\theta, \quad N_\theta = C_{12}\varepsilon_z + C_{22}\varepsilon_\theta, \quad N_{z\theta} = C_{66}\varepsilon_{\theta z} + 2D_{66}\frac{1}{R}\kappa_{\theta z},$$

$$M_z = D_{11}\kappa_z + D_{12}\kappa_\theta, \quad M_\theta = D_{12}\kappa_z + D_{22}\kappa_\theta, \quad M_{\theta z} = M_{z\theta} = 2D_{66}\kappa_{\theta z},$$

$$Q_\theta = K_2\gamma_\theta, \quad Q_z = K_1\gamma_z, \quad N_{\theta z} = C_{66}\varepsilon_{\theta z}\ K_1 = 5h(\theta,\ z)G_{13}/6,$$

$$K_2 = 5h(\theta,\ z)G_{23}/6, \quad B_{11} = B_{22} = E/(1-\nu^2), \quad B_{66} = E/2(1+\nu),$$

$$B_{12} = \nu E/(1-\nu^2), \quad C_{ij} = B_{ij}h(\theta, z), \quad D_{ij} = B_{ij}h^3(\theta,\ z)/12, \tag{9.3}$$

where G_{13} and G_{23} are the transverse shear moduli; E is Young's modulus; ν is Poisson's ratio.

The motion of an element of the mid-surface is described by the equation

$$\frac{\partial N_z}{\partial z} + \frac{1}{R}\frac{\partial N_{\theta z}}{\partial \theta} = \rho h\frac{\partial^2 u}{\partial t^2}, \quad \frac{1}{R}\frac{\partial N_\theta}{\partial \theta} + \frac{\partial N_{z\theta}}{\partial z} + \frac{1}{R}Q_\theta = \rho h\frac{\partial^2 v}{\partial t^2},$$

$$\frac{\partial Q_z}{\partial z} + \frac{1}{R}\frac{\partial Q_\theta}{\partial \theta} - \frac{1}{R}N_\theta = \rho h\frac{\partial^2 w}{\partial t^2}, \quad \frac{\partial M_z}{\partial z} + \frac{1}{R}\frac{\partial M_{\theta z}}{\partial \theta} - Q_z = \rho\frac{h^3}{12}\frac{\partial^2 \psi_z}{\partial t^2},$$

$$\frac{1}{R}\frac{\partial M_\theta}{\partial \theta} + \frac{\partial M_{z\theta}}{\partial z} - Q_\theta = \rho\frac{h^3}{12}\frac{\partial^2 \psi_\theta}{\partial t^2}, \quad N_{z\theta} - \frac{1}{R}M_{\theta z} - N_{\theta z} = 0, \tag{9.4}$$

where $N_z, N_\theta, N_{z\theta}, N_{\theta z}$ and Q_z, Q_θ are the tangential and shearing forces; $M_z, M_\theta, M_{z\theta}, M_{\theta z}$ are the bending and twisting moments; ρ and $h = h(\theta, z)$ are the density of the material and the thickness of the shell.

Assuming that all particles of the shell undergo harmonic vibrations with circular frequency ω and considering that

$$u(\theta, z, t) = \tilde{u}(\theta, z)e^{i\omega t}, \quad v(\theta, z, t) = \tilde{v}(\theta, z)e^{i\omega t}, \quad w(\theta, z, t) = \tilde{w}(\theta, z)e^{i\omega t},$$

$$\Psi_\theta(\theta, z, t) = \tilde{\Psi}_\theta(\theta, z)e^{i\omega t}, \quad \Psi_z(\theta, z, t) = \tilde{\Psi}_z(\theta, z)e^{i\omega t}$$

(hereafter the sign "~" is omitted), we represent the equations of motion as

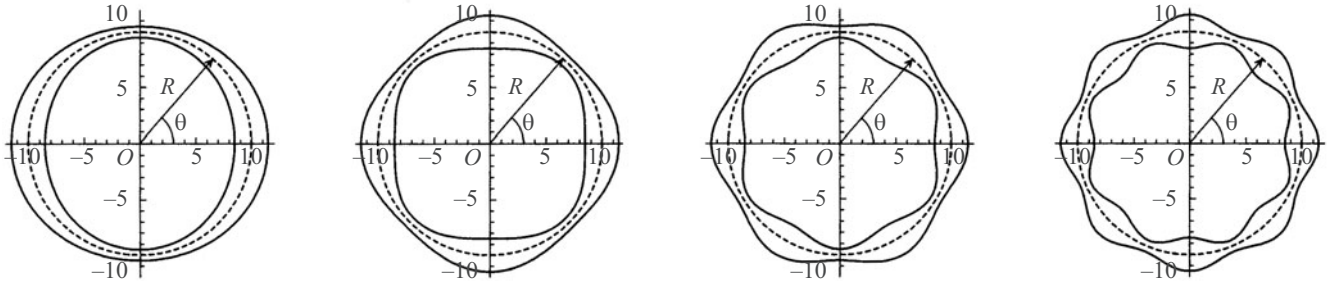

p = 2 *p* = 4 *p* = 6 *p* = 8

a *b* *c* *d*

Fig. 28

$$\frac{\partial N_z}{\partial z}+\frac{1}{R}\frac{\partial N_{\theta z}}{\partial \theta}+\rho h\omega^2 u=0, \qquad \frac{1}{R}\frac{\partial N_\theta}{\partial \theta}+\frac{\partial N_{z\theta}}{\partial z}+\frac{1}{R}Q_\theta+\rho h\omega^2 v=0,$$

$$\frac{\partial Q_z}{\partial z}+\frac{1}{R}\frac{\partial Q_\theta}{\partial \theta}-\frac{1}{R}N_\theta+\rho h\omega^2 w=0, \qquad \frac{\partial M_z}{\partial z}+\frac{1}{R}\frac{\partial M_{\theta z}}{\partial \theta}-Q_z+\rho\omega^2\frac{h^3}{12}\psi_z=0,$$

$$\frac{1}{R}\frac{\partial M_\theta}{\partial \theta}+\frac{\partial M_{z\theta}}{\partial z}-Q_\theta+\rho\omega^2\frac{h^3}{12}\psi_\theta=0. \tag{9.5}$$

Substituting formulas (9.2)–(9.3) into (9.5), we obtain a governing system of differential equations for the functions $u(z,\theta)$, $v(z,\theta)$, $w(z,\theta)$, $\Psi_z(z,\theta)$, $\Psi_\theta(z,\theta)$ and their derivatives:

$$L_i\left(u, \frac{\partial u}{\partial \theta}, \frac{\partial u}{\partial z}, \frac{\partial^2 u}{\partial^2 \theta}, \frac{\partial^2 u}{\partial^2 z}, \frac{\partial^2 u}{\partial \theta\,\partial z}, v, \frac{\partial v}{\partial \theta}, \frac{\partial v}{\partial z}, \frac{\partial^2 v}{\partial^2 \theta}, \frac{\partial^2 v}{\partial^2 z}, \frac{\partial^2 v}{\partial \theta\,\partial z},\right.$$

$$w, \frac{\partial w}{\partial \theta}, \frac{\partial w}{\partial z}, \frac{\partial^2 w}{\partial^2 \theta}, \frac{\partial^2 w}{\partial^2 z}, \frac{\partial^2 w}{\partial \theta\,\partial z}, \Psi_\theta, \frac{\partial \Psi_\theta}{\partial \theta}, \frac{\partial \Psi_\theta}{\partial z}, \frac{\partial^2 \Psi_\theta}{\partial^2 \theta}, \frac{\partial^2 \Psi_\theta}{\partial^2 z}, \frac{\partial^2 \Psi_\theta}{\partial \theta\,\partial z},$$

$$\left.\Psi_z, \frac{\partial \Psi_z}{\partial \theta}, \frac{\partial \Psi_z}{\partial z}, \frac{\partial^2 \Psi_z}{\partial^2 \theta}, \frac{\partial^2 \Psi_z}{\partial^2 z}, \frac{\partial^2 \Psi_z}{\partial \theta\,\partial z}, \omega^2\right)=0, \tag{9.6}$$

where L_i $(i=\overline{1,5})$ are linear operators, and adding boundary conditions, we arrive at a two-dimensional boundary-value problem.

Problem-Solving Method. To solve the two-dimensional boundary-value problem posed, we use the spline-collocation method to reduce it a one-dimensional problem that can be solved with the discrete-orthogonalization and incremental-search methods [1–5].

The solution of (9.6) can be represented as

$$u(z,\theta)=\sum_{i=0}^{N}u_i(\theta)\varphi_{1i}(z), \qquad v(z,\theta)=\sum_{i=0}^{N}v_i(\theta)\varphi_{2i}(z), \qquad w(z,\theta)=\sum_{i=0}^{N}w_i(\theta)\varphi_{3i}(z),$$

$$\Psi_z(z,\theta)=\sum_{i=0}^{N}\Psi_{z_i}(\theta)\varphi_{4i}(z), \qquad \Psi_\theta(z,\theta)=\sum_{i=0}^{N}\Psi_{\theta_i}(\theta)\varphi_{5i}(z), \tag{9.7}$$

where $u_i(\theta)$, $v_i(\theta)$, $w_i(\theta)$, $\Psi_{\theta i}(\theta)$, $\Psi_{zi}(\theta)$ are functions of θ; $\varphi_{ji}(z)$ $(j=1,\ldots,5,\ i=0,\ldots,N)$ are linear combinations of cubic *B*-splines on a uniform partition $\{\Delta: 0=z_0<z_1<\ldots<z_N=L\}$ that satisfy the boundary conditions at $z=0$ and $z=L$.

The system of equations (9.6) is reduced to

$$\overline{Y}'=A(\theta,\omega)\overline{Y}, \tag{9.8}$$

TABLE 23

p	Ω	$\alpha = 0$	$\alpha = 0.1$	$\alpha = 0.2$	$\alpha = 0.3$
2	Ω_1	0.0899	0.0900	0.0901	0.0905
	Ω_2	0.1083	0.1071	0.1060	0.1048
	Ω_3	0.1089	0.1087	0.1083	0.1077
4	Ω_1	0.0899	0.0905	0.0909	0.0910
	Ω_2	0.1083	0.1063	0.1039	0.1013
	Ω_3	0.1089	0.1089	0.1089	0.1088
6	Ω_1	0.0899	0.0898	0.0895	0.0890
	Ω_2	0.1083	0.1057	0.1030	0.1001
	Ω_3	0.1089	0.1084	0.1080	0.1076
8	Ω_1	0.0899	0.0898	0.0894	0.0888
	Ω_2	0.1083	0.1059	0.1033	0.1005
	Ω_3	0.1089	0.1091	0.1092	0.1089

where $\overline{Y} = \{\overline{u},\ \overline{u}',\ \overline{v},\ \overline{v}',\ \overline{w},\ \overline{w}',\ \overline{\Psi}_z,\ \overline{\Psi}'_z,\ \overline{\Psi}_\theta,\ \overline{\Psi}'_\theta\}^T$; $A(\theta, \omega)$ is a $10(N+1)\times 10(N+1)$-matrix. The boundary conditions are

$$B_1\overline{Y}(0) = \overline{0}, \qquad B_2\overline{Y}(\pi) = \overline{0}, \tag{9.9}$$

where B_1 and B_2 are $5(N+1)\times 10(N+1)$-matrices.

The boundary-value eigenvalue problem (9.8), (9.9) is solved using the discrete-orthogonalization and incremental-search methods.

We analyzed the natural frequency spectrum of a clamped circular cylindrical shell with thickness circumferentially varying as $H = H_0(1+\alpha\cos p\theta)$, $H_0 = 2$, $p = 2l$, $l \in \mathbb{N}$, $\alpha = 0$, 0.1, 0.2, 0.3. Figure 28 illustrates how the thickness of the shell varies in the circumferential direction with the parameter p ($p = 2, 4, 6, 8$) for $\alpha = 0.3$.

Table 23 summarizes the first three dimensionless frequencies $\Omega_m = \omega_m H_0\sqrt{\rho / G}$ (m is frequency number).

When $p = 2, 4$, as the parameter α is increased, the first frequency increases and the second and third frequencies decrease. When $p = 6, 8$, all the three frequencies decrease with increasing α.

Table 24 collects the calculated values of the parameter p for a circular cylindrical shell with thickness circumferentially varying as $H = H_0(1+\alpha\cos p\theta)$, $H_0 = 2$, $p = 2l$, $l = 1, \ldots, 20$ and $\alpha = 0.3$.

It can be seen that the effect of the parameter p on the natural frequencies of the shell is stronger when $2 \le p \le 8$. Beginning with $p = 8$, the first three frequencies monotonically decrease with increasing p.

We studied the influence of change in the length of the shell within $15 \le L \le 150$ on the natural frequencies of closed circular cylindrical shells with the radius of the mid-surface remaining constant ($R = 10$). Shells with thickness circumferentially varying as $H = H_0(1+\alpha\cos p\theta)$, $p = 2$, $H_0 = 2$, $\alpha = 0.2$, and shells of constant thickness ($\alpha = 0$) were compared considering various boundary conditions. The calculated values of Ω are given in Table 25.

TABLE 24

p	Ω_1	Ω_2	Ω_3
2	0.0905	0.1048	0.1077
4	0.0910	0.1013	0.1088
6	0.0890	0.1001	0.1076
8	0.0888	0.1005	0.1089
10	0.0887	0.1004	0.1085
12	0.0885	0.1003	0.1083
14	0.0884	0.1002	0.1082
16	0.0882	0.1001	0.1080
18	0.0881	0.1000	0.1079
20	0.0880	0.0999	0.1077
22	0.0879	0.0998	0.1076
24	0.0878	0.0997	0.1075
26	0.0877	0.0997	0.1075
28	0.0877	0.0996	0.1074
30	0.0876	0.0996	0.1073
32	0.0876	0.0996	0.1073
34	0.0875	0.0995	0.1072
36	0.0875	0.0995	0.1072
38	0.0874	0.0995	0.1072
40	0.0874	0.0994	0.1071

The first natural frequencies can be compared. The effect of the parameter α on the frequencies is strong in short shells with hinged edges (to 8%) and is less strong for quite short ($15 \le L \le 20$) shells with clamped edges (to 2%).

At greater lengths of the cylinder, the influence of the parameter α is insignificant. The first frequency tends to zero with increasing length of the cylinder, which is in agreement with the results for thin shells in [13, 14].

Let us analyze the effect of varying the radius of mid-surface within $10 \le R \le 20$ at constant length $L = 20$ on the natural frequencies of a shell with various boundary conditions. Shells with thickness circumferentially varying as $H = H_0(1 + \alpha \cos p\theta)$, $p = 2$, $H_0 = 2$, $\alpha = 0.2$, and shells of constant thickness ($\alpha = 0$) were compared considering various boundary conditions. The calculated values of Ω are given in Table 26.

TABLE 25

L	L / R	Hinging		Clamping	
		$\alpha = 0$	$\alpha = 0.2$	$\alpha = 0$	$\alpha = 0.2$
15	1.5	0.1256	0.1257	0.0987	0.0902
20	2.0	0.0899	0.0901	0.0707	0.0706
25	2.5	0.0703	0.0704	0.0547	0.0546
30	3.0	0.0579	0.0581	0.0450	0.0449
35	3.5	0.0497	0.0498	0.0389	0.0389
40	4.0	0.0439	0.0439	0.0350	0.0350
45	4.5	0.0397	0.0397	0.0325	0.0324
50	5.0	0.0366	0.0366	0.0307	0.0307
55	5.5	0.0343	0.0343	0.0273	0.0273
60	6.0	0.0325	0.0325	0.0238	0.0239
65	6.5	0.0303	0.0296	0.0209	0.0211
70	7.0	0.0276	0.0270	0.0185	0.0187
75	7.5	0.0252	0.0247	0.0165	0.0167
80	8.0	0.0231	0.0227	0.0148	0.0150
85	8.5	0.0213	0.0210	0.0133	0.0136
90	9.0	0.0197	0.0194	0.0120	0.0123
95	9.5	0.0182	0.0180	0.0109	0.0112
100	10.0	0.0169	0.0167	0.0100	0.0103
105	10.5	0.0157	0.0156	0.0091	0.0094
110	11.0	0.0146	0.0146	0.0084	0.0086
115	11.5	0.0137	0.0136	0.0078	0.0080
120	12.0	0.0128	0.0128	0.0072	0.0074
125	12.5	0.0120	0.0120	0.0066	0.0069
130	13.0	0.0112	0.0113	0.0062	0.0064
135	13.5	0.0106	0.0106	0.0057	0.0059
140	14.0	0.0099	0.0100	0.0054	0.0056
145	14.5	0.0094	0.0094	0.0050	0.0052
150	15	0.0088	0.0089	0.0047	0.0049

TABLE 26

R	R / L	Hinging		Clamping	
		$\alpha = 0$	$\alpha = 0.2$	$\alpha = 0$	$\alpha = 0.2$
10.0	0.5000	0.0899	0.0901	0.0707	0.0706
10.5	0.525	0.0888	0.0890	0.0701	0.0700
11.0	0.550	0.0878	0.0880	0.0697	0.0696
11.5	0.575	0.0869	0.0871	0.0693	0.0692
12.0	0.600	0.0861	0.0863	0.0689	0.0688
12.5	0.625	0.0853	0.0855	0.0686	0.0685
13.0	0.650	0.0846	0.0847	0.0683	0.0682
13.5	0.675	0.0839	0.0840	0.0679	0.0668
14.0	0.700	0.0833	0.0833	0.0676	0.0644
14.5	0.725	0.0827	0.0826	0.0670	0.0622
15.0	0.750	0.0821	0.0819	0.0655	0.0601
15.5	0.775	0.0815	0.0808	0.0643	0.0581
16.0	0.800	0.0805	0.0796	0.0625	0.0563
16.5	0.825	0.0795	0.0786	0.0606	0.0546
17.0	0.850	0.0786	0.0776	0.0588	0.0531
17.5	0.875	0.0777	0.0767	0.0571	0.0515
18.0	0.900	0.0769	0.0758	0.0555	0.0501
18.5	0.925	0.0762	0.0750	0.0540	0.0487
19.0	0.950	0.0755	0.0743	0.0526	0.0474
19.5	0.975	0.0748	0.0736	0.0513	0.0462
20.0	1.000	0.0742	0.0729	0.0500	0.0451

The greater the ratio R / L the stronger the effect of the parameter α on the natural frequency of the shell. In all cases, the first frequency decreases with increasing radius of the mid-surface of the shell. The frequencies differ by 2% if the shell is clamped and by 10% if the shell is hinged.

We also analyzed the natural frequency spectrum of closed circular cylindrical shells with thickness circumferentially varying as $H = H_0 (1 + \alpha \cos p\theta)$. Applying the spline-collocation and discrete-orthogonalization methods makes it possible to analyze the effect of the parameters p and α on the natural frequency spectrum of the shell when the geometrical parameters R and L of the shell are changed and to compare the obtained results with those for a cylindrical shell of constant thickness with various boundary conditions. Thus, varying the parameters p and α, it is possible to control the natural frequency spectrum of shells of variable thickness. Problems on the free vibrations of cylindrical shells with thickness varying in two directions were solved in [11, 42].

The stress state of hollow circular isotropic and orthotropic cylinders of finite length with clamped ends was analyzed in [81].

Conclusions. We have reviewed publications and generalized the results on the static and dynamic deformation of a wide class of shells with variable parameters obtained using classical and refined problem formulations. Solving static and dynamic problems for such shells involves computational difficulties. In this connection, an effective discrete–continuous numerical–analytic approach has been developed. It employs the spline-collocation method to reduce the starting system of partial differential equations with variable coefficients to one-dimensional boundary-value problems for systems of ordinary differential equations of high order that can be solved with the stable numerical discrete-orthogonalization method (in combination with the incremental-search method in the dynamic case). This approach was used to analyze the stress–strain state and free vibrations of rectangular plates, shallow circular and noncircular cylindrical and conical shells with variable thickness and anisotropic properties using classical and refined problem formulations.

Emphasis was placed on the reliability of numerical results. The effect of mechanical and geometrical parameters, boundary conditions, and type of load on the displacement and stress fields and dynamic characteristics of shells has been analyzed. The results obtained are indicative of the high capability of the proposed approach (along with the finite-difference and finite-element methods) to solve problems in the mechanics of shells.

REFERENCES

1. J. H. Ahlberg, E. N. Nilson, and J. L. Walsh, *The Theory of Splines and Their Applications*, Academic Press, New York (1967).
2. S. A. Ambartsumyan, *General Theory of Anisotropic Shells* [in Russian], Nauka, Moscow (1974).
3. R. E. Bellman and R. E. Kalaba, *Quasilinearization and Nonlinear Boundary-Value Problems*, Elsevier, New York (1965).
4. V. L. Biderman, *Mechanics of Thin-Walled Structures* [in Russian], Mashinostroenie, Moscow (1977).
5. V. Z. Vlasov, *General Theory of Shells and Its Applications in Engineering*, NASA TTF 99, April (1964).
6. S. K. Godunov, "Numerical solution of boundary-value problems for systems of linear ordinary differential equations," *Usp. Mat. Nauk*, **16**, No. 3, 171–174 (1961).
7. S. K. Golushko and Yu. V. Nemirovskii, *Direct and Inverse Problems in the Mechanics of Elastic Composite Plates and Shells* [in Russian], Fiz.-Mat. Lit., Moscow (2008).
8. A. L. Goldenveizer, *Theory of Elastic Thin Shells* [in Russian], Nauka, Moscow (1976).
9. E. I. Grigolyuk and E. A. Kogan, *Statics of Elastic Layered Shells* [in Russian], NII Mekh. MGU, Moscow (1999).
10. A. Ya. Grigorenko, "Calculation of natural vibrations of rectangular plates of variable thickness by the spline-collocation method," *Prikl. Mekh.*, **27**, No. 2, 123–126 (1990).
11. A. Ya. Grigorenko, T. L. Efimova, and L. V. Sokolov, "Free vibrations of nonclosed orthotropic shells of variable thickness," *Methods for Solving Applied Problems in Solid Mechanics* [in Russian], **13**, (2012), pp. 99–105.
12. A. Ya. Grigorenko, T. L. Efimova, and S. V. Puzyrev, "Analysis of the free vibrations of orthotropic rectangular plates with linearly varying thickness," *Mat. Metody Fiz.-Mekh. Polya*, **49**, No. 3, 153–161 (2006).
13. A. Ya. Grigorenko and S. A. Mal'tsev, "Solving problems of the free vibrations of conical shells of variable thickness," *Dop. NAN Ukrainy*, No. 7, 63–69 (2009).

14. A. Ya. Grigorenko and S. A. Mal'tsev, "Free vibrations of conical shells with thickness varying in two directions," *Dop. NAN Ukrainy*, No. 11, 60–69 (2009).
15. A. Ya. Grigorenko and A. Yu. Parkhomenko, "Free vibrations of shallow shells of variable thickness: Refined numerical solution," *Dop. NAN Ukrainy*, No. 12, 50–54 (2009).
16. Ya. M. Grigorenko, *Isotropic and Anisotropic Layered Shells of Revolution with Variable Stiffness* [in Russian], Naukova Dumka, Kyiv (1973).
17. Ya. M. Grigorenko and M. N. Berenov, "Solving two-dimensional problems of the bending of rectangular plates using spline-approximation," *Dop. AN URSRm Ser. A*, No. 8, 22–25 (1987).
18. Ya. M. Grigorenko, E. I. Bespalova, A. T. Vasilenko, and L. N. Petrova, "Computer solution of static problems for shells of revolution under arbitrary loadingm" in: *Proc. 4th All-Union Conf. on the Use of Computers in Structural Engineering* [in Russian], Naukova Dumka, Kyiv (1968), pp. 46–51.
19. Ya. M. Grigorenko and A. T. Vasilenko, "Numerical solution of boundary-value problems of the stress state of shells of revolution," in: *Abstracts of 5th All-Union Conf. on the Theory of Plates and Shells* [in Russian], Nauka, Moscow (1965), pp. 18–19.
20. Ya. M. Grigorenko and A. T. Vasilenko, *Static Problems for Anisotropic Inhomogeneous Shells* [in Russian], Nauka, Moscow (1992).
21. Ya. M. Grigorenko, A. T. Vasilenko, and G. P. Golub, *Statics of Anisotropic Shells with Finite Shear Stiffness* [in Russian], Naukova Dumka, Kyiv (1987).
22. Ya. M. Grigorenko, G. G. Vlaikov, and A. Ya. Grigorenko, *Numerical Analytic Solution of Shell Problems Based on Various Models* [in Russian], Akademperiodika, Kyiv (2006).
23. A. N. Guz, *Stability of Three-Dimensional Deformable Bodies* [in Russian], Naukova Dumka, Kyiv (1971).
24. A. N. Guz, I. S. Chernyshenko, V. N. Chekhov, et al., *Theory of Thin Shells Weakened by Holes*, Vol. 1 of the five-volume series *Methods of Shell Design* [in Russian], Naukova Dumka, Kyiv (1980).
25. Yu. S. Zav'yalov, Yu. I. Kvasov, and V. L. Miroshnichenko, *Spline-Function Methods* [in Russian], Nauka, Moscow (1980).
26. A. V. Karmishin, V. A. Lyaskovets, V. I. Myachenkov, and A. N. Frolov, *Statics and Dynamics of Thin-Walled Shell Structures* [in Russian], Mashinostroenie, Moscow (1975).
27. S. G. Lekhnitskii, *Theory of Elasticity of an Anisotropic Body*, Mir, Moscow (1981).
28. Kh. M. Mushtari, "Some generalizations of the theory of thin shells with application to problems of the stability of elastic equilibrium," *Prikl. Mat. Mekh*., **2**, No. 14, 439–456 (1939).
29. Kh. M. Mushtari and K. Z. Galimov, *Nonlinear Theory of Elastic Shells* [in Russian], Tatknigoizdat, Kazan (1957).
30. V. V. Novozhilov, *Thin Shell Theory*, Noordhoff, Groningen (1964).
31. B. L. Pelekh, *Theory of Shells with Finite Shear Stiffness* [in Russian], Naukova Dumka, Kyiv (1973).
32. O. A. Avramenko, "Stress–strain analysis of nonthin conical shells with thickness varying in two coordinate directions," *Int. Appl. Mech*., **48**, No. 3, 332–342 (2012).
33. V. Birman, *Plate Sructures*, *Ser. Solids Mechanics and Applications*, Spinger, Berlin (2011).
34. V. D. Budak, A. Ya. Grigorenko, and S. V. Puzyrev, "Solution describing the natural vibrations of rectangular shallow shells with varying thickness," *Int. Appl. Mech*., **43**, No. 4, 432–441 (2007).
35. V. D. Budak, A. Ya. Grigorenko, and S. V. Puzyrev, "Free vibrations of rectangular orthotropic shallow shells with varying thickness," *Int. Appl. Mech*., **43**, No. 6, 670–682 (2007).
36. L. H. Donnel, *Beams*, *Plates*, *and Shells*, McGraw-Hill, New York (1976).
37. W. Flugge, *Stresses in Shells*, Springer, Berlin (1967).
38. A. Ya. Grigorenko, "Investigation of the dynamical characteristics of anisotropic in homogeneous cylinders with circular and non-circular cross section on the base of the numerical research," in: *2nd Eur. Conf. Comput. Mech.* (Cracow, Poland, June 26–29), Abstract and Full Paper on Enclosed CD-ROM (2001), pp. 846–847.
39. A. Ya. Grigorenko and T. L. Efimova, "Spline-approximation method applied to solve natural-vibration problems for rectangular plates of varying thickness," *Int. Appl. Mech*., **41**, No. 10, 1161–1169 (2005).
40. A. Ya. Grigorenko and T. L. Efimova, "Application of the spline-approximation method for solving the problems on axisymmetric natural vibrations of thick-wall orthotropic cylinders," *Int. Appl. Mech*., **44**, No. 10, 1137–1147 (2008).

41. A. Ya. Grigorenko and T. L. Efimova, “Free axisymmetric vibrations of solids cylinders: Numerical problem solving,” *Int. Appl. Mech*., **46**, No. 5, 499–508 (2010).
42. A. Ya. Grigorenko, T. L. Efimova, and L. V. Sokolova, “On the approach to studying free vibrations of cylindrical shells of variable thickness in the circumferential direction within a refined statement” *J. Math. Sci*., **181**, No. 4, 548–563 (2010).
43. A. Ya. Grigorenko, I. I. Dyyak, and V. M. Makar, “Influence of anisotropy on the response characteristics of finite cylinders under free vibrations,” *Int. Appl. Mech*., **37**, No. 5, 628–637 (2001).
44. A. Ya. Grigorenko and I. A. Loza, “Axisymmetric waves in layered hollow cylinders with axially polarized piezoceramic layers,” *Int. Appl. Mech*., **47**, No. 6, 707–713 (2011).
45. A. Grigorenko and V. Makar, “Free vibrations of the thick hollow anisotropic cylinders,” in: *Abstracts of 8th Int. Conf. on Modern Building Materials*, *Structures and Techniques* (May 19–21, 2004), Technika, Vilnius (2004), pp. 759–764.
46. A. Ya. Grigorenko and S. A. Mal’tsev, “Natural vibrations of thin conical panels of variable thickness,” *Int. Appl. Mech*., **45**, No. 11, 1221–1231 (2009).
47. A. Ya. Grigorenko, W. H. Muller, R. Wille, and S. N. Yaremchenko, “Numerical solution of the problem on the stress-strain state in hollow cylinders using spline-approximations,” *J. Math. Sci*., **180**, No. 2, 135–145 (2012).
48. A. Ya. Grigorenko and A. Yu. Parkhomenko, “Free vibrations of shallow nothin shells with variable thickness and rectangular planform,” *Int. Appl. Mech*., **46**, No. 7, 776–789 (2010).
49. A. Ya. Grigorenko and A. Yu. Parkhomenko, “Free vibrations of orthotropic shallow shells with variable thickness and rectangular planform,” *Int. Appl. Mech*., **46**, No. 8, 877–889 (2010).
50. A. Ya. Grigorenko and T. V. Tregubenko, “Numerical and experimental analysis of natural vibration of rectangular plates with variable thickness,” *Int. Appl. Mech*., **36**, No. 2, 268–271 (2000).
51. A. Ya. Grigorenko and G. G. Vlaikov, “Some problems of the theory of elasticity for anisotropic shells of noncircular cross-section,” in: *Proc. 7th Conf. on Shell Structures*, *Theory and Applications*, *Golansk-Jurata* (Poland) (2002), pp. 97–98.
52. A. Ya. Grigorenko and G. G. Vlaikov, *Some Problems of the Theory of Elasticity for Anisotropic Bodies of Cylindrical Form*, Inst. Mekh. NAN Ukrainy i Teckn. Tsentr NAN Ukrainy, Kyiv (2002).
53. A. Ya. Grigorenko and G. G. Vlaikov, “Numerical analysis of anisotropic circular and non-circular cylinder,” in: *CMM-2003-Computer Methods in Mechanics* (June 3–6, Gliwice, Poland): Abst. and Full Paper on Enclosed CD-ROM (2003), pp. 141–142.
54. A. Ya. Grigorenko and G. G. Vlaikov, “Investigation of the static and dynamic behaviour of anisotropic cylindrical bodies with noncircular cross-section,” *Int. J. Solids Struct*., **41**, 2781–2798 (2004).
55. A. Ya. Grigorenko, O.V. Vovkodav, and S. N. Yaremchenko, “Stress–strain state of nothing orthotropic spherical shells of variable thickness,” *Int. Appl. Mech*., **48**, No. 1, 80–93 (2012).
56. A. Ya. Grigorenko and N. P. Yaremchenko, “Stress–strain state of shallow shells with rectangular planform and varying thickness: Refined formulation,” *Int. Appl. Mech*., **43**, No. 10, 1132–1141 (2007).
57. A. Ya. Grigorenko and N. P. Yaremchenko, “Stress–state of nothin orthotropic shells with varying thickness and rectangular planform,” *Int. Appl. Mech*., **44**, No. 8, 905–915 (2008).
58. A. Grigorenko, N. Yaremchenko, and S. Yaremchenko, “Spline–based investigation of stress–strain of anisotropic rectangular shallow shells of variable thickness in refined formulation,” in: *Proc. Int. Symp. on Advances in Applied Mechanics and Modern Information Technology*, Baku, Azerbaijan (2011), pp. 171–175.
59. A. Grigorenko and S. Yaremchenko, “Spline-approximation method for investigation of mechanical behavior of anisotropic inhomogeneous shells,” in: *Proc. 9th Int. Conf. on Modern Building Materials*, *Strucruct. and Techniques*, Technika, Vilnius (2007), pp. 918–924.
60. A. Grigorenko and S. Yaremchenko, “Investigation of static and dynamic behaviour of anisotropic inhomogeneous shallow shells by spline approximation method,” *J. Civ. Eng. Manag*., **15**, No. 1, 87–93 (2009).
61. A. Grigorenko and S. Yaremchenko, “Static problems for noncircular cylindrical shells: Classical and refined theories,” in: *Proc. 9th Conf. on Shell Structures and Applications*, 2, Gdansk-Jurata, Taylor and Francis Group, London, UK (2009), pp. 241–244.

62. A. Grigorenko and S. Yaremchenko, “Solution of stress-strain problems for noncircular cylindrical shells based upon different models,” in: *Proc. 10th Int. Conf. on Modern Building Materials Structures and Techniques*, II, VGTV leidyklos, Technika, Lithuania (2010), pp. 885–889.
63. Ya. M. Grigorenko, “Solution of problems in the theory of shells by numerical-analysis methods,” *Int. Appl. Mech*., **20**, No. 10, 881–897 (1984).
64. Ya. M. Grigorenko, “Some approaches to modelling and numerical solution of the deformation problems of the flexible shells of revolution,” in: *Eur. Mech. Colloq. EUROMECH 292*, *Modelling of Shells with Nonlinear Behaviour*, Germany, September 2–4 (1992), pp. 12.1–12.2.
65. Ya. M. Grigorenko, “Influence of anistropy and non-homogeneity on the deformation of flexible shells,” in: *Euromech Colloq. 317*, *Buckling Strength of Imperfection-Sensitive Shells* (March 21–23, 1994), Liverpool (1994), p. 44.
66. Ya. M. Grigorenko, “Some approaches to the numerical solution of linear and nonlinear problems on deforming of elastic shell systems,” in: *Proc. 3rd Int. Congr. Industr. and Appl. Math*., Germany, Hamburg, July 3–7 (1995), p. 294.
67. Ya. M. Grigorenko, “Nonconvential approaches to static problems for noncircular cylindrical shells in different formulations,” *Int. Appl. Mech*., **43**, No. 1, 35–53 (2007).
68. Ya. M. Grigorenko, “Using discrete Fourier series to solve boundary-value stress problems for elastic bodies with complex geometry and structures,” *Int. Appl. Mech*., **45**, No. 5, 470–513 (2009).
69. Ya. M. Grigorenko and O. A. Avramenko, “Stress–strain analysis of closed nonthin orthotropic conical shells of varying thickness,” *Int. Appl. Mech*., **44**, No. 6, 635–643 (2008).
70. Ya. M. Grigorenko and O. A. Avramenko, “Influence of geometrical and mechanical parameters on the stress-strain state of closed nothin conical shells stress–strain analysis of closed nonthin orthotropic conical shells of varying thickness,” *Int. Appl. Mech*., **44**, No. 10, 1119–1127 (2008).
71. Ya. M. Grigorenko, O. A. Avramenko, and S. N. Yaremchenko, “Spline-approximation solution of two-dimensional problems of statics for orthotropic conical shells in a refined formulation,” *Int. Appl. Mech*., **43**, No. 11, 1218–1227 (2007).
72. Ya. M. Grigorenko and M. N. Berenov, “Numerical solution of problems in the statics of flattened shells on the basis of the spline collocation method,” *Int. Appl. Mech*., **24**, No. 5, 458–463 (1988).
73. Ya. M. Grigorenko and M. N. Berenov, “Solution of problems of the statics of shallow shells and plates with hinged and rigidly–fastened opposing edges,” *Int. Appl. Mech*., **26**, No. 1, 25–31 (1990).
74. Ya. M. Grigorenko, A. Ya. Grigorenko, and T. L. Efimova, “Spline-based investigation of natural vibrations of orthotropic rectangular plates of variable thickness within classical and refined theories,” *J. Mech. Struct*., **3**, No. 5, 929–952 (2008).
75. Ya. M. Grigorenko, A. Ya. Grigorenko, and L. S. Rozhok, “Solving the stress problem for solid cylinders with different end conditions,” *Int. Appl. Mech*., **42**, No. 6, 629–635 (2006).
76. Ya. M. Grigorenko, A. Ya. Grigorenko, and G. G. Vlaikov, *Problems of Mechanics for Anisotropic Inhomogeneous Shells on the Basis of Different Models*, Akademperiodika, Kyiv (2009).
77. Ya. M. Grigorenko, A. Ya. Grigorenko, and L. I. Zakhariichenko, “Stress–strain analysis of orthotropic closed and open noncircular cylindrical shells,” *Int. Appl. Mech*., **41**, No. 7, 778–785 (2005).
78. Ya. M. Grigorenko, A. Ya. Grigorenko, and L. I. Zakhariichenko, “Stress analysis of noncircular cylindrical shells with cross-section in the form of connected convex half-corrugations,” *Int. Appl. Mech*., **42**, No. 4, 431–438 (2006).
79. Ya. M. Grigorenko, A. Ya. Grigorenko, and L. I. Zakhariichenko, “Influence of geometrical parameters on the stress–strain state of longitudinally corrugated cylindrical shells,” *Int. Appl. Mech*., **45**, No. 2, 778–785 (2009).
80. Ya. M. Grigorenko and N. N. Kryukov, “Solution of problems of the theory of plates and shells with spline functions (survey),” *Int. Appl. Mech*., **31**, No. 6, 413–434 (1995).
81. Ya. M. Grigorenko and N. N. Kryukov, “Investigation of the asymmetric stressed–strained state of transversely isotropic cylinders under different boundary conditions at the ends,” *Int. Appl. Mech*., **34**, No. 7, 607–614 (1998).
82. Ya. M. Grigorenko, N. N. Kryukov, and Yu. I. Ivanova, “Solution of two-dimensional problems of the statics of flexible shallow shells by spline approximation,” *Int. Appl. Mech*., **31**, No. 4, 255–261 (1995).
83. Ya. M. Grigorenko, N. N. Kryukov, and Yu. I. Ivanova, “Spline-approximation solution of problems of the statics of orthotropic shallow shells with variable parameters,” *Int. Appl. Mech*., **36**, No. 7, 888–897 (2000).

84. Ya. M. Grigorenko, N. N. Kryukov, and N. S. Yakovenko, “Using spline-functions to solve boundary-value problems for laminated orthotropic trapezoidal plates of variable thickness,” *Int. Appl. Mech*., **41**, No. 4, 413–420 (2005).
85. Ya. M. Grigorenko and O. V. Tumashova, “Stress–strain state of flexible cylindrical panels with variable geometric parameters,” *Int. Appl. Mech*., **25**, No. 5, 454–461 (1989).
86. Ya. M. Grigorenko and O. V. Tumashova, “Computation of flexible finite-size cylindrical panels of noncircular cross section,” *Int. Appl. Mech*., **28**, No. 12, 839–842 (1992).
87. Ya. M. Grigorenko and S. N. Yaremchenko, “Stress analysis of orthotropic noncircular cylindrical shells of variable thickness in a refined formulation,” *Int. Appl. Mech*., **40**, No. 3, 266–274 (2004).
88. Ya. M. Grigorenko and S. N. Yaremchenko, “Influence of variable thickness on displacements and stresses in nonthin cylindrical orthotropic shells with elliptic cross-section,” *Int. Appl. Mech*., **40**, No. 8, 900–907 (2004).
89. Ya. M. Grigorenko and S. N. Yaremchenko, “Refined design of corrugated noncircular cylindrical shells,” *Int. Appl. Mech*., **41**, No. 1, 7–13 (2005).
90. Ya. M. Grigorenko and S. N. Yaremchenko, “Spline-approximation solution of two-dimensional problems of statics for orthotropic conical shells in a refined formulation,” *Int. Appl. Mech*., **43**, No. 11, 1218–1227 (2007).
91. Ya. M. Grigorenko and S. N. Yaremchenko, “Refined design of longitudinally corrugated cylindrical shells,” *Int. Appl. Mech*., **48**, No. 2, 205–211 (2012).
92. Ya. M. Grigorenko and L. I. Zakhariichenko, “Solution of the problem of the stress state of noncircular cylindrical shells of variable thickness,” *Int. Appl. Mech*., **34**, No. 12, 1196–2003 (1998).
93. Ya. M. Grigorenko and L. I. Zakhariichenko, “Analysis of the stress-strain state of non-circular cylindrical shells subject to thickness variation and weight retention,” *Int. Appl. Mech*., **35**, No. 6, 567–576 (1999).
94. Ya. M. Grigorenko and L. I. Zakhariichenko, “Design of corrugated cylindrical shells under different end conditions,” *Int. Appl. Mech*., **35**, No. 9, 897–905 (1999).
95. Ya. M. Grigorenko and L. I. Zakhariichenko, “Studying the effect of the spatial frequency and amplitude of corrugation on the stress-strain state of cylindrical shells,” *Int. Appl. Mech*., **39**, No. 12, 1429–1435 (2003).
96. L. Librescu, *Elastostatics and Kinetics of Anisotropic and Heterogeneous Shell-Type Structures*, Noordhoff Inter. Publishing, Leyden, Netherlands (1975).
97. A. E. H. Love, *Mathematical Theory of Elasticity*, Cambridge Univer. Press (1952).
98. E. Ramm and W. A. Wall, “Shell structures — a sensitive interrelation between physics and numerics,” *Int. J. Numer. Meth. Eng*., **60**, 381–427 (2002).
99. E. Ramm and W. A. Wall, “Computational methods for shells,” *Special Issue of Comp. Meth. Appl. Mech. Eng*., **184**, 2285–2707 (2005).
100. K. P. Soldatos, “Mechanics of cylindrical shells with non-circular cross-section. A survey,” *Appl. Mech. Rev*., **52**, No. 8, 237–274 (1999).
101. S. P. Timoshenko, *History of the Strength of Materials*, McGraw-Hill, New York (1953).